SYNTHESIS OF IONIC LIQUIDS AND THEIR APPLICATIONS IN CAPILLARY ELECTROPHORESIS

QIN WEIDONG

NATIONAL UNIVERSITY OF SINGAPORE
2003

SYNTHESIS OF IONIC LIQUIDS AND THEIR APPLICATIONS IN CAPILLARY ELECTROPHORESIS

QIN WEIDONG
(M. Eng., CISRI)

A THESIS SUBMITTED
FOR THE DEGREE OF DOCTOR OF PHILOSOPHY
DEPARTMENT OF CHEMISTRY
NATIONAL UNIVERSITY OF SINGAPORE
2003

ACKNOWLEDGEMENTS

LIST OF SYMBOLS AND ABBREVIATIONS

2,4,5-T	2,4,5-Trichlorophenoxyacetic acid	CZE	Capillary zone electrophoresis
2,4-D	2,4-Dichlorophenoxyacetic acid	D	Diffusion coefficient
		DAIM	Dialkylimidazolium
2,4-DB	4-(2,4-dichlorophenoxy) butyric acid	Dichlorprop	2-(2,4-dichlorophenoxy)propionic acid
2,4-DCBA	2,4-dichlorobenzoic acid		
3,5-DCBA	3,5-dichlorobenzoic acid	DMIMCl	1-decyl-3-methylimidazolium chloride
4-CPA	4-chlorophenoxyacetic acid		
α-CD	α-Cyclodextrin	DMSO	Dimethyl sulphoxide
A_p	Peak area	E	The electric field strength
BGE	Back ground electrolyte	ECD	Electron capture detection
BMIMCl	1-butyl-3-methylimidazolium chloride	EMIM	1-ethyl-3-methylimidazolium
		ESI	Electrospray ionization
bp	Base pairs	F	Faraday's constant
C	Concentration	FAB	Fast atom bombardment
C_{18}	Octadecylsilane	FASI	Field-amplified sample injection
CE	Capillary electrophoresis		
CEC	Capillary electrochromatography	FSCE	Free solution capillary electrophoresis
CGE	Capillary gel electrophoresis	GC	Gas chromatography
CIEF	Capillary isoelectric focusing	η	Viscosity
CITP	Capillary isotachophoresis	HBMIM	1-(4-hydroxy-butyl)-3-methylimidazolium
CPTCS	3-chloropropyl-trichlorosilane		
		HEC	Hydroxyethylcellulose
CPTMS	3-chloropropyl-trimethoxysilane	HMIM	1-hexyl-3-methylimidazolium
CRM	Consecutive reaction monitoring	HPLC	High-performance liquid chromatography
CTAC	Hexadecyltrimethylammonim chloride	I	Ionic strength
		I.D.	Internal diameter

iBMIM	1-isobutyl-3-methylimidazolium	Rs	Resolution
IE-OTCEC	Ion-exchange open tubular capillary electrochromatography	RSD	Relatively standard deviation
		S/N	The signal to noise ratio
		σ_A^2	Variance due to wall adsorption
IL	Ionic liquid	σ_D^2	Variance due to longitudinal diffusion
ILCC	IL-coated capillary		
L	Capillary length	SDS	Sodium dodecyl sulfate
LDR	Linear dynamic range	σ_E^2	Variance due to electrophoretic dispersion
LIF	Laser induced fluorescence		
l_{inj}	Length of the injected plug	σ_I^2	Variance due to injection overloading
LOD	Limit of detection		
MALDI-MS	Matrix-assisted laser desorption/ionization mass spectrometry	σ_J^2	Variance due to Joule heating
		σ_O^2	Variance due to other effects
		SL	Sildenafil
Mecoprop	2-(2-Methyl-4-chlorophenoxy)propanoic acid	SPE	Solid phase extraction
		σ_W^2	Variance due to width of the detection zone
MEKC	Micellar electrokinetic chromatography	T	Temperature
		TBE	Tris-Boric acid-EDTA
$\mu_{o\varepsilon}$	EOF rate	TIC	Total ion chromatogram
MS	Mass spectrometry	t_m	Migration time
N	Theoretical plate number	TR	Transfer ratio
NACE	Nonaqueous capillary electrophoresis	UK	UK103,320
		V	The applied voltage
PA	Polyacrylamide	v	Velocity
PACC	PA-coated capillary	VOCs	Volatile organic compounds
PEO	Poly(ethylene oxide)	z	Valence of ion
PGD	Potential gradient detector	ζ	Zeta potential
PVP	Polyvinylpyrrolidone	μ_{app}	Apparent mobility
q	Number of ionic charges	$\Delta\kappa_e$	Conductivity difference
r	Ionic radius	μ_{count}	Mobility of counterion
	Capillary internal diameter	ΔP	Pressure difference

λ_B	Conductivities of buffer
λ_S	Conductivities of sample solution
Ω_T	Temperature coefficient of electrophoretic mobility
$\Delta\mu$	Difference between electrophoretic mobilities
$\overline{\mu}$	Average electrophoretic mobility

LIST OF FIGURES

LIST OF TABLES

CONTENTS

SUMMARY

This work focuses on the synthesis of 1,3-dialkylimidazolium based ionic liquids (ILs) and methods development, optimization and applications of these materials in capillary electrophoresis (CE).

A series of ILs were synthesized with different methods and their yields were compared. The properties of the ILs were investigated with mass spectrometry (MS), indicating their different combining modes in organic solvents which would partially relate to their behavior in CE. A capillary electrophoresis (CE) method for determining the main impurity (1-methylimidazole) and by-products during the synthesis was developed with detection limits as low as 0.42 µg/ml.

The IL-cations are UV active and their electrophoretic mobilities are relatively stable over a wide pH range, making them suitable as background chromophores in CE. Research obtained in this study showed that 1-ethyl-3-methylimidazolium (EMIM) was a good chromophore between pH 3.5 and pH 11.5, while imidazole could only work below pH 7. Ammonium in human urine was successfully separated from the high-concentration potassium without additives and determined by CE using EMIM as background chromophore at pH 8.5.

Research on ILs as coating materials showed that the electroosmotic flow (EOF) of the capillary was reversed and its magnitude could be controlled by manipulating coating parameters such as reaction time. The interaction between the cationic analytes and the silica wall was reduced and hence the peak shapes and the recoveries were improved.

With careful design and operation, the co-migrating sildenafil and its metabolite were baseline separated and determined by CE-mass spectrometry. Application of IL-coated capillary (ILCC) in DNA separation depicts that in the presence of weak self-coating sieving matrix hydroxyethylcellulose (HEC), the fragments were separated in similar patterns as obtained in polyacrylamide-coated capillary with shorter analysis time due mainly to the anodic EOF. Also, the experimental data indicate electrostatic interaction between DNA and the cationic coating, which is dependent on the charge density of the fragments.

Combination of ILs as both background electrolytes and coating materials were employed in the separation of metal ions. Eleven metal ions were baseline separated in IL-coated capillary with detection limits as low as 0.27 ng/ml. The detection limits were lowered by two approaches. First, field-amplified sample injection was employed. Secondly, the sensitivity of potential gradient detector was improved by reducing the mobility of the background co-ion, the IL-cation, by addition of α-cyclodextrin (α-CD).

Fast separation of 7 phenoxy and benzoic acid herbicides was accomplished by using IL as additive. In phosphate-acetate buffer, the EOF of the capillary was reversed with addition of IL, and the analytes were baseline separated within 7 minutes under negative voltage. In addition, the resolution of position isomers was significantly improved. A solid-phase extraction (SPE) procedure was also developed and coupled with the CE method in the analysis of a local surface water sample for residual herbicides.

CHAPTER 1 INTRODUCTION

1.1 Ionic liquids

The ionic liquids (ILs) are those compounds composed of organic cations and inorganic or organic anions which are liquids at room temperature or whose melting points are slightly higher than ambient temperature. The first ambient temperature ionic liquid was synthesized in 1951 [1], an alkylpyridinium based salt (N-ethylpyridinium bromide-aluminium chloride). However, it was not until the discovery of the 1,3-dialkylimidazolium based ionic liquids in 1982 that this group of materials engendered dramatic interests [2] because the later exhibit both a wide liquidus range and electrochemical window that are useful in both electrochemistry and synthesis; moreover, the dialkylimidazolium based ILs are more stable [3]. Investigations have been carried out mainly on this group of compounds from then on. Low melting point ILs typically exhibit mixed organic and inorganic character. The cation containing imidazole ring and attached alkyl groups is relatively large compared to simple inorganic cations, accounting for the low melting point of the salt. The chemical property of the IL is determined prominently by the anion.

The research in this thesis is focused on applications of the 1,3-dialkylimidazolium based ILs. The terms "ionic liquid", "IL", "dialkylimidazolium based IL" and "ILs" in the thesis are related to the same group of ILs.

X^- can be Cl^-, Br^-; BF_4^-, PF_6^-, etc
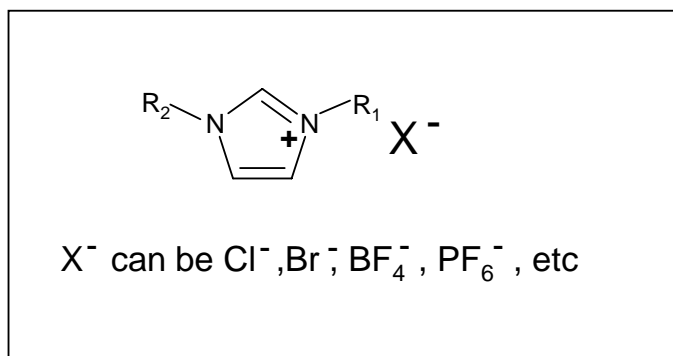
Fig. 1-1 Schematic representation of ionic liquid

Fig. 1-1 shows the schematic representation of the 1,3-dialkylimidazolium based IL. Generally R_1 and R_2 are alkyl groups as reported in many publications [3-5], but actually they can be any groups that can be added onto the imidazole ring via chemical reaction. Halides are the primary ILs synthesized, and are usually the beginning materials for other ILs. Tetrafluoroborate and hexafluorophosphate have drawn enormous interests owing to their feasibilities as electrolyte in solar battery and as solvents for liquid-liquid extraction. The following is the brief introduction of applications of this kind of materials. Although some of the applications are still potential, IL has shown promise.

1.1.1 Use as electrolyte in solar battery

The electrolytes used in many conventional solar cells are salts dissolved in organic solvents. There are some drawbacks with the electrolytes used: 1) because the organic solvents are volatile, the cell must be absolutely tight, leading to high cost; moreover, the life time of the cell is influenced by the leakage of the solvents [5]; 2) when the cell works at lower temperature than anticipated, the salts may precipitate out due to the reduced solubility. 3) The organic solvents are often incompatible with the glues used to

seal the cell. 4) For the dye-sensitized nanocrystalline solar cell, UV exciting of the dye-supporting semiconductor may cause oxidization of the salts [3].

ILs are liquids that are composed entirely of ions with negligible vapor pressure. But unlike the normal salts, they are liquids with wide liquidus range and are non-corrosive. They can be utilized in a wide range of electrochemical applications where high conductivity and ionic mobility are required. These properties as well as relatively low viscosity, the large electrochemical window, resistance to oxidation, low melting point, thermal stability, miscibility with other solvents or salts and hydrophobicity are the desirable qualities rendering them attractive alternatives for use as electrolytes and solvents in the solar cell. Furthermore, ILs are now appear to be undemanding and inexpensive to prepare. One of the ILs, 1-hexyl-3-methylimidazolium iodide, has been found to be of lowest viscosity at room temperature, not sensitive to water, and stable under the operational conditions of the photoelectrochemical cell utilizing the iodide/triiodide couple as redox mediator [5].

1.1.2 As solvent for extraction

Liquid-liquid extraction has been a widely used technique in separation science. However, the traditional solvent extraction, in which an organic solvent and an aqueous solution were used as the two immiscible phases, is increasingly challenged by the emphasis on clean manufacturing processes and environmentally benign technologies because it employs toxic, flammable, volatile organic compounds as solvents. The costs of solvents are high and disposal of spent extractants and diluents will also bring increasing costs through the impact of environmental protection regulations. A report

stated that the current worldwide usage of these organic materials has been estimated at over 5 billion dollars per annum [5]; these organics will have profound influence on environment and human health. Design of safe and clean separation media is now becoming an increasingly important role in the development of clean manufacturing processes.

The ILs used for liquid-liquid extraction are water and air stable; they have relatively favorable viscosity and density characteristics; they have high solubility in organic species while the water immiscible ionic liquids are also available. Water immiscible ILs may render such systems as being uniquely suited to the development of completely novel liquid-liquid extraction processes. The most important feature of the ILs for these purposes may be their very low vapor pressure due to the high coulombic forces present among the ions. With ionic liquids, one does not have the concerns as with volatile organic solvents. In addition, the R_1 and R_2 groups of the cation (**Fig. 1-1**) are variable and may be used to finely tune the properties of the IL. It was reported that such ionic liquids are able to solvate a wide range of species including organic, inorganic and organometallic compounds [6].

1.1.3 As solvent and catalyst for chemical reaction

Research was carried out in the early 1980s on IL feasibility as reaction media and it has attracted industrial interest from late 1990s.

Industrial chemical syntheses usually take place in liquid media, so the solvent properties play an important role in the reaction. Most chemical synthesis are catalyzed for the following reasons: 1) greater reaction selectivity and therefore less by-products; 2) enhanced reaction rates which means reduced plant size and hence the costs; 3) milder operating conditions (in terms of temperature and pressure) due to highly efficient catalysts, which may lead to both reduced energy consumption and enhanced safety. There are two factors determining the catalysis effects, one is the active site of the catalyst, another is the concentration of the catalyst. But classical solvent-catalysts system usually cannot simultaneously satisfy both the two requirements. For example, some metal-complex catalysts have to be dissolved in polar solvents in order to achieve the higher concentration. But the polar solvent often coordinates onto the active site of the catalyst and consequently blocks it.

Ionic liquids offer a highly polar but noncoordinating environment for chemical reactions. They can dissolve the metal complex catalyst to a high concentration while not blocking the active sites. Most of the known transition metal-catalyzed reactions can be carried out in ionic liquids. These include alkylation, acylation, reduction [7], oxidation, oligomerization, Diels-alder reaction [8,9] and polymerization [10-14]. Moreover, the solvation and solvolysis phenomena which occur in conventional solvents can be effectively suppressed in IL-media and therefore, waste production through side reactions are reduced to a minimum [5,15,16].

The ILs' wide liquid range is also an amazing parameter for chemical engineering. For chemical reactions, the higher the reaction temperature, the higher the reaction speed. It is important for the solvents to be in liquid state so that the reaction can take place

successfully. However, liquid ranges of most organic solvents are usually less than 100°C. As reported [4], some ILs have a liquid range of about 300°C (e.g. 1-ethyl-3 methylimidazolium chloride-aluminum chloride, the archetypal IL, is liquid and thermally stable from almost –100 to 200 °C), far in excess of the 100°C range for water or 44°C degree for ammonia.

In some cases, the ILs act as both solvents and catalysts for chemical reactions, for example, the 1-ethyl-3-methylimidazolium aluminum chloride (EMIMCl·AlCl$_3$) system can be used as a solvent and catalyst for Frieldel-Crafts reactions. A typical Friedel-Crafts reaction takes six or seven hours to produce about 80% yield of an isomer mixture; while in an IL, the reaction is complete in about 30 seconds with nearly 100% conversion [17]. Furthermore, the chemical properties of the IL such as complexing ability and acidity can be tuned at will.

The following characters of ILs also contribute to their ability as solvent for chemical reactions: very low vapor pressure, high heat conductivity, stable toward various organic chemicals, controlled miscibility with organic compounds, easy to separate from a large range of organic products, tunable Lewis acidity (for EMIMCl·AlCl$_3$ system), compatible with organometallics, and adjustable coordinating ability.

1.1.4 Use in capillary electrophoresis

With the increasing interests with this kind of new materials, some analysts expanded the application of ILs to capillary electrophoresis (CE). In the works of Vaher et al

[18], it was employed as electrolytes in nonaqueous capillary electrophoresis (NACE) for separation of water-insoluble dyes. Recently they also published a paper on the separation of phenolic mixture with NACE [19]. It was found that the EOF of the capillary was efficiently reversed, comparable to that of alkaline aqueous buffer in magnitude with addition of 4 mM IL in pure acetonitrile. Also, the ILs showed significant resolving ability towards position isomers: the peaks of resorcinol and pyrocatechol were baseline resolved in the presence of 1.3 mM 1-ethyl-3-methylimidazolium fluoroacetate. Stalcup and co-workers [20] used ILs as electrolytes in aqueous capillary electrophoresis for separation of phenolic compounds extracted from grape. They found that EOF of the capillary was reversed by adsorption of the IL cations onto the silica wall, and the magnitude of the anodic EOF increased with the amount of IL added. The neutral analytes were separated based on their different interaction abilities with dialkylimidazolium. Interestingly, they also found superior resolution ability of IL (1-butyl-3-methylimidazolium tetrafluoroborate) toward the mixtures. However, there is to date no reported systematic study of the application of ILs in this emerging area.

1.2 Capillary electrophoresis

There has been tremendous growth of capillary electrophoresis (CE) in the past decades since the launch of the first commercial CE instrument in 1989. CE is characterized by the use of narrow bore capillaries, usually in the range of 10-100 μm internal diameter (I.D.); operated at high applied potential (Normally less than 30 kV, but recently higher voltage, up to half million was utilized [21]). CE has notable advantages over the

previous methods in high separation efficiency: short analysis time, and low sample consumption. Nowadays it is widely used in analytical laboratories.

The separation mechanism of CE is based on the differences in mobilities of species (either caused by the different electrophoretic mobilities or by their different partition abilities between the aqueous buffer and the other phase) in small capillaries. The pioneering work of Hjerten [22] demonstrated the separation of inorganic and organic ions, peptides, proteins, and bacteria in a tube of 3mm I.D. in 1967. He termed it as free solution electrophoresis. But due to overloading of the samples, the high efficiencies of the technique were unable to obtained. By using capillaries of 200 μm I.D., plate heights smaller than 10 μm were obtained in the work of Mikkers et al [23].

The most widely accepted initial demonstration of the power of CE was carried out by Jorgenson and Lukacs [24]. Their paper included a brief discussion of simple theory of dispersion in CE and provided the first demonstration of high separation efficiency with high field strength in narrow capillaries. Applications also include the separation of protein and peptides, tryptic mapping, DNA sequencing, serum analysis, analysis of neurotransmitters in single cells and chiral separations. The technique provides efficiencies up to two orders greater than high-performance liquid chromatography (HPLC). With the more and more sophisticated instruments commercially available since the beginning of 1990s, CE is now gaining popularity, not only as an alternative analytical tool for some routine analytical application, but also a promising technique in some modern field.

1.2.1 System and Mechanism

1.2.1.1 System setup
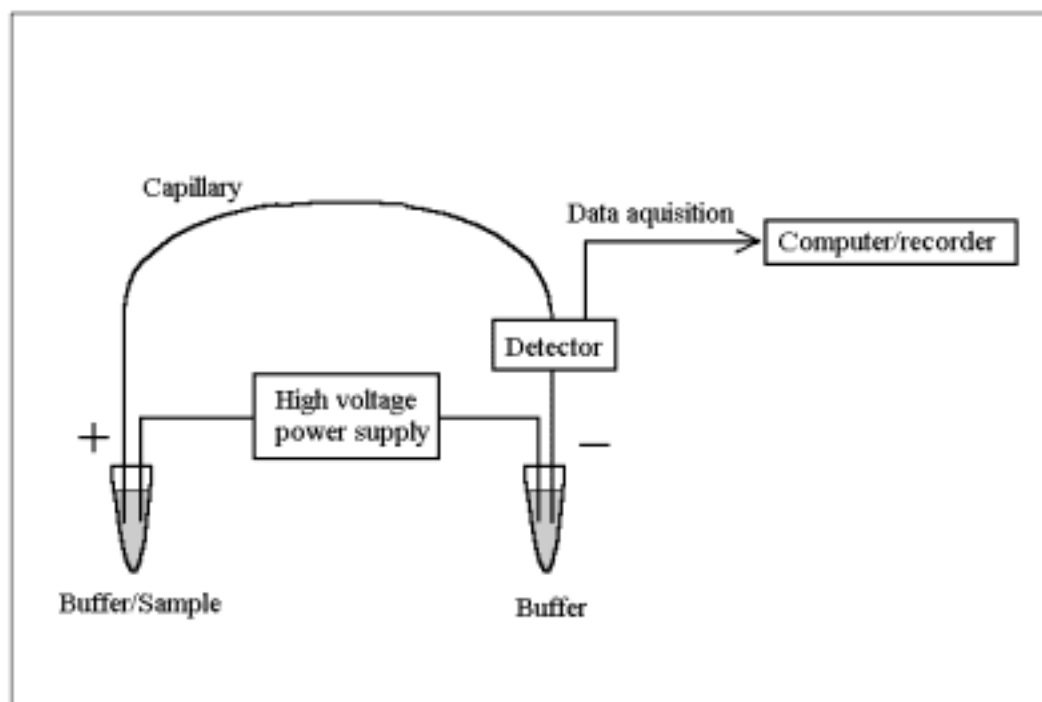
Fig. 1-2 Diagram of the essential components of a capillary electrophoresis system

A typical CE apparatus is shown in **Fig. 1-2**. It consists of a high-voltage power supply, two buffer reservoirs, a capillary and a detector. Separations are carried out in a capillary tube whose length differs in the range of 20 to 100 cm. The capillary is filled with running buffer and the sample is introduced by dipping one end into the sample and applying an electric field (electrokinetic injection) or by applying gas pressure (hydrodynamic injection) or by gravity. Migration through the capillary is driven by an electric field, and analytes are detected as they pass the window at the far end. The signal from the detector is usually sent to an integrator or recorder; but nowadays more and more computers are used in data acquisition, the electropherograms are saved digitally and the separation performance and quantification are evaluated by

professional software. Further, the computer-interfaced CE system can usually be operated under automated mode, which is helpful in improving reproducibility of the operation favoring its application in industrial analysis.

1.2.1.2 Capillary

The capillary is the crucial part of the CE system; they can be differentiated by dimensions, shapes and materials. The dimensions (length and radius) are important for the electric field and the heat dissipation as will be discussed. The capillary material is important for successful separation since it determines parameters such as magnitude and direction of EOF, heat dissipation and wall-analyte interaction. By far, fused silica has been the material of choice for its superior characteristics compared to other materials, including optical transparency across the UV and visible regions, high thermal conductance, mechanical stability when coated with polyimide and feasibility of manufacture with inner diameters down to a few microns.

Efforts were also made using polymeric materials as alternatives by many authors. Polymeric materials such as polyester (PE), polyurethane (PU), polypropylene (PP), polymethylmethacrylate (PMMA), ethylene vinylacetate (EVA) and others have been tested and used for CE separations [25-27]. Although the polymer hollow fibers also exhibit cathodic EOF as in fused silica capillaries, it is lower [25]. Because all polymer materials have their own physical and chemical properties, the quality of separations and selectivities may differ from one to another. But in general because their low heat conductivity, they are not good at dissipating heat and hence the separation voltage is lower compared to that across fused silica capillary, leading to long analysis time, low efficiency and even poor reproducibility. Other disadvantages of using these polymer

materials as separation capillary also include UV absorbance and hydrophobic interactions of the capillary with analytes which may cause significant adsorption problems. The advantage of using the polymer capillaries lies in the ease of preparing dynamic or permanent capillary coatings for a particular separation [27,28].

1.2.1.3 Migration of ions under electric field

Under the influence of an applied electric field, sample ions will move towards their appropriate electrode; cations move towards the cathode and anions towards the anode. When a particle moves in a solution, it also experiences a frictional retarding force that is proportional to its velocity and the solution viscosity. Its migration speed is such determined that the electric driving force is in magnitude equal to frictional retarding force. So the speed of their movement towards the electrode is governed by their size, charge state and the properties of the solution as well. Smaller molecules with a large number of charges will move more quickly than larger or less charged compounds. The electrophoretic mobility μ_{ep} is theoretically expressed as

$$\mu_{ep} = \frac{q}{6\pi\eta r} \tag{1-1}$$

where, q is the number of ionic charges, η is the solution viscosity and r the hydrodynamic radius.

The velocity of a particle is linked to its electrophoretic mobility by

$$v_{ep} = \mu_{ep} E = \mu_{ep} \frac{V}{L} \tag{1-2}$$

where, v_{ep} is the velocity; E is the electric field strength; V is the applied voltage, and L is the total capillary length. Eq (1-2) shows that the velocity is directly related to the magnitude of the strength of the applied electric field.

The time t taken by a solute to migrate through a capillary of length l is:

$$t = \frac{l}{v_{app}} = \frac{l}{\mu_{app}E} = \frac{Ll}{\mu_{app}V} \tag{1-3}$$

For the components of different mobilities, their migration time will be different and thus they are physically separated. Please note that in eq (1-3), the velocity and the mobility of the particle are expressed as v_{app} and μ_{app} (apparent mobility) respectively. This term also includes the movement arising from the electroosmotic flow (EOF) of the bulk electrolyte. This is because when an electric field is applied across a capillary, electroosmotic flow moving longitudinally is usually generated (which will be discussed later); separation of the analytes depends upon their apparent mobilities. Under some operational modes such as micellar electrokinetic chromatography (MEKC), the neutral analytes migrate in the presence of EOF with different velocities according to their individual partition coefficients between the pseudo-stationary phase and the aqueous buffer; a similar situation applies to the migration under capillary electrochromatography mode (CEC) while under capillary gel electrophoresis (CGE) mode, the mobility of the macromolecules are determined by their sizes, not solely by the charge-to-size ratios. In CGE, migration velocities decrease with molecular size in the presence of the sieving matrices, although electrophoretic mobilities generally increase with size (up to 400 bp for DNA). Even under capillary zone electrophoresis (CZE) mode, the mobilities of the analytes may be influenced by complexing reagents,

buffer pH and ion-pair effects. While the electrophoretic mobilities are useful in qualitative evaluation and explanation of the phenomena, the apparent mobilities are useful in quantitative prediction for separation.

1.2.1.4 Electrolyte system

The electrolyte system is also called the electrophoretic media, background electrolytes, or carrier electrolytes. It plays key important role in CE because it provides the chemical environments that solutes migrate in. The functions of buffers, includes supplying a medium for maintaining a small electric current between the anode and the cathode and to provide a medium that resists changes in pH. The properties of the electrolyte system influence the EOF, electrophoretic mobilities of analytes and analyte-wall interactions. A suitable electrolyte system must ensure the correct electrophoretic behavior of all individual solutes, the overall stability of the system and satisfactory separation of the analytes. The following are the factors relating to the buffer properties:

The types and the concentrations of the anions or cations in the buffer may affect the mobilities of the analytes and the properties of the capillary surface hence the EOF rate. Also, buffer influences the current produced and amount of Joule heat generated. For example, using of potassium or chloride ions in buffer may lead to high current.

Buffer pH is one of the key parameters for optimizing selectivity in separation. It affects the ionic state of the silanols on capillary surface thus EOF and thereby analysis speed and resolution. The ionic equilibrium states of the analytes are also influenced by buffer pH, so changes in pH may cause changes in effective mobilities of the analytes (weak acids or bases) and even their migration orders: the merged peaks under one pH can be

separated under another. Effective buffer systems have a range of approximately two pH units centered on the pKa value of the acid/base conjugate pair.

Modifiers are a group of chemicals affecting electrophoretic parameters; they are usually added to enhance the CE separation [29]. Their functions include improving analyte solubility, manipulating or suppressing EOF; preventing adsorption of analytes and improving reproducibility and peak shape, etc.

1.2.1.5 Detection

Detection is always an important issue in almost all analytical separation methods because it provides information for qualifying and /or quantifying analytes. Sensitive, selective and universal detectors are highly demanded for CE. A general challenge encountered in CE detection techniques is to maximize sensitivity without a losing or reducing separation efficiencies. Probably all the detectors now used in CE were adapted or modified from those previously used in HPLC. Detectors in CE include mainly those based on ultraviolet-visible (UV-Vis) absorbance, fluorescence absorbance, electrochemistry and mass spectrometry. Indirect detection is applicable to optical and some of the electrochemical (such as potential gradient) detection methods.

1.2.1.5.1 UV-Vis detection

UV-Vis is to date the most widely used detection technique in CE because it is easy to operate and widely available. The principle of UV-Vis detection in CE is determined by Lambert-Beer's law under certain assumptions. UV detection is performed on-column for high efficiency and convenience in operation; but this leads to lower sensitivity

compared to that in HPLC because of the very short optical path length which is approximately the inner diameter of the capillary. There is always a trade-off between the use of low cell volumes (small-diameter capillary) for high separation performance and the use of larger diameter for high sensitivity.

1.2.1.5.2 Fluorescence detection

Fluorescence detectors, using either an arc lamp or a laser as the excitation source, are also increasingly used in CE. The fluorescence detector adopting low cost and widely available incoherent light sources, can provide sensitivity 1-2 orders higher than the UV absorbance detector [30]. In 1985, Gassmann and co-workers published their pioneering work on complying laser induced fluorescence (LIF) detection with CE [31]. Compared with the previously used fluorescence detector, the sensitivity of the LIF detector is further improved owing to the monochromaticity and coherent nature of the light sources, which can focus a large amount of light onto the detection window. Currently, LIF is the best choice as far as the detection sensitivity is concerned for on-column detection. Fluorescence detection has been used for quite a number of analytes, especially for those containing primary amines, such as amino acids, peptides, and it is now an important detection tool in DNA sequencing [32].

1.2.1.5.3 Electrochemical detection

Electrochemical detection, based on potentiometric measurement [33], conductivity measurement [34,35], or amperometric detection [36], can be coupled to CE either by on-column or off-column format. Compared to the limited light pass length encountered

in the optical detection method (in CE), the electrochemical detection method suffers little or no loss in detection sensitivity.

Both potentiometric and conductivity measuring methods are suitable for detecting ionic analytes; sensitivity of these detectors depends strongly on the composition and concentration of the electrophoretic media. Potentiometric detection is based on measuring the Nernst potential changes at the surface of an indicator electrode or across an ion-selective barrier [37]. Conductivity detection was reported by Mikkers et al in 1979 [23]. It is a universal, relatively simple method for detection of ionic species in solution. On-column conductivity detection was first reported by Zare and co-workers [38] by fixing platinum wires through diametrically opposed holes on a capillary tube.

Amperometric detection is based on electron transfer between the electroactive solutes and the surface of a solid electrode under the influence of a constant potential. Wallingford and Ewing first reported such a detection system in CE with a porous glass coupler to decouple the electrode from the separation voltage [39]. Since then, there have been several reports on further improvements and applications of this technique. It is particularly useful in detection of solutes easily oxidized or reduced and is potentially one of the most sensitive detection techniques for CE separations. The disadvantage of the amperometric detection is that it is only suitable to those compounds that are readily oxidized on the electrode. Development of indirect detection may expand its application range.

1.2.1.5.4 Indirect detection

In indirect detection method in CE, the detector response is a result of the absence of a detector-active component in the electrophoretic media owing to the charge displacement for maintaining electroneutrality in the presence of ionic analytes. This general approach applicable to UV-Vis [40], Fluorescence [41,42], and electrochemical [43] techniques. A comprehensive study of indirect detection methods has been given by Yeung [44].

Generally, the indirect detection method has the following advantages: 1) it is universal; it can be expanded to compounds which are detector-inactive; 2) quantitation may be easier with indirect direction for analytes sequencing if tedious chemical derivatization procedure used for the direct detection can be avoided.

During electrophoresis, the analyte physically displace a component which may be a chromophore, fluorophore or electroactive species. It is important that the mechanism for displacement is clear and unambiguous (e.g., the replaced species is the only co-ion in the buffer), and the operation conditions are amenable to optimization at low analyte concentration.

An important parameter used in indirect detection is the transfer ratio, TR, which is defined as the number of coions in the buffer displaced by an analyte. Another parameter is the dynamic reserve, DR, which is defined as the ratio of the background signal to the background noise. The limit of detection (C_{lim}) of the indirection method can be expressed as [44]

$$C_{\lim} = \frac{C_m}{DR \times TR} \qquad\qquad (1\text{-}4)$$

where, C_m is the concentration of the relevant co-ion detector-active species. In indirect detection, a large background is required hence there exists degraded DR value. Theoretical calculation and experimental demonstration has shown that the well-matched mobilities between the analytes and the detector-active species will provide low detection limit as well as well-shaped peaks that favor quantitative determination. The detection limit of indirect detection is high compared with the direct detection mode, but is still impressive.

1.2.1.5.5 Mass spectrometry

Mass spectrometry (MS) is a detection technique of high sensitivity, universality and specificity; it has the advantage of providing structural information for the analytes [45]. For the electropherograms obtained from unknown samples or samples containing complicated matrices or contaminants, identification problems can be solved by coupling CE with MS. The main difficulty of coupling CE with MS lies in the fact that the MS system operating under high vacuum and interfacing to CE can reduce hydrodynamic flow in the capillary. An interface is needed for transferring the analytes and electrolyte liquid from the capillary while vaporizing for MS analysis without thermal degradation.

Since the pioneering work of Olivares et al in 1987 [46], there have been rapid developments in CE-MS. MS operated in two ionization modes, electrospray ionization (ESI) [47,48] and fast atom bombardment (FAB) [49,50e] have been coupled to CE for

on-line analysis. While matrix-assisted laser desorption/ionization mass spectrometry (MALDI-MS) [51] is also commonly used CE off-line analysis because the operation conditions may be less complicated and the detector has high sensitivity and wide mass-detection range [52].

1.2.2 Operation Modes of CE

From its invention, the CE method has generated great interest and undergone rapid development. A number of operation modes have been developed by combining electrophoresis with other techniques such as chromatography, and more new modes are being added into this family. These modes can be performed with the standard CE system described above. In this section, some often used modes and those closely related to the research topic of this thesis are briefly discussed.

1.2.2.1 Capillary zone electrophoresis (CZE)

In CZE mode, a narrow band of sample is placed between two identical buffer solutions in a capillary and a voltage is applied across it. Charged solutes migrate at different rates in the potential field according to their charge-to-size ratios. Generally, components with high charge-to-size ratios will move fast. Separation of components is based on the difference of their mobilities in a uniform electrophoretic medium [24,53,54]. Selectivity may be manipulated by changing pH so as to vary equilibriums between various subspecies of analytes or by introducing additives to the buffer. Ideally, each substance will be eventually separated from the others and form separated "zones". To date, CZE has been applied in separating charged species ranging from small inorganic ions to macromolecules such as proteins.

1.2.2.2 Micellar electrokinetic chromatography (MEKC)

The main limitation of CZE is its inability to separate neutral compounds. In 1984, Terabe et al. [55] introduced a modified version of CZE in which surfactant-based micelles were included in the running buffer to provide a two-phase pseudo-chromatographic system for separating neutral and ionic compounds by making use of partition equilibria of solutes between aqueous buffer and the pseudo-stationary phase. Since then, there have been increasing numbers of papers on this topic [56,57]. The analytes include herbicides, pesticides, drugs and bioactive peptides, etc. The pseudo-phases used in MEKC include not only ionic surfactants, (e.g. sodium dodecyl sulfate (SDS), hexadecyltrimethylammonim chloride (CTAC)), but also neutral surfactants such as polyoxyethylene-t-octylphenol (Triton X-100). Other materials such as charged cyclodextrin, and polymer ions have also been employed [58].

1.2.2.3 Capillary gel electrophoresis (CGE)

The first work on CGE carried out in late 1980s [59,60] showed an opportunity for significant advances in the practice of separation science, and dramatic interests have since then been generated by the promise of the combination of separation ability of hydrophilic gels for biopolmers with the fast, quantitative, and microsample capabilities of CE. In CGE, separations are carried out in gel-filled columns. The gels contain pores which act as sieves and solutes are separated based on their charges as well as sizes. Solutes having very close molecular weights have been separated by the high efficiencies of this technique. Karger and co-workers [61] reported achievements of single-base separation of oligonucleotides within minutes. Drossman et al demonstrated

the utility of CGE in the fast sizing of DNA fragments [32]. Molecular-weight sizing of proteins has been accomplished in gels with buffer containing SDS. Recent developments were to use entangled polymer solutions which eliminates the problem of bubble formation in gel preparation and provides better run-to-run reproducibility with only slightly inferior separation efficiencies [62,63].

1.2.2.4 Capillary electrochromatography (CEC)

CEC combines the techniques of micropacked liquid chromatography and capillary electrophoresis. The capillary is packed with a chromatographic packing which can retain solutes by the normal distribution equilibria upon which chromatography depends. However, separation in CEC depends not only on partition of the solutes between mobile phase and stationary phase but also their different electrophoretic mobilities as well. CEC combines the simplicity of controlling retention and selectivity in HPLC by manipulation of mobile phase and stationary phase and high separation efficiency due to the flat electroosmotic profile in CE. The work of Knox and Grant [64] demonstrated the lower plate height in CEC than in HPLC. Furthermore, there is no column back pressure and longer columns than in HPLC can be used. Nowadays, CEC is applied in separating a wide range of materials including phenols, PAHs, amines, carbonyls, dyes, and even inorganic and small organic ions.

However, this technique also encounters some problems [65]. One is the difficulty in fabricating the frits holding the packing materials; another is the bubbles formed around the packing materials and the frits during electrophoresis, which would lead to unstable baseline or interruption of the current. Several solutions to the problem have been

developed of which the simplest is to bond the appropriate moiety to the capillary wall and utilize solute-bonded phase interactions in a manner similar to open-tubular GC [66,67]. This technique is termed as open-tubular capillary electrochromatography (OT-CEC) and has been study actively because of its simplicity in operation [68,69].

1.2.2.5 Capillary isoelectric focusing (CIEF)

Isoelectric focusing is achieved by the electrophoretic migration of ampholytes in a pH gradient [70]. Before Hjerten and co-workers [71,72] transferred it to CE for focusing protein in glass capillary, the technique had long been used in slab gel electrophoresis. Before separation, the anodic end of the capillary is placed into an acidic solution, and the cathodic end in a basic solution; hence a pH gradient will be formed through the capillary after a voltage is applied. During the separation the samples will migrate in the solution until they reach a region of pH (for protein, the isoelectric points or p*I* values) where they become electrically neutral and therefore stop migrating. Zones are consequently focused until a steady state condition is reached. After focusing, the zones can be driven to the detector either by a salt mobilization or the pressurized mobilization. The technique has advantages of good reproducibility, useful concentrating effect and high resolution.

1.2.2.6 Capillary isotachophoresis (CITP)

CITP is characterized by discontinuous buffer systems consisting of leading and terminating electrolytes, between which the samples migrate under electric field. Thus, it is different from other modes, such as CZE, which are operated in a uniform buffer. The procedure can be separated into two stages: during the separation stage, individual

components of the sample migrate at different velocities according to their electrophoretic mobilities, forming separated zones; during the isotachophoretic migration, the equilibrated zones are separated into individuals and migrate at the same velocity. The advantage of CITP is the concentrating effect for diluted samples.

1.2.3 Concepts related to CE

Quite a number of concepts in CE should be concerned during operation; these include EOF, the analyte-wall interaction, and mobilities of the analytes that have been discussed in section 1.2.1. There are several criteria for evaluating the separation performance, such as analysis time (which can be observed directly from electropherograms), resolution, efficiency, etc. Theoretically, there exist links among these factors, and understanding the relations behind these concepts is critical for optimization of the separation conditions.

The concepts described in this section are basic to CE and they are closely related to the work in the subsequent chapters. In fact, most of the equations and assumptions in this section are based on CZE; theory and concepts related to other operation modes, such as open tubular capillary electrochromatography (OTCEC), are regarded as specific cases which will be discussed in the individual chapters.

1.2.3.1 Electroosmotic flow (EOF)

When dealing with CE we have to consider EOF. It has a significant impact on analysis time and resolution, two important criteria in separation.

The EOF is the bulk flow of solvent in the capillary under an applied electric field. As shown in **Fig. 1-3**, the silanol groups (Si-OH) on surface of the fused silica capillary. In buffer of pH higher than 2.5 the silanols dissociate; the negative charges attract cations from the buffer and this layer of positive charges forms the double layer, which would creates a potential difference very close to the wall (zeta potential, ζ). According to Stern's model [73], a rigid double layer of adsorbed ions (Stern layer) is in equilibrium with an outer diffuse layer (Debye-Huckel or Gouy Chapman layer). The cationic electric double layer extends into the diffuse layer which is mobile. When a voltage is applied across the capillary, the mobile cations in the diffuse layer migrate toward the cathode, causing the bulk solvent to migrate in the same direction.
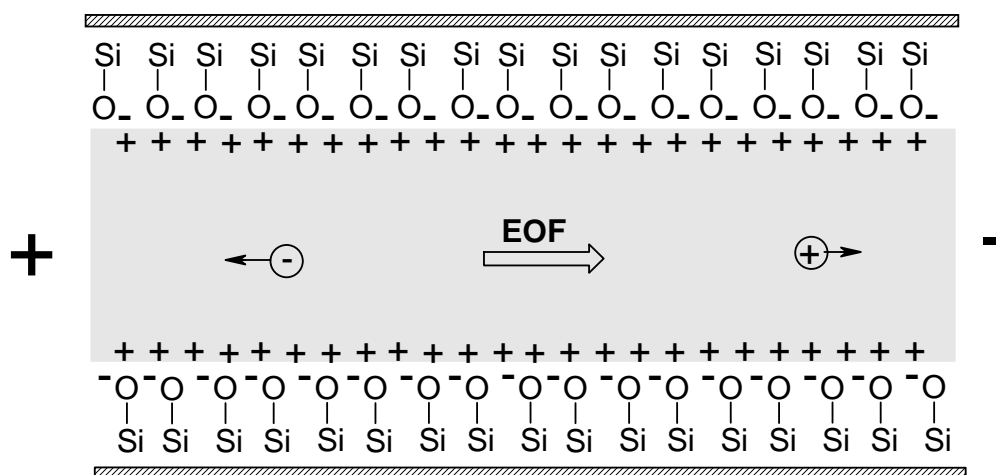
Fig. 1-3 Schematic representation of migration direction of anion, cation and EOF in a fused silica capillary

The magnitude of the EOF depends on the surface concentration of silanol groups and on their degree of dissociation. The latter increases with increasing pH of the background electrolyte (BGE). The magnitude of EOF is given by eq (1-5)

$$\mu_{eo} = \frac{\varepsilon\zeta}{4\pi\eta} \qquad\qquad (1\text{-}5)$$

where, μ_{eo} is the EOF rate, η is buffer viscosity and ζ is zeta potential.

The velocity of the electroosmotic flow, v_{eo}, can be calculated similarly from eq (1-2). The EOF rate is highly dependent upon electrolyte pH as the zeta potential is largely governed by the ionization of the acidic silanol on the capillary wall. Below pH 4, the ionization is small and the EOF flow rate is therefore not significant; above pH 8, the silanols are fully ionized and EOF is high.

The EOF is generated by the entire length of the capillary and thus produces constant flow rate along the capillary. This means the flow profile of EOF is plug-like (**Fig. 1-4**) and the solutes are being swept along the capillary at the same rate, which minimizes sample dispersion. This is an advantage of CE over HPLC where hydrodynamic pumping produces laminar flow (**Fig. 1-4**). In laminar flow, the solution is pushed from one end of the column and the solution at the edges of the column is moving slower than that in the middle, which results in a distribution of velocities across the column. Therefore, laminar flow broadens the peaks more than the plug-like flow as they travel along the column.

As expressed in eq (1-3), the overall migration time of a solute is related to both the mobility of the solute and EOF. The apparent mobility (μ_{app}) is measured from the migration time, and is the sum of both μ_{ep} and μ_{eo}. Reproducible migration time requires that the EOF should be controlled or even suppressed. But sometimes it is necessary.

EOF can be measured readily either by injection of a neutral solute such as acetone or dimethyl sulfoxide (DMSO) and measuring the time taken from the injection end to the detector, or using the method described by Vigh et al [74] for weak EOF.
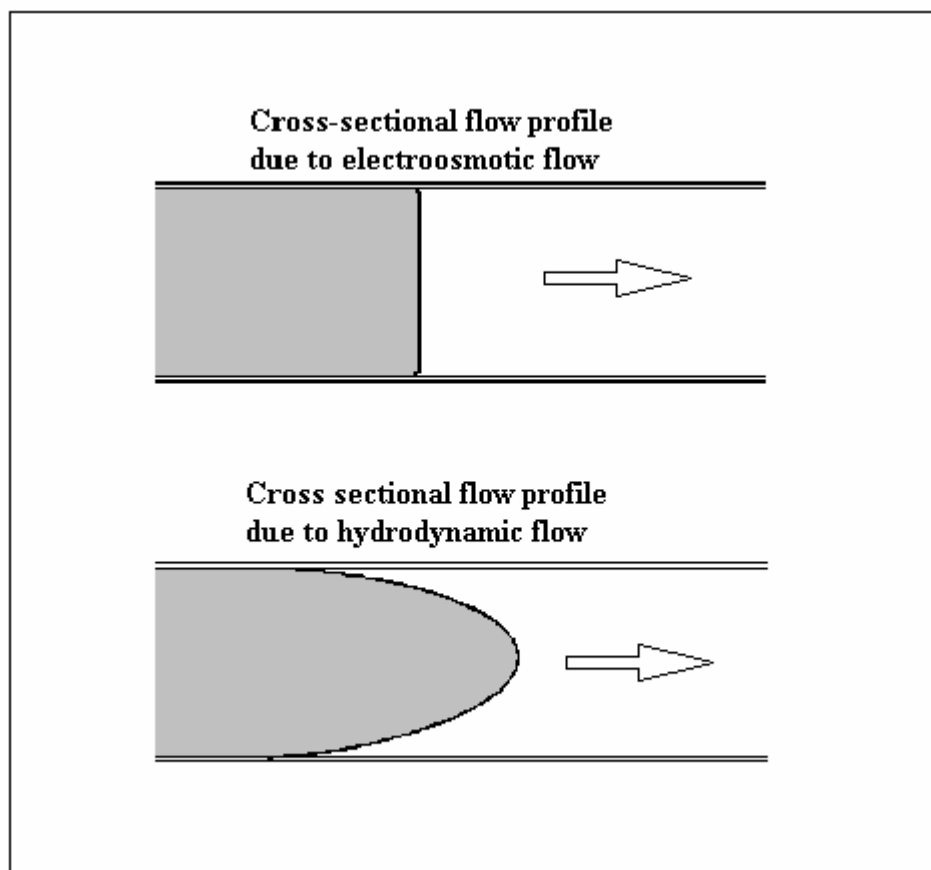
Fig. 1-4 Comparison of flow profiles of chromatography and CE

1.2.3.1.1 Control of EOF

It is desirable to manipulate the magnitude of EOF in order to optimize the separation performance under some circumstances. As can be implied from eq (1-5), change of the following parameters can vary EOF.

26

Buffer concentration

Increasing the buffer concentration will serve to reduce the double layer thickness, leading to the decreased EOF. Fujiwara and Honda [75] reported in detail the effect of NaCl concentration on the intensity of EOF.

Organic solvents

Introduction of organic solvents reduce the permittivity (ε) of the buffer [76] while increasing the viscosity and hence reduce the EOF according to eq (1-5). It was also reported [77] that addition of organic solvents would dramatically lower EOF and zeta potential by shifting the pk values of the silanols to higher pH ranges.

Cations

Cationic ions adsorbed onto the silica surface partially neutralize the deprotonated silanols and hence reduce the surface charge density. In the work of Atamna et al [78] and Issaq et al [79], 0.1 M each of the alkali metal acetates was used as buffer and the correlations between EOF and the crystal radius was investigated. It was found that the larger the crystal radius, the higher the effect of the cation in quenching EOF. Another approach was to add alkylamines into the background electrolyte. Cohen and Grushka [80] hypothesized that the amines changes EOF by shielding the wall from impurities in the buffer that otherwise might be adsorbed onto it and by changing the nature of the double layer. Meanwhile other long-chain amines were tested for feasibility in varying EOF. In 1986, Altria and Simpson [81] used cetyltrimethylammonium to reduce the magnitude of EOF; other salts such as tetradecyltrimethylammoniun bromide, and benzylthiouronium chloride have also been employed [82-84]. Recently, the

dialkylimidazolium based ionic-liquids (ILs) were investigated as background electrolytes by some authors [85,86], it was found that in acetonitrile, 2% 1-butyl-3-methylimidazolium can reverse EOF by adsorption onto the silica wall; while reversed EOF was observed in the presence of ca. 50 mM 1-ethyl-3methylimidazolium in water matrix buffer.

Chemical modification

Jorgenson and Lukas [87] treated the capillary with trimethylchlorosilane to reduce the number of the ionizable silanols on the capillary surface; Hjerten [88] modified the surface by first introducing a bifunctional compound, (γ-methacryloxypropyl)-trimethoxysilane to produce a Si-O-Si covalent, attachment for a monomer for subsequent polymerization.

Polymers

Addition a polymer which adsorbs onto the capillary wall to the buffer greatly increase the effective viscosity of the buffer near the capillary-buffer interface and hence effectively reduces the magnitude of EOF. Herrin and co-workers [89] reported the influence of different noncovalently bond polymers for this purpose.

1.2.3.2 Separation efficiency and the influence factors

1.2.3.2.1 Theoretical plate number

The plate number N is often used in assessing separation efficiency. The theoretical plate number is determined by

$$N = \frac{l}{\sigma_T{}^2} \qquad\qquad (1\text{-}6)$$

where l is the distance migrated by a zone and $\sigma_T{}^2$ is the total spatial variance of the concentration profile of the zone (band broadening) caused during the migration.

1.2.3.2.2 Band broadening

Band broadening is encountered in all separations and thus has been actively studied both theoretically and experimentally. The band is the volume of buffer in the capillary that the analytes are localized. All analyte bands broaden during the separation process, leading to a decrease in both detection sensitivity and peak resolution.

One of the main advantages of CZE over conventional chromatography is that it minimizes or eliminates most sources of band broadening that occur in the later; indeed, broadening is 6-10 times higher in chromatographic systems. That does not mean we can neglect this effect during operation; careless in buffer design or operation will result in high band broadening.

A number of dispersive factors contribute to the spreading of the sample zone. Band broadening is usually expressed as variance σ^2. The total variance σ_t^2 is the sum of individual variances due to different sources of dispersion:

$$\sigma_t^2 = \sigma_D{}^2 + \sigma_E{}^2 + \sigma_J{}^2 + \sigma_A{}^2 + \sigma_I{}^2 + \sigma_W{}^2 + \sigma_O{}^2 \qquad\qquad (1\text{-}7)$$

where $\sigma_D{}^2$ represents the variance due to longitudinal diffusion (molecular diffusion); $\sigma_E{}^2$ the variance due to electrodispersion; $\sigma_J{}^2$ the variance due to Joule heating; $\sigma_A{}^2$ the variance due to wall adsorption; $\sigma_I{}^2$ the variance due to injection overloading; $\sigma_W{}^2$ the variance due to the width of the detection zone and $\sigma_O{}^2$ the variance due to other effects.

Longitudinal diffusion

Longitudinal diffusion is one of the main factors contributing to the zone dispersion in CE. The initial sharp sample plug broadens through diffusion during migration through the capillary. The degree of diffusion depends on the difference between the concentrations of the sample zone and the background electrolyte (BGE) and on the diffusion coefficients of the analytes. For a particle in solution, its diffusion coefficient can be defined by Fick's law as

$$D = \frac{kT}{6\pi\eta r} \tag{1-8}$$

where k is a constant; T is the temperature, r is the hydrodynamic radius of the molecule, and η the viscosity of the solution.

The Einstein equation for diffusion in liquids is written as:

$$\sigma_D{}^2 = 2Dt \tag{1-9}$$

where, t is the migration time. As a consequence of eq. (1-8), the diffusion is low for large molecules such as proteins that have small diffusion coefficients. Therefore, it is possible to obtain theoretical plates (N) of several million for these macromolecules. Because diffusion is dependent directly on temperature and inversely on viscosity,

lowering the temperature of the buffer will reduces diffusion and consequently, band broadening.

Electrodispersion

Electrodispersion is caused by the conductivity differences between the sample zone and the BGE that lead to different mobilities between these two zones. If the sample has a higher mobility than the BGE, the front edge of the sample zone, which diffuses in the direction of migration, encounters a higher voltage drop on entering the buffer zone. This causes the diffusion sample to accelerate away from the solute zone, which results in zone fronting. When the solute at the trailing edge diffuses into the BGE it also encounters an increase in voltage drop but in the direction of the migration which accelerates the analytes back into the sample zone, keeping the trailing edge sharp (**Fig. 1-5**). When the sample zone has lower conductivity than the BGE the opposite effect is obtained. Neutral species are unaffected by this conductivity differences.
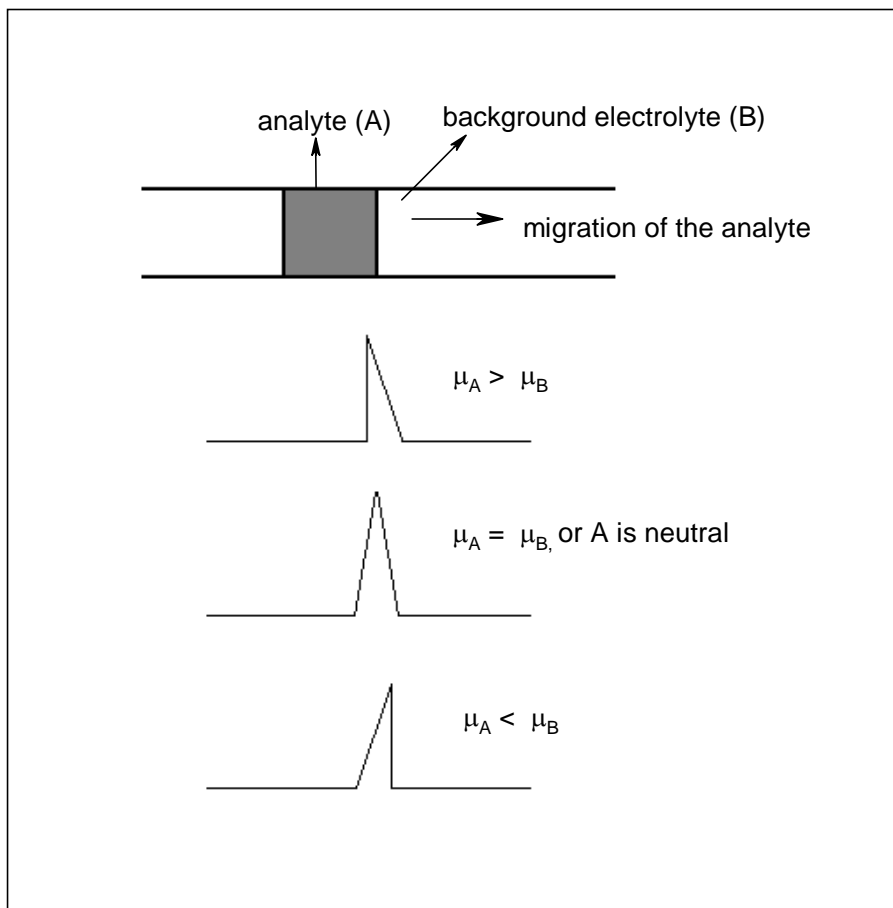
Fig. 1-5 Schematic illustration showing the mechanism of band broadening due to electrical conductivity differences between the sample zone and the running buffer.
μ_A and μ_B in the figure represent the mobilities of the analyte and the background co-ion, respectively.

Hjerten [90] has derived a simple approximate expression to describe conductivity-induced band broadening:

$$\sigma_E^2 = \frac{(\mu_{app}Et)^2}{16}\left(\frac{\Delta\lambda_e}{\lambda_e}\right)^2 \qquad (1\text{-}10)$$

where, μ_{app} is the apparent mobility of the analyte in the buffer, E is the electric field strength, t is the migration time, $\Delta\lambda_e$ is the conductivity difference between the BGE and the migrating zone, and λ_e is the conductivity of the buffer. Thus, one should make $\Delta\lambda_e$ as small as possible to lower the electrodispersion. The $\Delta\lambda_e$ can be expressed as

$$\Delta\lambda_e = \frac{zCF}{\mu_A}(\mu_A - \mu_{count})(\mu_{co} - \mu_A) \tag{1-11}$$

where *z* is the valence of the sample ion, *C* is the molar concentration of the sample, *F* is Faraday's constant, and μ_A, μ_{count}, and μ_{co} are the mobilities of the sample ion, counterion and coion, respectively.

Heat dissipation

Joule heat is the major factor limiting the analysis speed, efficiency and resolution in CE. It is inevitably generated as result of the electric current passing through the electrolyte solution, and the amount of heat generated would be quite significant if very high voltage is applied through a BGE of high ionic strength. Moreover, the heating also leads to a radial temperature gradient because the heat is better dissipated near the wall than in the center. Joule heating and the temperature gradient generated therefore can adversely affect the quality of the separation in a number of ways [91]. First, temperature gradients can cause density gradients in the buffer which will lead to convection. Secondly, an increase in temperature will cause a decrease in viscosity and hence an increase in electrophoretic mobility. Thus, the ions in the center of the capillary will move fast than those closer to the wall, resulting in deformation of migrating zones which contributes to band broadening and peak distortion. Furthermore, viscosity changes affect the EOF and may result in parabolic flow profiles and consequently a decrease in peak efficiency. In addition, if the temperature of the buffer becomes too high, thermal decomposition of the analytes may occur. The poor dissipation of Joule heating may also cause poor reproducibility of migration time and peak areas.

On-capillary detection

The length of the detector window (l_{det}) and the time constant of the detector can contribute to peak dispersion. For practical purposes, the contribution of detection to peak variance is defined as [57]:

$$\sigma_W^2 = \frac{l_{det}^2}{12} \tag{1-12}$$

For the high theoretical plates, the maximum allowable detector length is [92]

$$l_{det} = \frac{0.4L}{\sqrt{N}} \tag{1-13}$$

where L is the total length of the capillary and N is the theoretical plate number.

Wall adsorption of the analytes

The tendency of the capillary wall to adsorb solute species is mainly due to the electrostatic charge of the silica surface; other factors include hydrophobic interaction and hydrogen bonding. The interaction of analytes with the capillary wall has a negative influence on the overall efficiency of a CE separation. Even very small degrees of interaction can dramatically increase the variance. Martin et al. [93] developed an expression relating variance to the degree of solute-wall interaction:

$$\sigma_A^2 = \frac{C_M r^2 v}{D} t \tag{1-14}$$

where v is the velocity of the solute moving through the capillary; C_M is the constant determined by eq (1-15)

$$C_M = \frac{4 + (4n+16)k' + (n^2 + 10n + 20)k'^2}{4(n+2)(n+4)(1+k')^2} \tag{1-15}$$

In the above equation, *k'* is the solute capacity factor and *n=r/k* +3/2 in which *k* is the thickness of the electrical double layer adjacent to the wall.

They proposed that under ideal CE conditions (i.e., no solute-wall interaction (*k'*=0)), the theoretical plate height of a 50 cm long, 50 μm I.D. capillary under 36300V/cm was estimated to be 3.34×10^{-11} m (corresponding to $\sigma = 1.67 \times 10^{-11}$ m^2). Thus, pure electroosmosis does not significantly contribute to band broadening. But the finite value of *k'* has a dramatic impact on the peak height.

Generally, the solute-wall interactions can be alleviated by 1) operating at pH values where the silanol group are uncharged; 2) using high ionic strength BGE to reduce the effective charge of the surface; 3) using zwitterionic salts or other additives competing with the analytes for the charged sites of the silica surface; 4) modifying the silica surface.

Injection and related broadening

CE is a microanalytical technique and the injection of sample in CE can have dramatic effects on the performance. Principally, introducing a great volume of sample can enhance detection sensitivity. However, the large volume usually negatively influences the number of theoretical plates, resolution, reproducibility and reliability of the results. Investigations [57,94,95] suggest that it is the length of the sample plug rather than the volume that influences performance parameters. If the injection plug is longer than the dispersion caused by diffusion, the efficiency and resolution can be diminished. The

contribution of the sample injection to the total peak dispersion can be expressed as [96]:

$$\sigma_I^2 = \frac{l_{inj}^2}{12}$$

(1-16)

where l_{inj} is the length of the injected plug. Practically, it is 1-2% of the total capillary length. However, specialized techniques such as sample stacking can

Generally samples are injected into capillaries by hydrodynamic injection or electrokinetic injection, or simply by gravity. For hydrodynamic injection and gravity, a pressure difference between injection and the detection ends is employed to drive sample into the capillary.

The sample plug length injected into the capillary can be calculated by Poiseuille's equation

$$l_{inj} = \frac{r^2 \Delta P}{8 \eta L} t$$

(1-17)

where ΔP is the pressure difference between the two ends of the capillary; r is the capillary inner radius; L is the total length of the capillary; η is the viscosity of the solution; t is the injection time. The variance due to hydrodynamic injection, derived form eq (1-16), can be expressed as:

$$\sigma_I^2 = \frac{r^6 \Delta P^2 t}{1536 L^2 \eta^2 D}$$

(1-18)

in the above equation, D is the diffusion coefficient of the analyte.

Under electrokinetic injection mode, a sample enters into the capillary by joint efforts of electrophoretic migration and electroosmotic flow under the influence of an electric field. The quantity Q of a component injected into the capillary can be represented by [97]

$$Q = \frac{C(\mu_{ep} + \mu_{eo})\pi r^2 V t}{L} \qquad (1-19)$$

where μ_{ep} and μ_{eo} are the electrophoretic mobility of the component and electroosmotic mobility, respectively; C is the concentration of the component in the sample solution; V is the applied voltage.

Eq (1-19) holds if the conductivity of the sample and the buffer in the capillary are equal. If this condition is not met, the following equation may be more precise:

$$Q = \frac{C(\mu_{ep} + \mu_{eo})\pi r^2 E \lambda_B t}{\lambda_S} \qquad (1-20)$$

where E is the field strength; λ_B and λ_S are the conductivities of buffer and sample solution, respectively. Eq (1-20) suggests that neutral analytes may be electrokinetically injected into the capillary when the EOF is directed toward the detector.

The variance caused by electrokinetic injection is determined by

$$\sigma_I^2 = \frac{r^6 E^6 \lambda_A^2 \Omega_T^2 (\mu_{ep} + \mu_{eo})^2 t}{1536 D \lambda_B^2} \qquad (1-21)$$

where, Ω_T is the temperature coefficient of electrophoretic mobility.

Other factors, such as siphoning caused by height difference between the ends of the electrophoresis capillary, also may contribute to the variance.

1.2.3.2.3 Resolution

In order to achieve complete separation of two components, the separation of the band centers of the two neighboring peaks must be increased so that they do not merge together. The resolution (*Rs*) between two peaks is defined by:

$$R_s = \frac{2 \times (t_2 - t_1)}{W_1 + W_2} \tag{1-22}$$

where, t_2 and t_1 are the migration times and W_1 and W_2 are the basal widths (in unit of time) of the peaks 1 and 2, respectively. If the peak widths W_1 and W_2 are very similar, the above equation reduces to Rs=Δt/W.
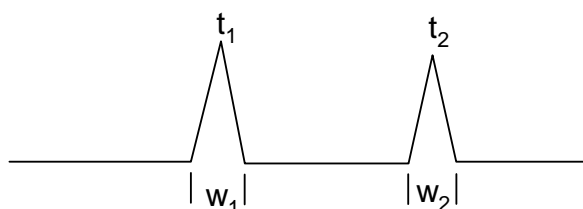
Fig. 1-6 Schematic representation of two peaks in electropherogram

Theoretically, resolution is affected by factors including peak efficiency and selectivity. The following equation describes resolution under CZE mode [98].

$$R = \frac{N^{1/2}}{4} \frac{\Delta\mu}{\bar{\mu} + \mu_{eo}} \tag{1-23}$$

in eq (1-23), $\dfrac{\Delta\mu}{\overline{\mu}+\mu_{eo}}$ is regarded as the selectivity of the two components, where

$\Delta\mu$ and $\overline{\mu}$ are the difference and average of the mobilities of the two components, respectively, and μ_{eo} is the magnitude of EOF.

1.3 Scope of study

The experiments in this thesis can be divided into two parts: synthesis (Chapter 2) and application (Chapter 3 to 6).

In Chapter 2, methods of synthesizing different ILs were described. Purity of the reagents used as buffer electrolyte in CE is important for good performance especially for the CE conducted using IL cations as background chromophores. A method for detecting by-products and precursors of ILs was developed; it was also applied to the real sample analysis and a reaction mechanism study. Also the mass spectrometric studies of the ILs were presented.

In Chapter 3, the 1-ethyl-3-methylimidazolium (EMIM) based ILs were tested as background chromophores for indirect detection of inorganic cations. The EMIM was also employed in determination of NH_4^+ in human urine.

Coating the internal capillary surface is one important approach in manipulating EOF, controlling analyte-wall interaction and therefore enhancing separation performance. In Chapter 4, IL was covalently bonded onto the silica capillary surface and the EOF was

reversed. The covalently modified silica capillaries were used for determination of sildenafil (SL) and its metabolite UK-103,320 (UK) in human serum; in another application, they were used in separation of ΦX174 DNA-Hae III digest fragments.

In Chapter 5, investigations were carried out to improve both resolution and detection sensitivity of 11 cations by using IL as both background electrolyte and coating material. Factors influencing separation and detection were studied.

ILs was used as additives in buffer in Chapter 6. The effect of ILs on migration time, selectivity was investigated.

References

[1] F.H. Hurley, T.P. Wier, J. Electrochem. Soc. 98 (1951) 203

[2] J.S. Wilkes, M.J. Zaworotko, J. Chem. Soc. Chem. Commum. (1992) 965

[3] P. Bonhote, A.P. Dias, N. Papageorgiou, K. Kalyanasundaram, M. Gratzed, Inorg. Chem. 35 (1996) 1168

[4] N. Papageorgiou, Y. Athanassov, M. Armand, P. Bonhote, H. Pettersson, A. Azam, M. Gratzel, J. Electrochem. Soc. 143 (1996) 3099

[5] K.R. Seddon, J. Chem. Techol. Biotechmol. 68 (1997) 351

[6] C.L. Hussey, Pure & Appl. Chem. 60 (1988) 1763

[7] Y. Chauvin, L. Mussmann, H. Olivier, Anew. Chem. Int. Ed. Eng. 34 (1995) 23

[8] H. Olivier, A. Hanlon, D. Fayne, P. Mccormac, Tetrahedron Lett. (1997) 3097

[9] H. Olivier, A. Hirschauer, French Pat. Appl. 96 1692 (1996) (To Institut Francais Du Petrole)

[10] Y. Chauvin, S. Einloft, H. Olivier, Ind. Eng. Chem. (1995) 1149.

[11] G. Wilke, B. Bogdanovic, P. Hart, O. Heimbach, W. Kroner, W. Oberkirch, K. Tanaka, E. Steinrucke, D. Walter, H. Aimmerman, Angew. Chem., Int. Ed. Eng. 5 (1996) 151

[12] K. Nomura, M. Ishino, M. Hazama, G. Suzukamo, J. Mol. Catal. A 126 (1997) L93

[13] G. Roberts, C.M. Lok, C. J. Adams, K.R. Seddon, M.E. Earle, J. Hamill, World Pat. Appl. 98/07680 (1998) (To Unichema Chemie)

[14] G. Roberts, C.M. Lok, C. J. Adams, K.R. Seddon, M.E. Earle, J. Hamill, World Pat. Appl. 98/07679 (1998) (To Unichema Chemie)

[15] Y. Chauvin, H. Olivier-Bourgigou, Chemtec 25(1995) 26

[16] J.G. Huddleston, H.D. Willauer, R.P. Swatloski, A.E. Visser, R. D. Rogers, Chem. Commun. (1998) 1765

[17] A. E. Visser, R. P. Swarloski and R.D. Rogers, Green Chemistry 2000, 1-4

[18] M. Vaher, M. Koel, M. Kaljurand, Chromatographia 53 (2001) S302

[19] M. Vaher, M. Koel, M. Kaljurand, Electrophoresis 23 (2002) 426

[20] E.G. Yanes, S.R. Gratz, M.J. Baldwin, S.E. Robison, A.M. Stalcup, Anal. Chem. 73 (2001) 3838

[21] J.W. Jorgenson, "Capillary Electrophoresis At Half A Million Volts", 25th International Symposium On Capillary Chromatography, Riva Del Garda, Italy, May 13-17, 2002

[22] S. Hjerten, Chromatogr. Rev. 9 (1967) 122

[23] F.E.P. Mikkers, F.M. Everacts, T.P.E.M. Verheggen, J. Chromatogr. 169 (1979) 11

[24] K.D. Lukacs, J.W. Jorgenson, Anal. Chem. 53 (1981) 1298

[25] P.Z. Liu, A. Malik, M.C.J. Kuchar, W.P. Vorkink, M.L. Lee, J. Microcol. Sep. 5 (1993) 245

[26] S. Chen, M.L. Lee, J. Microcol. Sep. 9 (1997) 57

[27] H. Bayer, H. Engelhardt, J. Microcol. Sep. 8 (1996) 479

[28] X. Ren, P.Z. Liu, M.L. Lee, J. Microcol Sep. 8 (1997) 529

[29] R. Kuhn, S. Hoffstetter-Kuln, Capillary Electrophoresis Principles and Practice, Springer-Verlag Berlin Heidelberg 1993

[30] J.S. Green, J.W. Jorgenson, J. Chromatogr. 352 (1986) 337

[31] E. Gassmann, J.E. Kuo, R.N. Zare, Science, 230 (1985) 813

[32] H. Drossmann, J.A. Luckey, A.J. Kostichka, J. D'cunha, L.M. Smith, Anal. Chem., 62 (1990) 900

[33] C. Haber, I. Silvstri, S. Roosli, W. Siman, Chimia 45 (1991) 117

[34] X. Huang, M.J. Gordon, R.N. Zare, J. Chromatogr. 425 (1998) 385

[35] X. Huang, M.J. Gordon, R.N. Zare, J. Chromatogr. 480 (1998) 285

[36] Y.F. Yik, H.K. Lee, S.F.Y. Li, S.B. Khoo, J. Chromatogr. 585 (1991) 139

[37] R. Virtanen, Acta Polytech. Scand. 123 (1974) 1

[38] X. Huang, T.K. Pang, M.J. Dordon, R.N. Zare, Anal. Chem. 59 (1987) 2747

[39] R.A. Willlingford, A.G. Ewing, Anal. Chem. 59 (1987) 1762

[40] S. Hjerten, K. Elenbring, F. Kilar, J.L. Liao, A.C.J. Chen, C.J. Siebert, M.D. Zhu, J. Chromatogr. 403 (1987) 47

[41] W.G. Kuhr, E.S. Yeung, Anal. Chem. 60 (1988) 1832

[42] W.G. Kuhr, E.S. Yeung, Anal. Chem. 60 (1988) 2642

[43] T.M. Olefirowicz, A.G. Ewing, J. Chromatogr. 499 (1990) 713

[44] E.S. Yeung, Acc. Chem. Res. 22 (1989) 125

[45] J.P. Landers (Ed.), Handbook of Capillary Electrophoresis, 2nd Ed. CRC Press, 1997, P. 791

[46] J.A. Olivares, N.T. Nguyen, C.R. Yonker, R.D. Smith, Anal. Chem. 59 (1987) 1230

[47] R.D. Smith, J.A. Olivares, N.T. Nguyen, H.R. Udseth, Anal. Chem. 60 (1988) 436

[48] R.D. Smith, H.R. Udseth, Nature, 331 (1988) 639

[49] R.M. Caprioli, W.T. Moore, M. Martin, B.B. Dague, J. Chromatogr. 480 (1989) 247

[50] S.M. Wolf, P. Vouros, C. Norwood, E. Jackim, J. Am. Soc. Mass Spectrum. 3 (1992) 757

[51] T. Keough, R. Takigiku, M.P. Lacey, M. Purdon, Anal. Chem. 64 (1992) 1594

[52] G. Ghoudhary, J. Chakel, W. Hancock, A. Toores-Duarte, G. Mcmahon, I. Wainer, Anal. Chem. 71 (1999) 855

[53] J.W. Jorgenson, K.D. Lukas, J. Chromatogr. 218 (1981) 209

[54] J.W. Jorgenson, K.D. Lukas, Clin. Chem. 27 (1981) 1551

[55] S. Terabe, K. Otsuka, K. Ichikawa, A. Tsuchiya, T. Ando, Anal. Chem. 56 (1984) 111

[56] S. Terabe, K. Otsuka, T. Ando, Anal. Chem. 57 (1985) 834

[57] S. Terabe, K. Otsuka, T. Ando, Anal. Chem. 61 (1989) 251

[58] N. Nishi, J. Chromatogr. A 780 (1997) 243

[59] A.S. Cohen, B.L. Karger, J. Chromatogr. 397 (1987) 409

[60] A.S. Cohen, A. Paulus, B.L. Karger, J. Chromatogr. 24 (1987) 15

[61] B.L. Karger, A.S. Cohen, US Patent 4,865,707

[62] M. Zhu, D.L. Hansen, S. Burd F. Gannon, J. Chromatogr. 480 (1989) 311

[63] R. Sonoda, H. Nishi, K. Noda, Chromatographia 48 (1998) 569

[64] J.H. Knox, I.H. Grant, Chromatographia 32(1991) 317

[65] C.Y. Liu, Electrophoresis, 22 (2001) 612

[66] V. Schurig, D. Schmalzing, M. Schleimer, Angew. Chem. Int. Ed. Engl. 30 (1991) 987

[67] C.Y. Liu, C.C. Hu, C.L. Yang, J. Chromatogr. A 773 (1997) 199

[68] S. Mayer, V. Schurig, J. High Resol. Chromatogr. 15 (1992) 129

[69] S. Mayer, V. Schurig, J. Liq. Chromatogr. 16 (1993) 915

[70] P.D. Grossman, J.C. Colburn, Capillary Electrophoresis: Theory and Practice, Academic Press, San Diego, 1992, Pp. 191

[71] S. Hjerten, J.L. Liao, K. Yao, 387 (1987) 127

[72] S. Hjerten, M.D. Zhu, J. Chromatogr. 346 (1985) 245

[73] O. Stern, Electrochem. 30 (1924) 508

[74] B.A. Williams, G. Vigh, Anal. Chem. 68 (1996) 1174

[75] S. Fujiwara, S. Honda, Anal. Chem. 58 (1986) 1811

[76] S. Fujiwara, S. Honda, Anal. Chem. 59 (1987) 487

[77] C. Schwer, E. Kenndler, Anal. Chem. 63 (1991) 1801

[78] I.Z. Atamna, H.J. Issaq, J. Chromatogr. 588 (1991) 315

[79] H.J. Issaq, I.Z. Atamna, G.M. Muschik, G.M. Janini, Chromatographia 32 (1991) 155

[80] N. Cohen, E. Grushka, J. Chromatogr. A 678 (1994) 167

[81] K. Altria, C. Simpson, Anal. Proc. 23 (1986) 453

[82] X. Huang, J.A. Luckey, M.J. Gordon, R.N. Zare, Anal. Chem. 61 (1989) 766

[83] H.H. Lauer, D. Mcmanigill, Anal. Chem. 587 (1986) 166

[84] K. Altria, C. Simpson, Chromatographia 24 (1987) 527

[85] M. Vaher, M. Koel, M. Kaljurand, Electrophoresis 23 (2002) 426

[86] E.G. Yanes, S.R. Gratz, M.J. Baldwin, S.E. Robison, A.M. Stalcup, Anal. Chem. 73 (2001) 3838

[87] J.W. Jorgenson, K.D. Lukacs, Science 222 (1983) 266

[88] S.Hjerten , J. Chromatogr. 347 (1985) 191

[89] B. Herrin, S. Shafer, J. Van Alstine, J. Haris, R. Snyder, J. Colloid Interfac. Sci. 115 (1987) 46

[90] S. Hejerten, Electrophoresis, 11 (1990) 665

[91] J. Knox, Chromatographia 26 (1988) 329

[92] X. Huang, W.F. Coleman, N. Zare, J. Chromatogr. 480 (1989) 95

[93] M. Martin, G. Guichon, Y. Walbroehl, J.W. Jorgenson, Anal. Chem. 57 (1985) 561

[94] N.A. Guzman, M.A. Trebilcock, J.P. Advis, J. Liq. Chromatogr. 14 (1991) 997

[95] X. Huang, W.F. Coleman, R.N. Zare, J Chromatogr. 504 (1990) 1

[96] K. Otsuka, S. Terabe, J. Chromatogr. 480 (1989) 91

[97] D.J. Rose, J.W. Jorgenson, Anal. Chem. 60 (1988) 642

[98] J.C. Giddings, Sep. Purify. Sci. 4 (1969) 181

CHAPTER 2 SYNTHESIS AND TEST OF IONIC LIQUIDS

The most often-studied ILs are those based on 1-alkyl-3-methylimidazolium. The halides, which can be synthesized readily with relatively high yield, are often the starting materials for the ILs of other anions (**Fig. 2-1**). A number of synthetic methods are frequently used and cited in the literature; the methods were employed or modified in the synthesis in the present work and were compared for the yields.
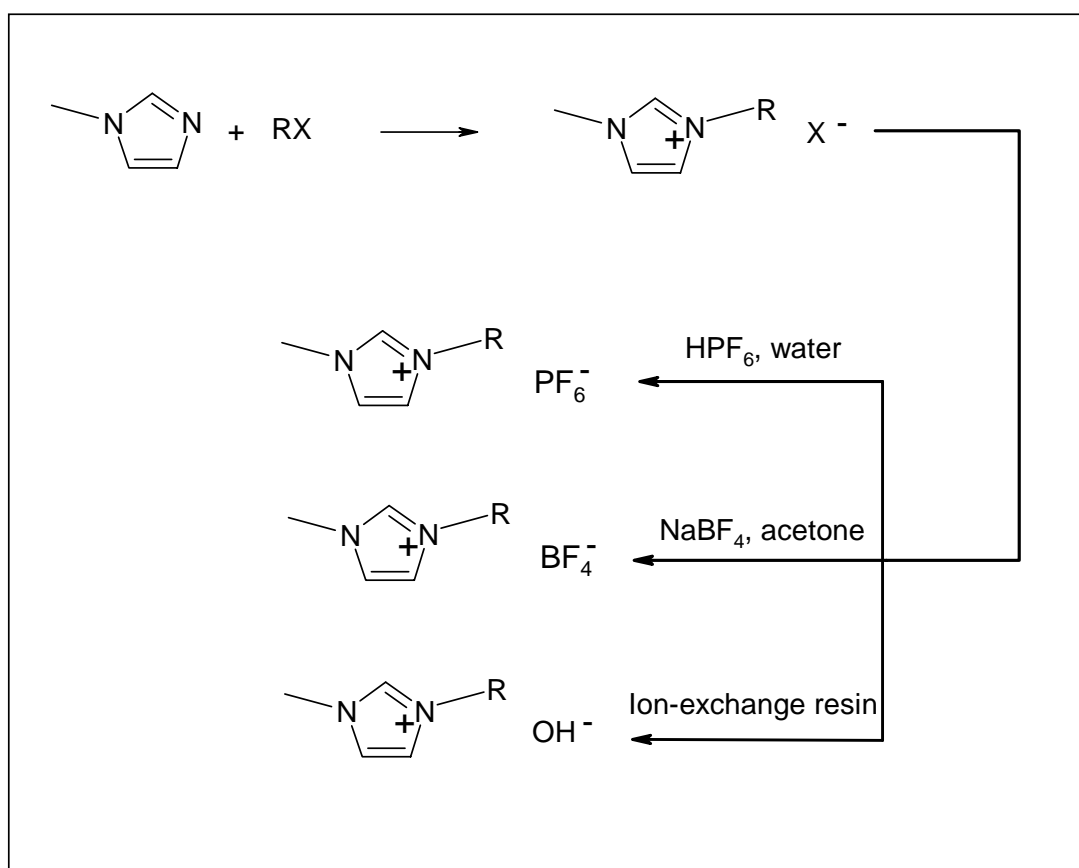
Fig. 2-1 Schematic representation of synthesis of ionic liquids

RX in **Fig. 2-1** is an alkyl halide, where, X=Cl, Br, or I. The ILs synthesized in this work are tabulated in Table 2-1. Because the 1-ethyl-3-methylimidazolium (EMIM) based ILs are commercially available, we will not discuss their synthesis here.

2.1 Chemicals

Sodium tetrafluoroborate, lithium tetrafluoroborate and imidazole were purchased from Fluka (Buchs, Switzerland). 1-ethyl-3-methylimidazolium chloride, 1-bromobutane, 1-bromohexane, 1-methylimidazole, 1,2-dimethylimidazole, 1-bromo-2-methylpropane, 70% hexafluorophosphoric acid (water solution), 1-chlorodecane and 4-bromo-1-butanol were products of Aldrich (Milwaukee, WI, USA). Triethylamine and dimethylsulfoxide (DMSO) were obtained from Merck (Darmsradt, Germany). The 2-ethylimidazole (purity $\geq$ 98%) was obtained from Acros Organics (NJ, USA). α-Cyclodextrin (α-CD) was purchased from Sigma (Louis, MO, USA). HPLC grade ethyl acetate was a product of J. T. Baker (Phillipsburg, NJ, USA).

2.2 Apparatus

Most of CE experiments in this thesis were carried out on the following instruments and hence they are described here. For the specific apparatus used, they will be described in the appropriate chapters.

Capillary: fused-silica capillaries of 50 (or 75 for mass spectrometer in Chapter 4) μm I.D. and 360 μm O.D. were purchased from Polymicro Technologies (Phoenix, AZ, USA).

High voltage supplier: A CE-L1 (CE Resources, Singapore, Republic of Singapore), a Prince CE System (Lauerlabs, Emmen, Netherlands) or a Spellman CZE 1000R (Plainview, NY, USA) power supply was used to apply high voltage across the capillary and inject sample.

UV-Vis detector: UV detection was carried out with a Linear Instrument UVIS 200 (Reno, NV, USA) or Perkin Elmer LC 290 (Wellesley, MA, USA) detector.

Data recording and processing: Electropherograms were recorded and evaluated with a CSW17 data acquisition system (DataApex, Prague, The Czech Republic) or with an HP 3394A integrator (Hewlett-Packard, Avondale, PA, USA).

CE-MS system: For CE-MS separation, a Finnigan LCQ ion trap instrument (San Jose, CA, USA) coupled with an electrospray ionization (ESI) source was connected to a capillary of 75 μm I.D. A Prince CE System was employed as the high-voltage supplier. The mass spectrometer was controlled, and the data from the instrument was recorded and evaluated, by the Xcalibur 1.0 software (Finnigan).

Apparatus for solution preparation: The ultrapure water in the experiments was prepared by a MILLI-Q system (Bedford, MA, USA). All solutions were filtered by 0.20 μm Millipore filters (Bedford, MA, USA) or 0.20 μm Minisart (Goettingen, Germany) filters.

2.3 Synthesis of ILs

2.3.1 1, 3-Dialkylimidazolium (DAIM) halides

There are numerous reported methods on the synthesis of this group of basic ILs, but we found that the reaction temperature, solvent, reaction time, crystallization procedure as well as the reactants themselves have influence on the yields. We tried the following reactions and measured their yields in order to obtain the optimal synthetic parameters. In each method, synthesis of one halide-IL was given as example and other halides were synthesized using the same parameters unless otherwise stated.

Method 2-1 The method was modified from the procedure described by Dzyuba and Bartsch [1]. A 250 ml two-neck round-bottomed flask with stirring bar was connected to a reflux condenser which was filled with cooling water while both the inlet and outlet of the condenser were blocked for convenience of the subsequent operations. 0.1 mol 1-methylimidazole and 0.1 mol alkyl halide were slowly added into the flask through a funnel. After addition, the funnel was replaced by a thermometer whose tip was below the surface of the liquid. The flask was then put into an oil bath and was slowly heated to 140 °C at which the exothermic reaction between 1-methylimidazole and alkyl halide occurred. Care was taken to avoid overheating of the mixture; when the reaction

temperature reached 150 °C the flask was taken out of the bath to cool and placed back into the bath again when the temperature was below 125 °C. After 10 minutes, the flask was taken out and allowed to cool to room temperature. After that it was put into the oil bath for another 10 minutes and the same procedures were applied to control the temperature of the mixture. The resulting viscous liquid was allowed to cool to room temperature and was washed three times with 5 ml portions of ethyl acetate. After the last washing, the remaining ethyl acetate was removed by heating and stirring the liquid at 80°C under vacuum.

Method 2-2 In this method, recrystallization was employed for the product. Before reaction, 1-methyllimidazole was distilled from calcium hydride and 1-chlororbutane was distilled from magnesium sulphate. To a round-bottomed flask, equal moles of 1-methylimidazole and chlorobutane were added. Dry nitrogen was introduced into the flask and the mixture was heated under reflux for 5 hours. The mixture was left to cool overnight and the resulting solid was dissolved in a small aliquot of acetonitrile and filtered in a fume hood subsequently. Dry ethyl acetate was added to the filtrate and the mixture was cooled to −10°C, the resulting precipitate was isolated by filtration and recrystallized from a minimum amount of ethyl acetate; the solid was then dried in vacuum for 10 hours.

Method 2-3 [2-5], 1-butyl-3-methylimidazolium chloride (BMIMCl) was prepared by adding equal amounts of 1-methylimidazole and chlorobutane to a round bottomed flask fitted with a reflux condenser; the mixture was kept at 70 °C for 48 hours. The resulting viscous liquid was allowed to cool to room temperature and then was washed three

times with 50 ml portions of ethyl acetate. After the last washing, the remaining ethyl acetate was removed by heating the liquid to 70°C under vacuum.

Method 2-4 [6] To a 3-liter three-neck round-bottomed flask with stirring bar, 50 g of distilled, dry 1-methylimidazole and 160 ml of distilled dry acetonitrile were added and a reflux condenser was then connected to the flask. When the temperature reached 70°C, chlorobutane of 3-fold amount of 1-methylimidazole was slowly added into the solution via funnel. When addition was completed, the funnel was replaced by a thermometer whose tip was below the surface of the liquid. The reaction was performed in a hood for 3 days and a slightly yellow liquid was obtained. The condenser was then removed and subsequently the flask was connected to a vacuum pump to evaporate the acetonitrile and excess chlorobutane. When the residual volume was about 100 ml, the solution was allowed to cool to room temperature and then the put into a refrigerator at 5°C. BMIMCl crystallized slowly from the cooled solution. After crystallization was complete, the supernatant was removed and replaced by 30 ml of dry acetonitrile. A colorless crystal was obtained from the recrystallization step. It was then collected and ground to powder in a nitrogen-atmosphere glove box, and dried under vacuum.

2.3.2 DAIM tetrafluoroborate

Method 2-5 [7] In this reaction, the tetrafluoroboric acid first reacts with silver oxide to produce silver tetrafluoroborate, which will then react with DAIM halide and results in DAIM tetrafluoroborate. 23.2 g solid Ag_2O (0.1mol) was stirred with 36.9 g 48% aqueous HBF_4 (0.2 mol) in 200 ml of water until the Ag_2O had reacted completely with HBF_4 giving a clear solution. 34.9 g BMIMCl (0.2 mol) dissolved in water was then

added to the solution. After 2 hour of stirring, the AgCl precipitate was filtered out, and the filtrate was concentrate with a rotor-evaporator. The resulting clear, colorless solution was dried overnight under vacuum at 70°C.

Method 2-6 [4] The reaction is based on immiscibility of sodium chloride in acetone so that it is separated from the product. To a 50 mmol BMIMCl acetone solution was added 50 mmol sodium tetrafluoroborate. After 24-hour stirring, the reaction mixture was filtered through a celite filter and the volatiles were removed under reduced pressure at 60°C.

2.3.3 DAIM hexafluorophosphate

Method 2-7 [2-5] Synthesis of DAIM hexafluorophosphate was conducted in water because it is water-immiscible. But according to our experiments, this kind of IL is slightly dissolved in water (ca. 50 mM for $EMIMPF_6$ and solubility decreases with increasing alkyl length), thus it is important to control the amount of water in order to obtain high yield. 0.02 mol BMIMCl was dissolved in 100 ml deionized water in a 250-ml plastic beaker. The solution was stirred with a magnetic stirrer. 6.0 ml hexafluorophosphoric acid (ca. 70%) was added in to the solution. Addition was made slowly to prevent the reaction temperature from rising too high. As the addition proceeds, two phases were formed: the $BMIMPF_6$ formed the lower phase and the upper phase was acidic. After stirring for 12 hours, the upper phase was decanted and repeated washings of the ionic liquid with small aliquots of water were carried out until the upper aqueous phase was no longer acidic. The ionic liquid was heated under vacuum at 70°C to remove water (optional).
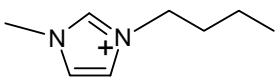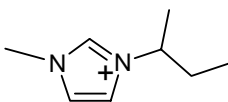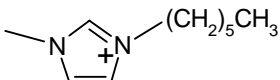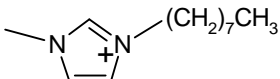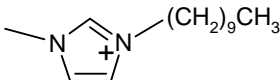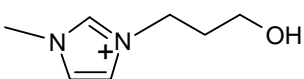
Method 2-8 [8] In a plastic beaker, a stirred solution of BMIMCl of 0.02 mol in 100 ml deionized water was cooled to 0°C in an ice-water bath, and hexafluorophosphoric acid was added slowly with rapid stirring. The resulting biphasic mixture was stirred for 2 hours, and then allowed to cool to room temperature. The (upper) aqueous phase was decanted; the ionic liquid phase was washed with 100 mM $NaHCO_3$ water solution and then extracted with dichloromethane. The organic phase was dried over $MgSO_4$ and filtered, the solvent was removed under reduced pressure and the ionic liquid was dried under vacuum at 70°C for 6 hours to produce colorless liquid.

2.3.4 DAIM hydroxide

Method 2-9 A column filled with Purolite A510 (Bala Cynwyd, PA, USA) anion ion-exchange resin was used during the preparation. The resin was activated by 4 N sodium hydroxide solution and rinsed with deionized water till the pH of the eluent was around 7. The EMIMCl solution was loaded and passed through the column at a flow rate of ca. 1ml/min. The eluent was collected at pH >13. The concentration of EMIM in the eluent was determined by CE with external standard method.

2.3.5 Comparison of the yields of the methods

Table 2-1 Comparison of the yields of DAIM based ILs

R	Structure of the cation	Abbrev. of cation	Anion	No.	Optimal Method and yield[a]
Butyl		BMIM	Cl^-	1	2-1 (86%)
			BF_4^-	2	2-5 (90%)
			PF_6^-	3	2-8 (79%)
			OH^-	4	97%
Isobutyl		*i*BMIM	Cl^-	5	2-1 (93%)
			BF_4^-	6	2-5 (82%)
			PF_6^-	7	2-8 (74%)
			OH^-	8	99%
Hexyl		HMIM	Cl^-	9	2-4 (90%)
			BF_4^-	10	2-5/6 (88%)
			PF_6^-	11	2-7/8 (82%)
			OH^-	12	98%
Octyl		OMIM	Cl^-	13	2-1 (94%)
			BF_4^-	14	2-6 (84%)
			PF_6^-	15	2-7 (82%)
			OH^-	16	100%
Decyl		DMIM	Cl^-	17	2-2 (91%)
			BF_4^-	18	2-6 (81%)
			PF_6^-	19	2-8 (86%)
			OH^-	20	95%
1-Hydroxy-Butyl		HBMIM	Cl^-	21	2-1 (87%)
			BF_4^-	22	2-5 (91%)
			PF_6^-	23	2-8 (76%)
			OH^-	24	99%

[a] for the ILs of hydroxide form (OH^-), only **Method 2-9** was employed. The corresponding data are the convert ratios based on the concentrations of the DAIM and halide impurities measured.

It was found that the chain length of alkyl halides affected its reactivity with 1-methylimidazole. From butyl to decyl, the longer the chain, the higher the reactivity. Cloudiness, indicating presence of IL, could be found after 20-minute heating of the mixture of decylchloride and 1-methylimidazole at 70°C, while for the yellowish 1-butyl-3-metylimidazolium, cloudiness did not appear until after ca. 4-hour reaction. Also alkyl bromide was found to have higher reactivity than chloride in most cases.

The yields of hexafluorophosphates are generally low mainly owing to considerable amount of water used both in synthesis and purification. For ***Method 2-7***, care should be taken not to use too much water during the washing procedures. Theoretically, ***Method 2-8*** may offer higher yield, but the organic solvent is harmful and the operation is complicated. If yield is not a crucial factor to be considered, ***Method 2-7*** is a better choice, especially in this work which does not require dry products.

High yields could be obtained with ***Method 2-5*** to convert bromides to tetrafluoroborates. For chlorides, ***Method 2-6*** is more suitable.

2.4 Mass spectrometry study of the ILs

The physical properties of the ILs such as melting point, density and viscosity are important parameters for their applications as electrolytes in solar batteries, solvents for chemical reaction and liquid-liquid extraction [9-11]. But in this study, the ILs will be dissolved in solvents as background electrolyte or additives, or be used as coating materials, so their physical properties may not significantly affect their performances in such applications and hence they will not be discussed in detail here. However,

understanding of the interactions between the IL-cation and IL-anion in solvents will be helpful in interpreting experimental phenomena and in experiment design.

Mass spectrometry (MS) is an important tool to obtain structural information of species in volatile solvents, and can also detect impurities in a mixture provided that the impurities are at significant levels that can be detected by the spectrometer. The aims of this experiment were to detect the impurities (mainly the residuals of the reactants) in the synthesized ILs. In order to obtain high specificity, selected reaction monitoring (SRM) mode was used for some fragments. Before SRM, full scan mode (under which the collision energy was set to zero) was first applied on the sample and operation parameters (infusion flow rate, capillary temperature and sheath gas pressure) were optimized to obtain the highest current for the mother fragments. During SRM, the collision energy (in this instrument, the energy is controlled by voltage applied between the capillary end the lens, and the percentage of the voltage) was optimized so that the intensity of the daughter fragments is significant. The synthesized ILs were analyzed by infusing their water-methanol (5:95, v/v) solution into the mass spectrometer with a syringe pump at a flow rate of 3 μl/min. The temperature of the capillary in the spectrometer was set to 260 °C. The sheath gas (N_2) pressure was at 50 arbitrary and the auxiliary gas pressure was set to zero. For the SRM mode, the voltage was in the range of 30 and 50 V, and the percentage was in the range of 10 to 25.

Table 2-2 m/z values of the analytes

Cation	m/z	Anion	m/z
BMIM	139.15	OH^-	17.01
EMIM	111.07	Cl^-	34.45
HMIM	167.17	Br^-	79.90
*i*BMIM	139.15	BF_4^-	86.80
DMIM	195.21	PF_6^-	145.18
HBMIM	157.13	TFMS	149.09

2.4.1 Monitoring the IL-cation

The most basic ILs synthesized are the halides, usually in chloride form which has a m/z of 34.5. Since the working m/z range of the mass spectrometer we used is 50-2000, it is reasonable to monitor the IL-cations, whose m/z are in the range of 100-200.

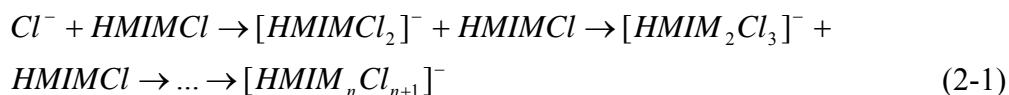The spectra of the cations show (for example in **Fig. 2-2**) no residual reactant 1-methylimidazole (the protonated quasi-molecule at m/z = 84 at positive ESI mode)

2.4.2 Association modes of the IL-cations and IL-anions in methanol

Positive and negative ESI modes were used to assess IL aggregation. More peaks were observed for negative ESI; these peaks were attributed to fragment aggregates.

Although methanol can be both as proton donor and acceptor [12], the ILs may not fully dissociate in it. As shown in **Fig. 2-3**, the cation and anion associate in the organic solvent under the operation conditions. For HMIMCl, the association of chloride with IL molecule by the following pattern:

$$Cl^- + HMIMCl \rightarrow [HMIMCl_2]^- + HMIMCl \rightarrow [HMIM_2Cl_3]^- +$$
$$HMIMCl \rightarrow ... \rightarrow [HMIM_nCl_{n+1}]^- \qquad\qquad (2\text{-}1)$$

It can be seen from **Fig. 2-3** that with the increasing collision energy, the association ability of anions with molecule decreases, especially for high-level aggregates (**Fig. 2-3**C). Under this situation, more IL molecules will be freed from the aggregations, and the concentration of the free IL-molecules in the organic solvent will increase hence the chance of cations associating with IL-molecules (with similar pattern as eq (2-1)) will be enhanced and the cationic aggregations can be detected (**Fig. 2-2**B and C). **Fig. 2-3** and **Fig. 2-4** show that in the presence of collision energy, the most stable negative aggregations are not the fragments consisting one anion and one IL molecule; in fact they are made up of one anion and two IL-molecules, i.e. $[(HMIM)_2Cl_3]^-$, $[(BMIM)_2Cl_3]^-$ and $[(BMIM)_2(PF_6)_3]^-$. However, association abilities of anions with IL-cations (or IL molecules) varied with ionization conditions. For example, BMIMCl and BMIMPF$_6$, **Fig. 2-4** shows that without collision, the high-level aggregation form of BMIMCl indicates higher abundance; when collision energy is applied, $[(BMIM)_2Cl_3]^-$ is the most abundant. But $[(BMIM)_2(PF_6)_3]^-$ shows the highest abundance both in the presence of and without the collision energy (**Fig. 2-4**A and B). The above experiments also suggest different ILs have different cation-anion association patterns in organic

solvent. As we know, the abundance of the fragments is related to the stability of that species.

More interesting results were obtained with EMIMCl. Under the positive ESI mode, the cationic aggregations can be observed (**Fig. 2-5**A and B), while under negative mode there is visually no significant fragment detected (the highest NL is 2.59×10^4 compared to 2.59×10^5 under the positive ESI mode). Moreover, the most stable fragment consists of one cation and one IL molecule ($[(EMIM)_2Cl]^+$); it appears even in the environment without collision energy applied.
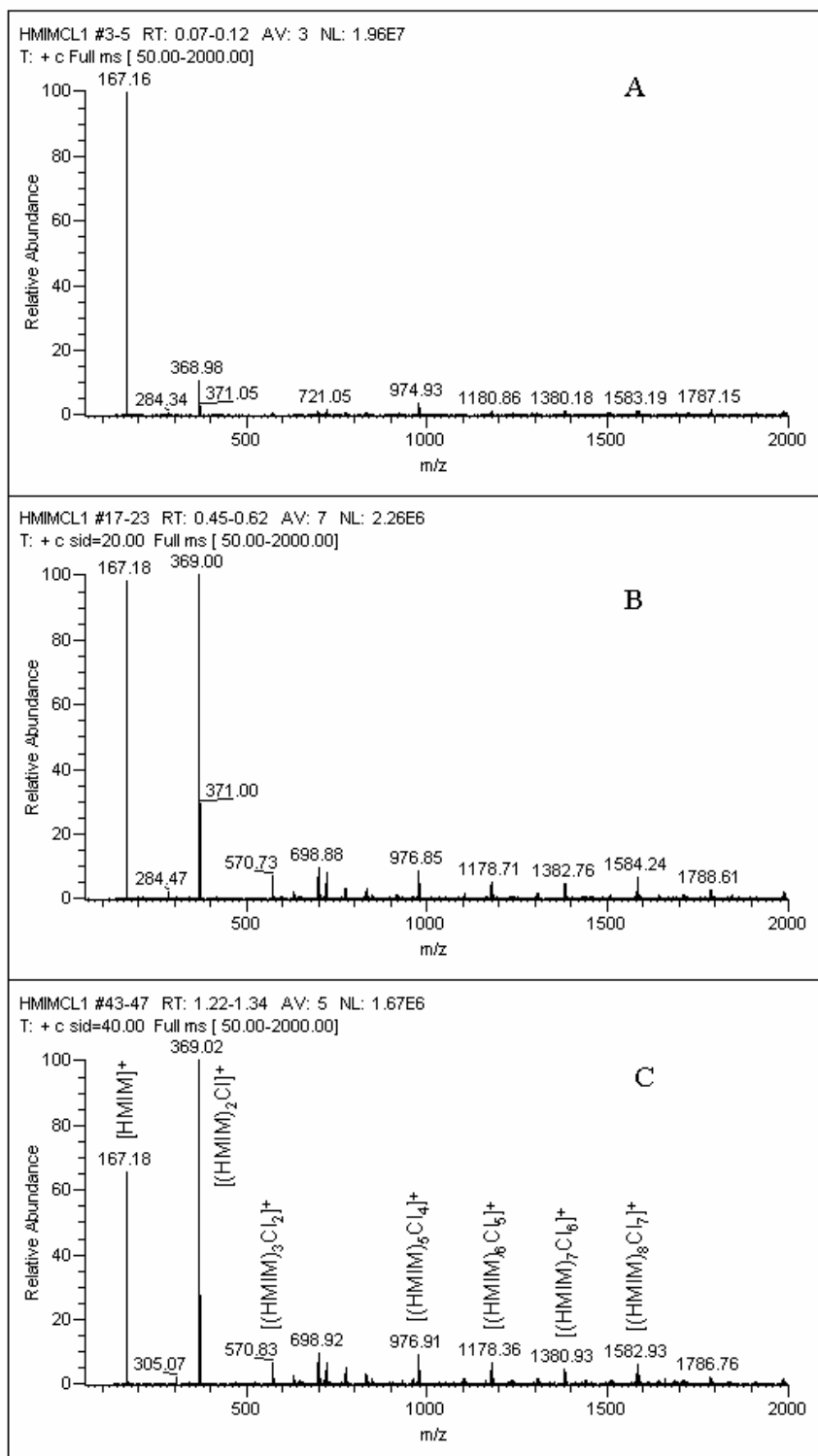
Fig. 2-2 Mass spectra of HMIMCl (positive ESI)
Experimental conditions: positive ESI mode, collision energy: A, 0V; B, 20 V; C, 40V
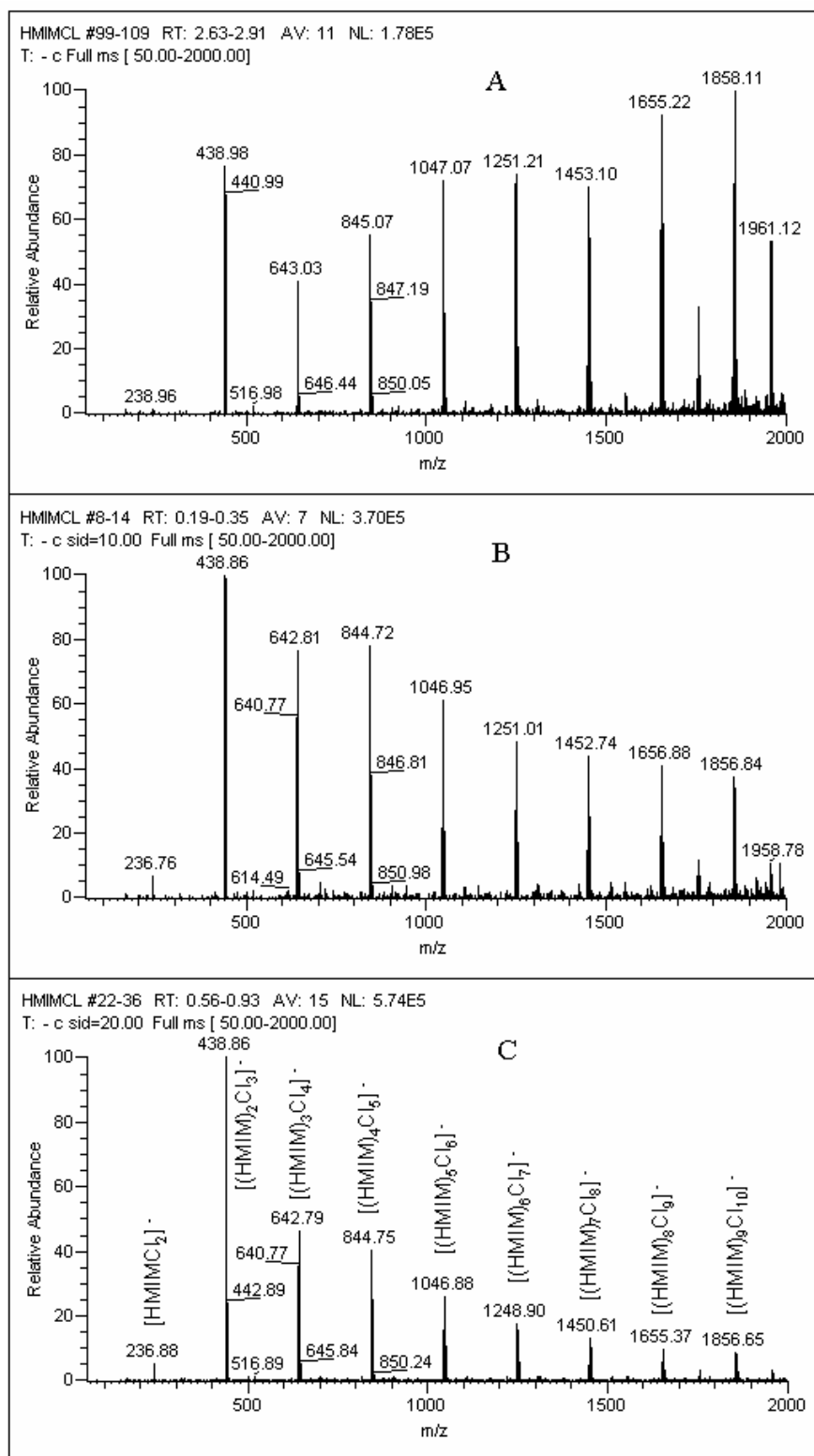
Fig. 2-3 Mass spectra of HMIMCl (negative ESI)
Experimental conditions: negative ESI mode, collision energy: A, 0V; B, 10 V; C, 20V
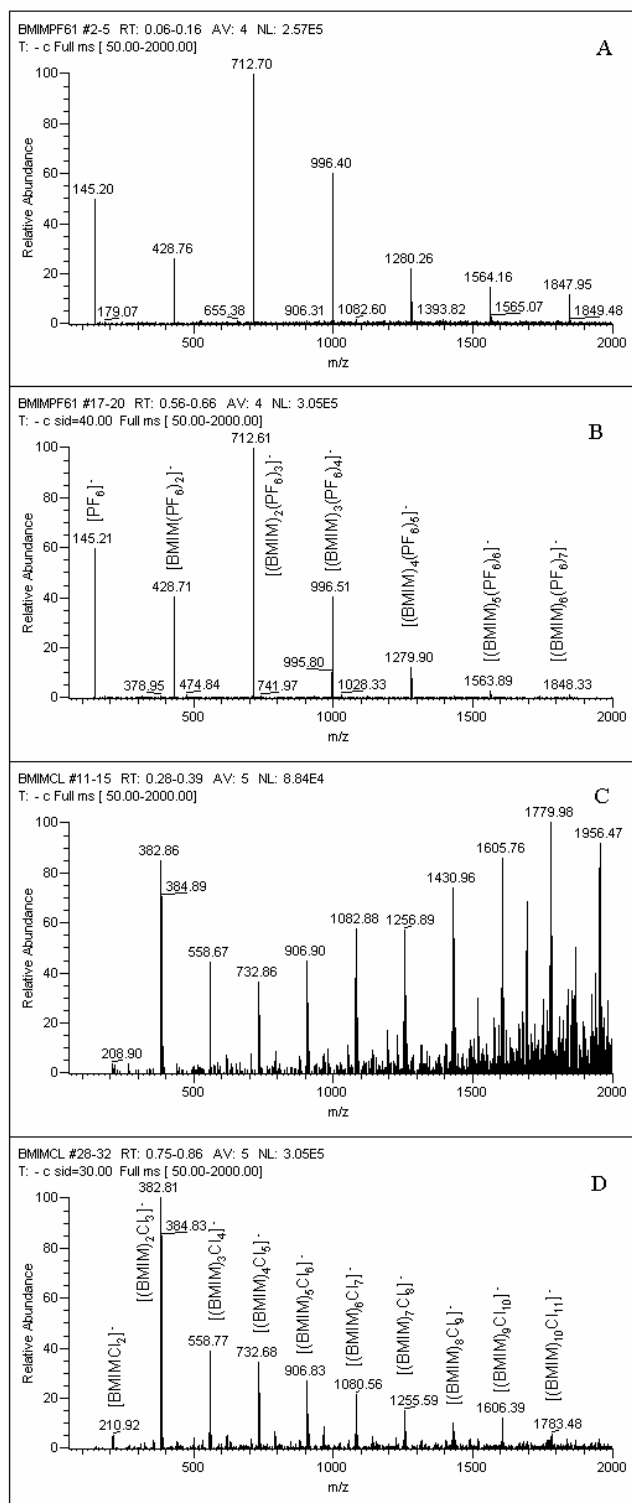
Fig. 2-4 Comparison of Mass spectra of BMIMCl and BMIMPF$_6$
Experimental conditions: negative ESI mode. IL and collision energy: A, BMIMPF$_6$, 0 V; B, BMIMPF$_6$, 40 V; C, BMIMCl, 0V; D, BMIMCl, 30 V.
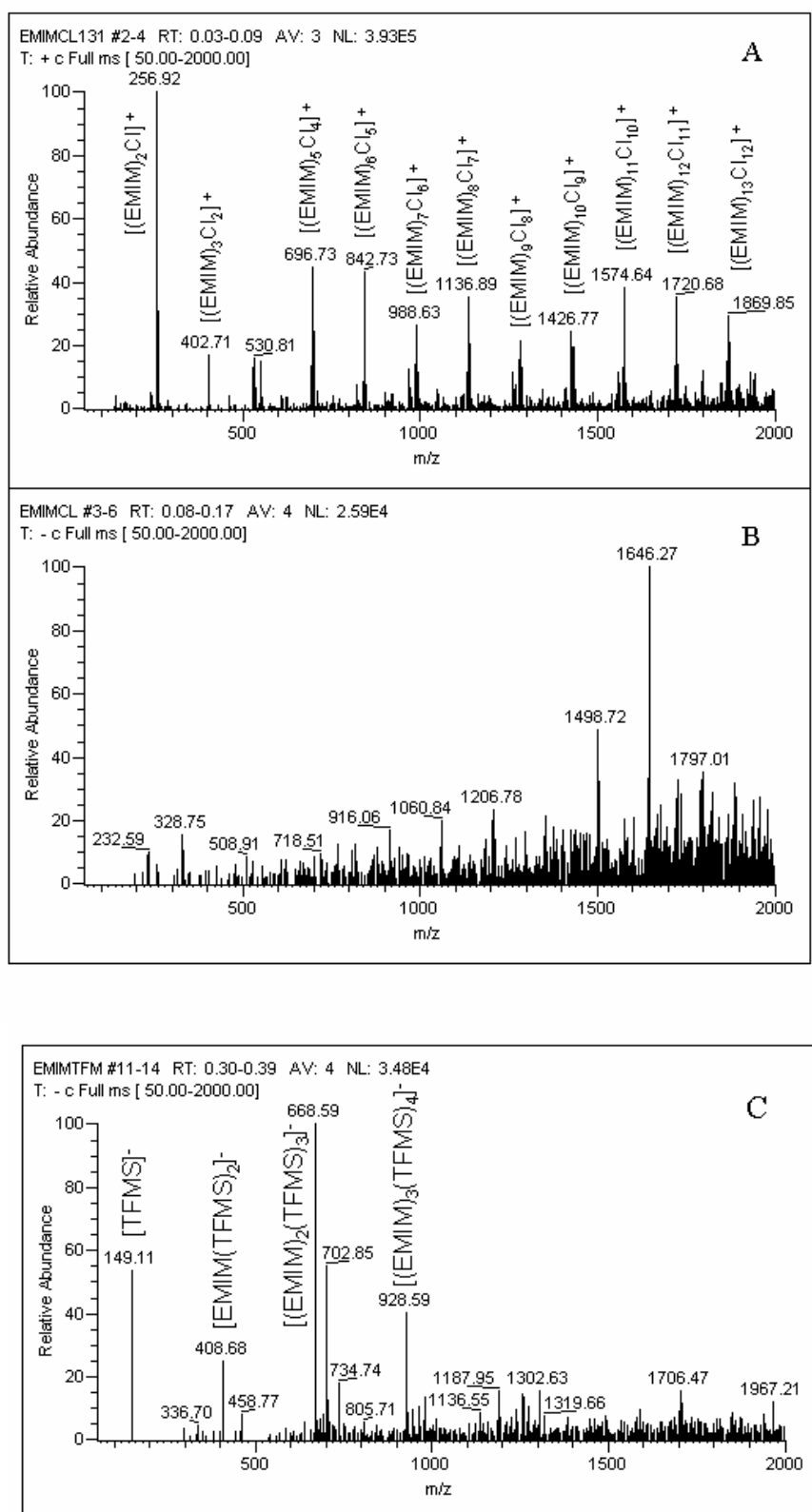
Fig. 2-5 Mass spectra of EMIMCl and EMIMTFMS
Experimental conditions: A, positive ESI mode, collision energy, 0 V; B, negative ESI mode, collision energy, 0 V;C, negative ESI mode, collision energy, 0 V.

2.4.3 Identification of species by MS^n

The components of aggregations were identified by MS/MS method. An example is shown in **Fig. 2-6**. Fragmentation may occur as

$$[(BMIM)_2(PF_6)_3]^- \rightarrow [BMIM(PF_6)_2]^- \rightarrow PF_6^- \qquad (2\text{-}2)$$
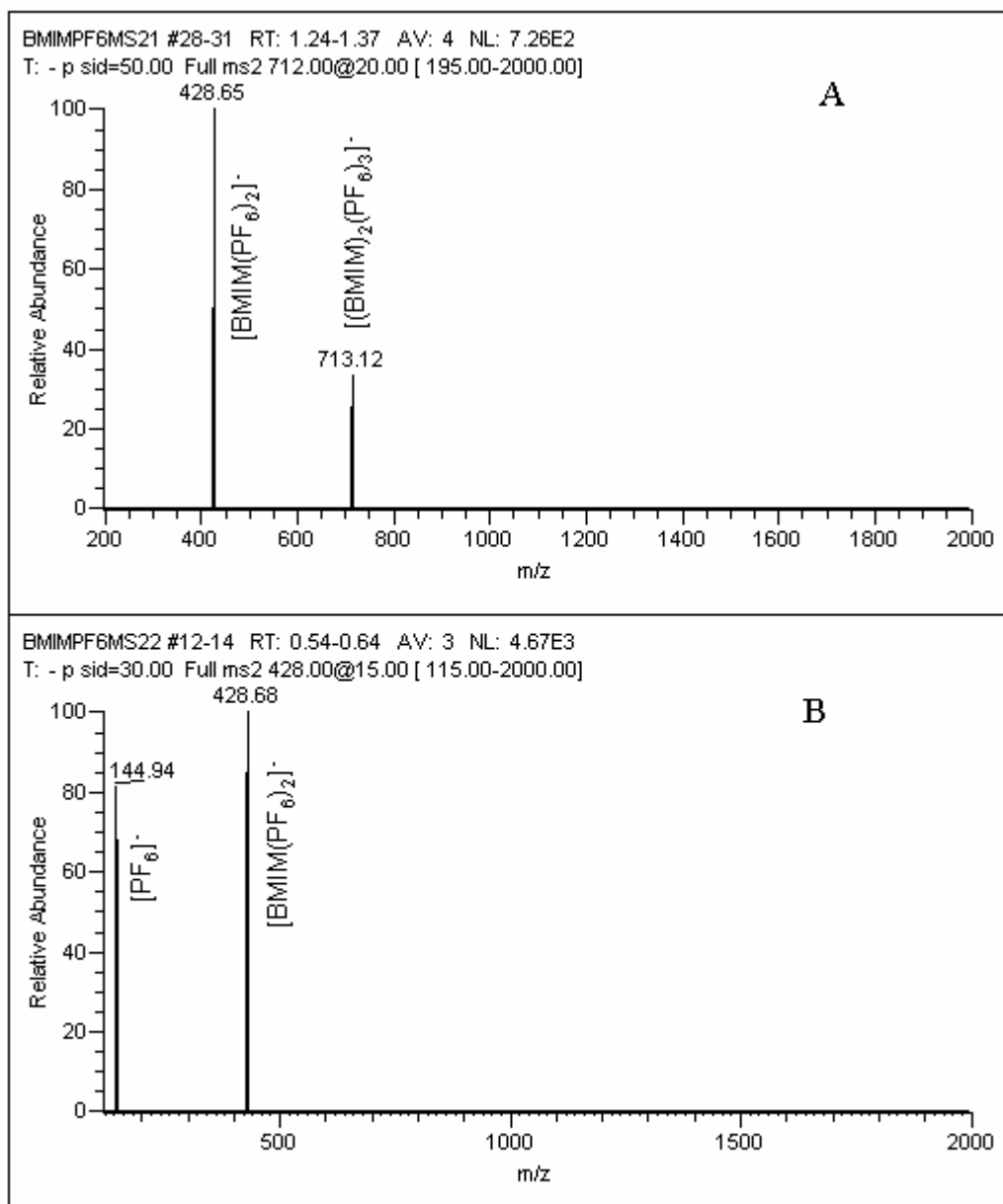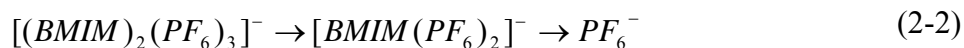
Fig. 2-6 MS/MS analysis of $[(BMIM)_2(PF_6)_3]^-$
Experimental conditions: negative ESI mode. A, 20% of the collision energy (50 V); B, 15% of the collision energy (30 V).
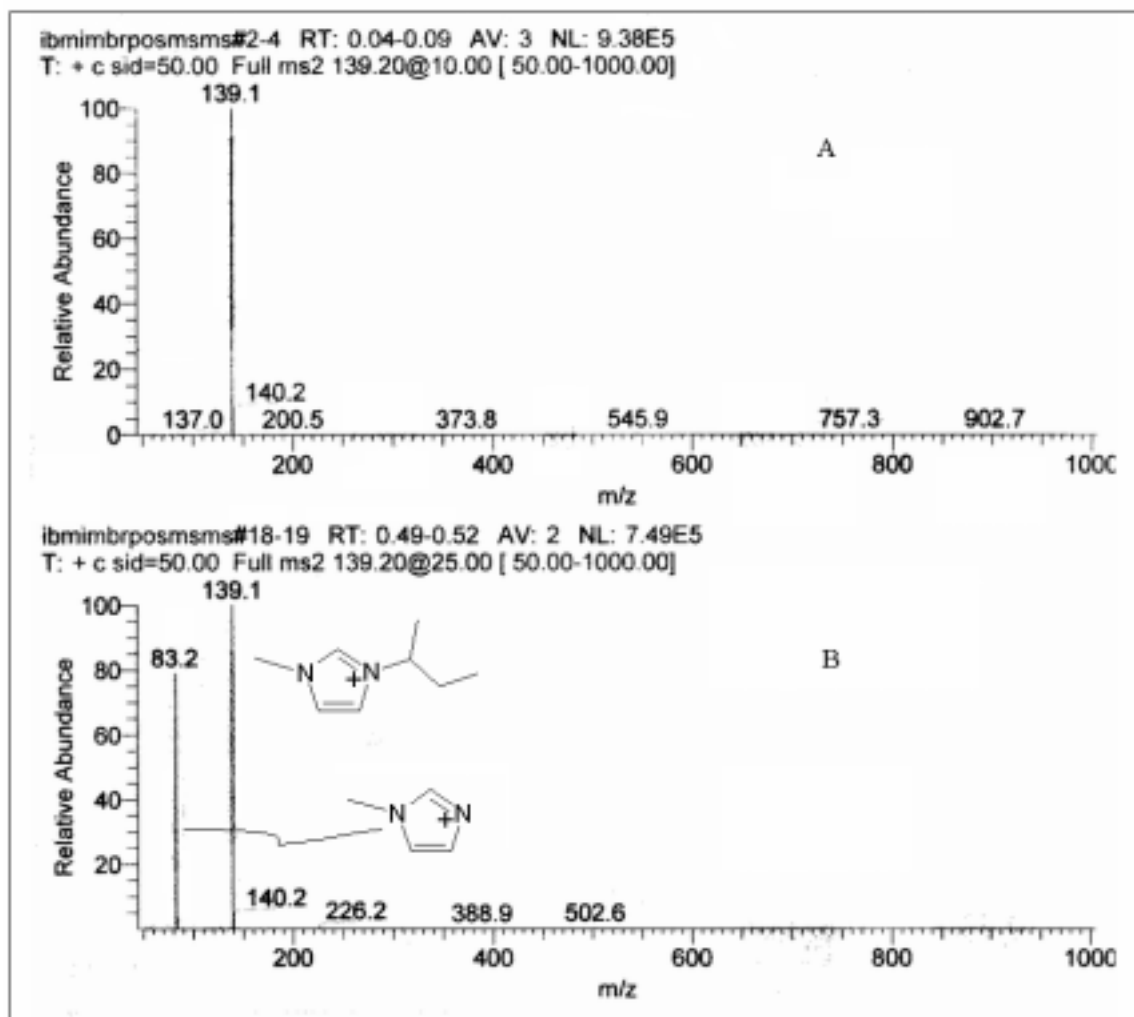
Fig. 2-7 MS/MS analysis of *i*BMIM
Experimental conditions: positive ESI mode. A, MS full scan (50 V); B, MS/MS on 25% of the collision energy (50 V).

For the DIAM cations, the MS/MS spectra indicated that under collision, the mother cation fragmented into 1-methylimidazole quasi-molecule and the long-chain alkyl group. For example, for *i*BMIM (spectra shown in **Fig. 2-7**):

$$(2\text{-}3)$$
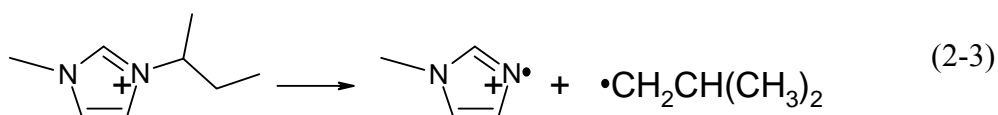
The above experiments suggest different interactions between the cations and anions. Such interaction will influence polarity and hydrophobicity of the aggregates, which

would have different affinities towards the analytes if they were used as BGE or additives in CE. It has been reported by a recent publication [12] that ILs with the same cation but different anions in aprotic solvent (acetonitrile) have different abilities in reversing the EOF of the capillary. Although our experiments in Chapter 3 showed that the electrophoretic mobilities of EMIM with different anion were the same in aqueous buffer when they were analyzed as samples in the range of 0.5-1.5 ppm, another report [13] demonstrated that ILs of different anions had different effects on analytes when they were used as buffer electrolytes of high concentration (50-300 mM). In this paper, the authors reported that the EMIM based ILs with tetrafluoroborate and hexafluorophosphate could separate the analytes (phenolic compounds), while no separation was obtained with trifluoromethanesulfonate (TFMS). The mass spectrum of EMIMTFMS was shown in **Fig. 2-5**C. It can be seen that it is significantly different from that of hexafluorophosphate (**Fig. 2-4**A and B); there is an order of magnitude in difference in their fragment abundances. In fact, EMIMTFMS is more similar to EMIMCl. The aggregation of IL in solutions was also found by other authors [14,15], one paper [15] pointed out that larger aggregates with a small charge density are generated in less polar solvents, small aggregates with a higher charge density are built in polar solvents. Among the above discussed anions, Chloride is a small ion. Compared with tetrafluoroborate and hexafluorophosphate, it has higher charged density and cannot form large aggregate in water solution. The larger aggregate may have stronger interaction with the phenolic compounds in the reference 13 of this chapter; this may partially explain why the tetrafluoroborate and hexafluorophosphate based ILs can improve the separation. Although we did not further investigate mechanisms behind the phenomena, we think understanding of these MS results may be of help in designing

electrophoretic buffer, especially for those using ILs as electrolytes in non-aqueous capillary electrophoresis.

It was also found that MS is not very sensitive in detecting impurities in the synthesized ILs, partially due to the low sample concentration infused or due to discrimination in sample introduction into the MS. There is a need to develop sensitive and reproducible method for assessing the quality of the products, which will be discussed in the following section.

2.5 Determination of the impurities in the ILs and the related imidazoles

The impurities in ILs will tremendously affect their performances. For instance, when they are used as battery electrolytes, large amount of impurities in the ionic liquids affect the transport numbers of the species involved in the system [16]. Previous studies suggest that different alkyl substitutes of the imidazolium cations, even the isomers, may result in different properties of the ILs [17]. Capillary electrophoresis is a microanalysis technique whose performance relies on the quality of buffers and the state of the internal capillary surfaces, etc. The impurities in the buffer will cause unexpected results not only from the interaction with analytes, but also from change in the properties of the capillary surface. As we mentioned in Chapter 1, a little adsorption of the electrolytes on the surface lead to tremendous influence on the electrophoretic results. Evaluating the purities of the starting materials or the products provides important information for application or for further purification.

A number of methods [17-20], such as NMR, IR, UV and MS, have been employed to test properties of ILs and detect impurities as well. These methods are either expensive to operate or are not suitable for routine quantitative analysis of the impurities typically present in ILs. Alkylimidazoles are the usual starting materials and are the main impurities in many IL products. Moreover, they are also basic starting materials in pharmacy industry [21] and commonly used chromophores in CE. Separation of these simple imidazoles has been actively studied [13,16,22,23]. In the work of Ong and Li [24], four imidazoles were baseline separated by MEKC within 12 minutes. A commercially available chemical, 2-ethylimidazole, was analyzed by high performance liquid chromatography (HPLC) and capillary electrophoresis (CE); but no quantitative or qualitative information of the impurities in the material was reported. Holbrey and co-workers [25] recently reported a colorimetric method determining imidazoles in EMIM based ILs. The concentration of 1-methylimidazole was measured by monitoring the change of the maximum absorbance wavelength of the solution caused by the coordination of copper (II) ion to 1-methylimidazole. The limit of detection (LOD) of this method was reported to be 0.2 mol% in EMIMCl. However, since determination of 1-methylimidazole is based on measuring the shift of the maximum absorbance wavelength, one cannot determine whether there is 1-methylimidazole in an IL without the spectrum of the pure standard. Moreover, other imidazoles such as imidazole and 1,2-dimethylimidazole may be interferences for the detection since they can also complex with cupric ion.

In acidic or neutral environment, the simple imidazoles are partially protonated, while the dialkylimidazolium are cations. They may be separated by CZE. The goal of this

work is to develop appropriate CZE working conditions to separate different 1,3-dialkylimidazolium cations (including isomers) and the related imidazoles. The method will be also applied in separation and detection of impurities in commercial chemicals as well as in monitoring the reaction process during preparation of the ILs used in this study.

2.5.1 Dependence of mobilities on pH

The effective mobilities of the analytes under different pH were measured to find the optimal separation pH. Dimethyl sulfoxide was employed as neutral marker for EOF and the effective mobilities were calculated by the following equation:

$$\mu_{ef} = \mu_{ap} - \mu_{eo} = \frac{Ll}{Vt} - \frac{Ll}{Vt_0} = \frac{Ll}{V}(\frac{1}{t} - \frac{1}{t_0}) \tag{2-4}$$

Where, μ_{ef}, μ_{ap}, μ_{eo}, L, l, V, t, t_0 are effective mobility, apparent mobility, EOF, length of capillary, length of capillary from injection side to detection window, voltage applied, migration time of the sample and migrating time of the EOF, respectively. **Fig. 2-8** shows that between pH 3 – 4.5, all the species except BMIM and *i*BMIM can be baseline separated. Imidazole and its derivatives are weak bases that can be protonated in acidic or weakly basic solutions (e.g. pKa values of imidazolium and 1-methylimidazolium are 6.993 and 7.16, respectively [26]). Since the above imidazoles are differently substituted, the pKa values of the imidazoliums will be different. Therefore changes of pH will have different effects on their degrees of dissociation and consequently their effective mobilities. Because the separation time was long under low pH due to the low EOF, the buffer pH was kept at 4.5 in our experiment.
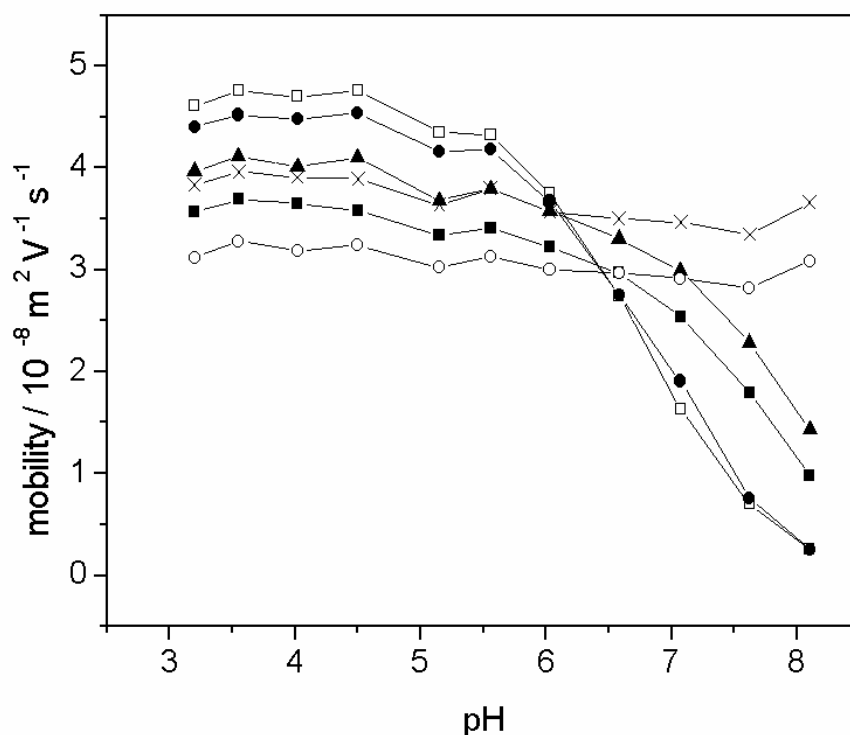
Fig. 2-8 Effect of pH on the mobilities of 1-alkyl-3-methylimidazoliums and the simple imidazoles
Buffer: 10mM NaH_2PO_4 adjusted to desired pH by 4M NaOH. Fused-silica capillary: 50μm I.D./ 360μm
O.D., 53.6 cm length/43.5 cm effective length. Voltage: +14 kV. Injection: 5s by gravity (8 cm height).
Detection wavelength: 210 nm. □= imidazole; ●=1-methylimidazole; ▲=1,2-dimethylimidazole;
✗=EMIM; ■= 2-ethylimidazole; ○= BMIM + *i*BMIM

2.5.2 Composition of the buffer and the buffer concentration

In order to obtain symmetric peaks for quantitation, the co-ion should be of similar
mobility as the analytes. It can be seen from **Fig. 2-8** that the mobilities of the analytes
range between 3.0-4.5 x 10^{-8} m^2 s^{-1} V^{-1}. Although the mobilities were not adjusted
against the ionic strength and viscosity of the buffer, they could be used as reference for
choosing buffer co-ions. In this experiment triethylamine was chosen as the co-ion in
the acidic buffer because its mobility (triethylammonium) is 3.48 x 10^{-8} m^2 s^{-1} V^{-1} [26].

71

It was reported by other authors [24] and also observed in this experiment that the baseline was not stable with ordinarily treated capillary (**Fig. 2-9**A). But we found that, without addition of any additives recommended by references 24 and 27, the capillary pretreated with 50 mM sodium acetate or 50 mM triethylammonium acetate for ca. 6 hours could offer stable baseline (**Fig. 2-9**B). It can be seen that the analysis time after pretreatment lengthened, which may result from decreased electroosmotic flow (the EOF decreased from ca. 2.5 to 2.0 x 10^{-8} m^2 s^{-1} V^{-1}).

The buffer concentration is another important parameter in CE; the high concentration favors the stacking of the analyte as well as reproducibility of results. From the buffer concentration of 2 mM onward, reproducible migration times and peak areas of the analytes could be obtained. Maybe because the target concentration was not very low, we did not observe obvious further stacking effect of the analytes with increasing buffer concentration. On the other hand, the analysis time was heavily influenced by the buffer concentration. At 15 mM, the analysis time was ca.11.7 minutes. Considering the above factors, the buffer concentration was chosen to be 5.0 mM
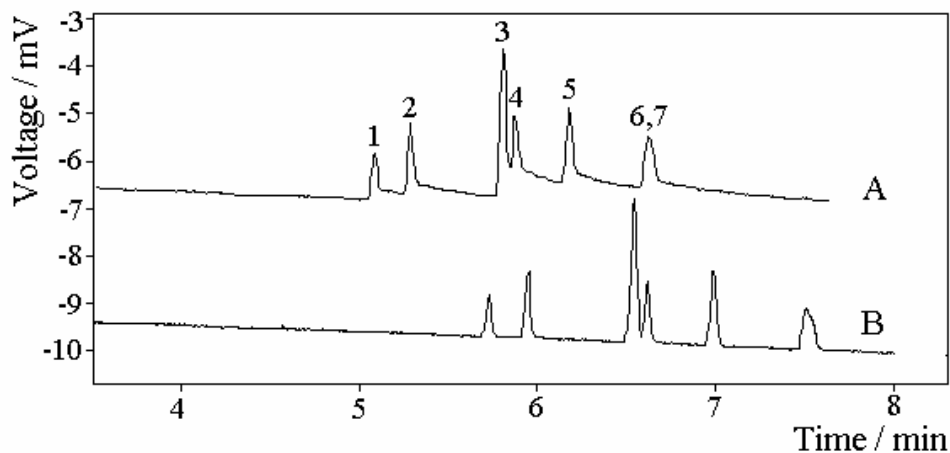
Fig. 2-9 Effect of capillary pretreatment
Capillary pretreatment: A, Fresh capillary was flushed by 0.5 M sodium hydroxide for 1 hour, followed by 10 minutes of deionized water, then by 10 minutes of running buffer; B, after flushed by 0.5 M sodium hydroxide, the capillary was rinsed with 50 mM sodium acetate for 6 hours and then flushed by deionized water and running buffer consecutively. Buffer: 5.0 mM sodium acetate adjusted by acetic acid to pH 4.5. Peaks (in the following order): 1, imidazole; 2, 1-methylimidazole; 3, 1,2-dimethylimidazole; 4, EMIM; 5, 2-ethylimidazole; 6, *i*BMIM; 7, BMIM. Other conditions as in **Fig. 2-8**.

2.5.3 Effect of α-CD

Cyclodextrins (CDs), also known as Schardinger dextrins, cycloglucopyranoses or cycloglucans, are cyclic oligosaccharide molecules built of glucopyranose units (**Fig. 2-10**). They can generally be dissolved in water to a certain extent. However, their cavities are hydrophobic and can form inclusion complexes with organic molecules according to their molecular sizes, structure conformations and hydrophobicities as well.

CD	No. of Glu	r (nm)
α	6	0.49
β	7	0.62
γ	8	0.79
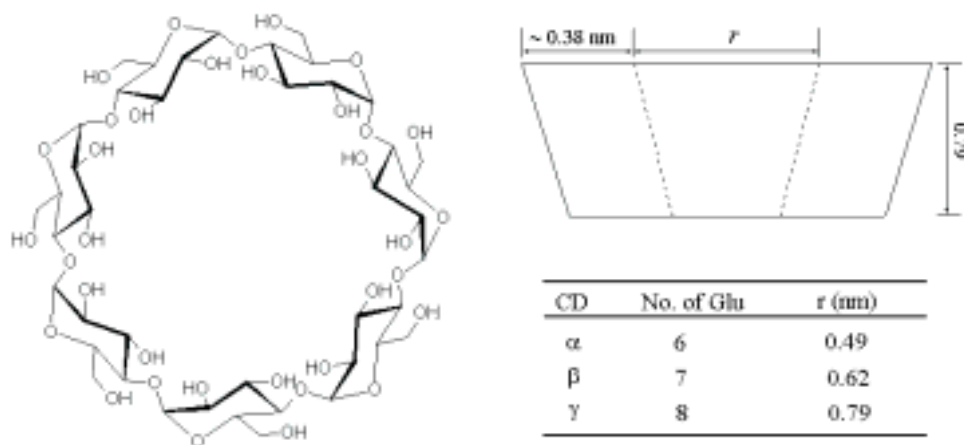
Fig. 2-10 Chemical structure and schematic model of cyclodextrin

The cavity diameter of α-CD is slightly larger than that of the imidazole ring, which may render the reagent the resolving abilities towards position isomers *i*BMIM and BMIM based on their slight steric differences. **Fig. 2-11** shows that the migration time of BMIM increases more significantly than those of others with addition of α-CD. Association of the analytes with the cyclodextrin increases migration times because of formation of bulky complex. With α−CD of 1.5 mM onward the isomers were baseline separated with BMIM migrating out first, followed by *i*BMIM. In order to further assess the complexation capability of α−CD with the isomers, the concentration of α−CD was increased till 30 mM (figures not shown). The peak patterns were similar to those in **Fig. 2-9**, but the mobility of BMIM decreased more. The complex formation constant of isomer−CD can be calculated by the equations derived by Armstrong et al [28]:

$$\frac{1}{(\mu_0 - \mu)} = \frac{1}{(\mu_0 - \mu_c)K[\alpha - CD]} + \frac{1}{(\mu_0 - \mu_c)} \tag{2-5}$$

Where, K is the complexation constant, $[\alpha-CD]$ is the concentration of α−CD in the buffer, μ_0, μ_c and μ are the mobility of the isomer in the α−CD-free buffer, the mobility of isomer-CD complex and the mobility of the isomer in the presence of α−CD,

respectively. Since introduction of α–CD also changed the buffer viscosity, the mobilities measured in these buffers should be adjusted. We measured the mobilities of imidazole in buffers containing 0, 10, 20, 30 mM α-CD and the viscosities of these buffers. After adjusted against the buffer viscosities, the mobility of imidazole in the above buffers remained relatively stable. So imidazole was chosen as internal standard and the adjusted mobilities of the isomers were calculated by $\mu = \mu_B \mu_{eI}/\mu_I$ (μ_B, μ_I and μ_{eI} are mobilities of isomers and imidazole in the α-CD containing buffer, and mobility of imidazole in the α-CD-free buffer, respectively). The *K* values of each isomer could be determined by plotting $(\mu_0-\mu)^{-1}$ versus $[\alpha-CD]^{-1}$. The regression equation for BMIM was $y= 0.341+0.0196x$ ($n=8$, $r=0.982$). *K* was calculated from dividing the intercept by the slope to yield 17.4 M^{-1}. For *i*BMIM, $y= -8.83+0.0322x$ ($n=8$, $r=0.127$). The poor regression data of *i*BMIM suggests there may be other interaction. Because eq (2-5) is based on 1:1 interaction, the data may suggest higher order complexation between *i*BMIM and α-CD. The concentration of α-CD in our work was 2.0 mM considering the analysis time.
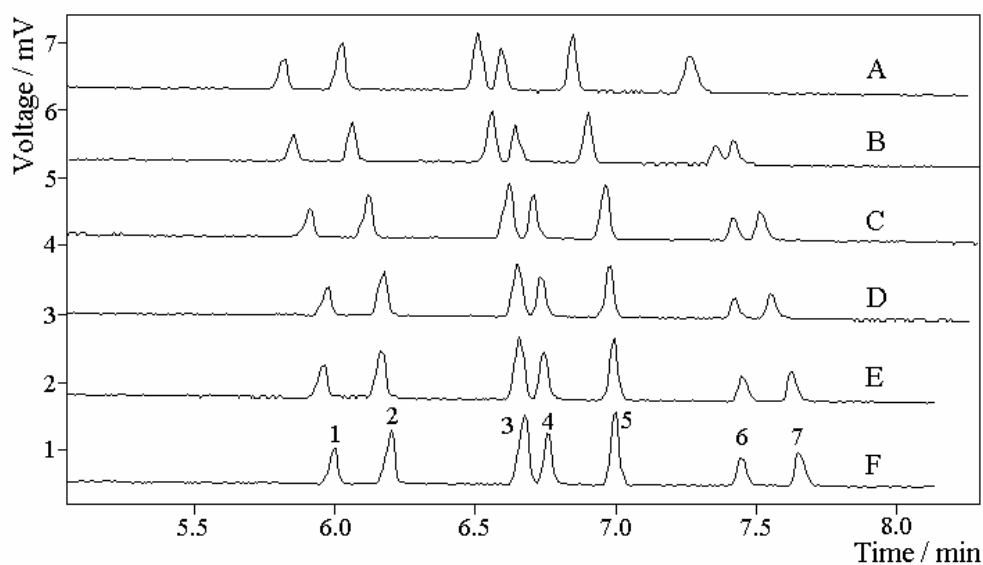
Fig. 2-11 Influence of α-CD concentration on the separation of the analytes
The concentration of α-CD increases from A (0.5 mM) to F (3.0 mM) with an interval of 0.5 mM. Other conditions and peak identifications are same as in **Fig. 2-9**.

2.5.4 Linearity, reproducibility and detection limits

Table 2-3 LOD, calibration data and precision obtained from the optimized conditions

Analytes	LOD	Correlation Coefficient	RSD% (N =5)	
	(ppm)	(N =7)	Migration Time	Peak Area
imidazole	0.44	0.999	0.64	1.9
1-methylimidazole	0.42	0.996	0.72	2.3
2-methylimidazole	0.54	0.996	0.49	1.9
1,2-imethylimidazole	0.60	0.993	0.58	2.1
EMIM	0.86	0.997	0.59	2.8
*i*BMIM	1.36	0.990	0.47	2.1
BMIM	0.92	0.992	0.53	2.1

LOD was determined at the signal to noise ratio (S/N) of three. Different concentrations ranging from 3 to 50 times of the LOD of each analyte were measured for the linear calibration. Five consecutive runs were performed for mixtures of 5 ppm each to assess the relatively standard deviation (RSD) of migration times and areas of the peaks. It can be seen from Table 2-3 that the LOD, linearity and reproducibility are within the regular working range for analysis of these compounds.

2.5.5 Applications

2.5.5.1 Detection of impurities in commercial chemicals

In order for comparison, the commercial EMIMCl was treated to remove the residual 1-methylimidazole. Eight grams of EMIMCl was transferred to a dry 200 ml round bottomed flask that would be kept at 90 °C. The melt was stirred with a magnet and bubbled with NaH dried ultra pure dinitrogen of 2 ml min^{-1} (measured under normal atmosphere). The flask was connected to a vacuum pump for 12 hours.

The commercially available EMIMCl and 2-ethylimidazole were used directly to prepare solutions of desired concentrations and then were analyzed with the optimized conditions obtained from the above experiments. Although the migration times changed (**Fig. 2-12**A-C) because of the high concentration of the matrix, the impurities were identified by spiking the solution with purified 1-methylimidazole and commercial imidazole. Imidazole (0.55% ± 0.04%) in 2-ethylimidazole and 0.27% ± 0.02% 1-methylimidazole in EMIMCl were found by the peak area method. For comparison, the concentration of 1-methylimidazole in EMIMCl was found to be 0.30 ± 0.04% by a colorimetric method (Shimadzu UV-160A, UV-Visible spectrophotometer); 0.61% ±

0.03% imidazole in the 2-ethylimidazole was detected with gas chromatography mass spectrometer (Shimadzu GCMS-QP506; the column: 30m, 0.25mm I.D., dimethylpolysiloxane). All the above data were obtained from three consecutive runs.
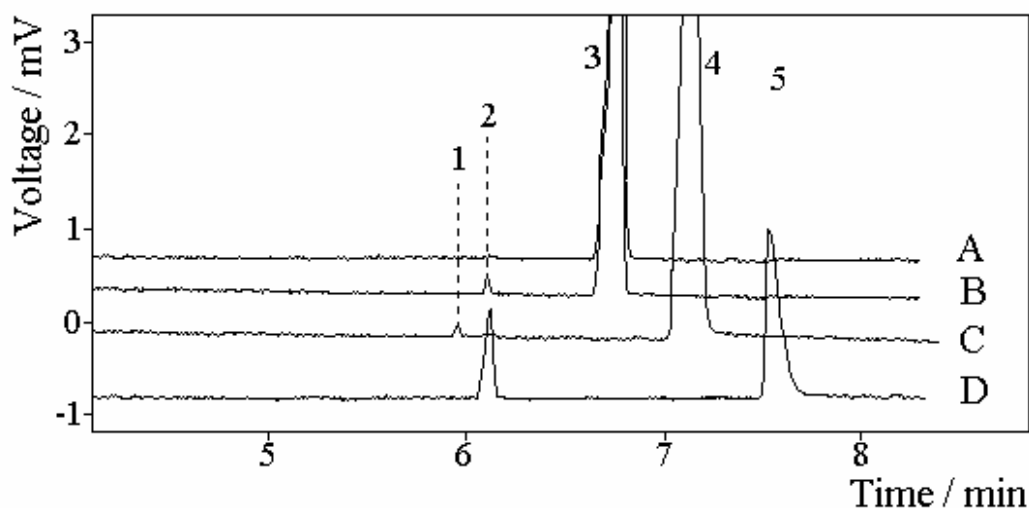
Fig. 2-12 Electropherogram of commercial chemicals and reaction mixture during synthesis of BMIMCl.

The concentration of α-CD was 2.0 mM. Other conditions are as in **Fig. 2-11**. The samples: A, 200 ppm treated EMIMCl; B, 200 ppm untreated EMIMCl; C, 200 ppm untreated 2-ethylimidazole; D, 60 ppm BMIMCl and 1-methylimidazole mixture. Peaks: 1, imidazole; 2,1-methylimidazole; 3, EMIM; 4, 2-ethylimidazole; 5, BMIM.

2.5.5.2 Process analysis during synthesis of BMIMCl

About 2 ml of the mixture was taken from the reaction mixture after 12 hours of reaction during the preparation of BMIMCl. After the excess 1-chlorobutane was evaporated, a 60 ppm deionized water solution was prepared and analyzed (**Fig. 2-12**D). We found that 73.1% ± 0.75% (n=3) (compared with 72.4 ± 0.87% (n=3) from colorimetric method) of 1-methylimidazole had changed into BMIM. Moreover, no peak corresponding to *i*BMIM was found. In order to confirm, *i*BMIM was spiked into the solution to 2 ppm and it could be quantitatively detected (not shown in the figure).

Our experiments suggested that no rearrangement of the n-butyl occurred during the synthesis.

2.6 Summary

DAIM based ILs can be synthesized with high yields and acceptable purities with the optimized methods. The mass spectra of the ILs reveal some of their association properties in organic solvent, which may be useful in interpreting the experimental phenomena and in experimental design.

The CE method developed can quickly separate and detect imidazole derivatives and 1,3-dialkylimidazolium cations with high resolution, low detection limits and good reproducibility. It can be employed in routine analysis such as impurity testing of commercial products as well as in reaction mechanism research and synthetic reaction process control.

References

[1] S.V. Dzyuba, R.A. Bartsch, J. Heterocyclic Chem. 38 (2001) 265

[2] D.W. Armstrong, L.F. He, Y. S. Liu, Anal. Chem. 71 (1999) 3873

[3] J.S. Wilkes, M. J. Zaworotko, J. Soc. Chem. Commun. (1992) 965

[4] P.A.Z. Suarez, J.E.L. Dullius, S. Einloft, R.F. Desouza, J. Dupont, Polyhedron 15 (1996) 1217

[5] J.G. Huddleston, H.D. Willauer, R.P. Swatloski, A.E. Visser, R.D. Rogers, Chem. Commun. (1998) 1765

[6] G.P. Smith, A.S. Dworkin, R.M. Pagni, S.P. Zing, J Am. Chem. Soc., 111 (1989) 525

[7] J. Fuller, R.T. Carlin, H.C. De-Long, D. Haworth, J. Chem. Soc., Chem. Commun. (1994) 209

[8] S.G. Cull, J.D. Holbrey, V. Vargas-Mora, K. R. Seddon, G.L. Lye, Biotechnology and Bioengineering, 69 (2000) 227

[9] P.A.Z. Suarez, V.M. Selbach, J.E.L. Dullius, S. Einloft, C.M.S. Piatnicki, D.S. Azambuja, R.F. De Souza, J. Dupont Electrochim. Acta 42 (1997) 2533

[10] M.J. Earle, P.B. Mccormac, K.R. Seddon, J. Chem. Soc. Chem. Commun. (1998) 2245

[11] P.A.Z. Suarez, S. Einloft, J.E.L. Dullius, R.F. De Souza, J. Dupont Chim. Phys.-Chim. Boil. 95 (1998) 1626

[12] M. Vaher, M. Koel, M. Kaljurand, Electrophoresis 23 (2002) 426

[13] E.G. Yanes, S.R. Gratz, M.J. Baldwin, S.E. Robison, A.M. Stalcup, Anal. Chem. 73 (2001) 3838

[14] P.J. Dyson, J.S. McIndoe, D.B. Zhao, Chem. Commun. (2003) 508

[15] D. Sandra, R. Wolfgang, K. Udo, 226th ACS National Meeting, New York, NY, United States, September 7-11, 2003

[16] J.R. Stuff, J Chromatogr. 547 (1991) 484

[17] A.G. Avent, P.A. Chaoner, M.P. Day, K.R. Seddon,, T. Welton, J. Chem. Soc. Dalton Trans. (1994), 3405

[18] K.M. Dieter, C.J. Dymek, N.E. Heimer, J.W. Roving, J.S. Wilks, J. Am. Chem. Soc. 110 (1988) 2722

[19] S. Dai, Y.S. Shin, L.M. Toth, C.E. Barnes, Inorg. Chem. 36 (1997) 4900

[20] A.K. Abdul-Sada, A.M. Greenway, K.R. Seddon,, T. Welton, Org. Mass Spectr. 28 (1993) 759

[21] M.D. Nair, K. Nagarajan, Prog. Drug Res. 27 (1983) 163

[22] M. Vaher, M. Koel, M. Kaljurand, Chromatographia 53 (2001) S201

[23] P. Bonhote, A.P. Dias, N. Papageorgiou,K. Kalyanasundaram, M. Gratzel, Inorg. Chem. 35 (1996) 1168

[24] C.P. Ong, C.L. Ng, H.K. Lee, S.F.Y. Li, J. Chromatogr. A 686 (1994) 319

[25] J.D. Holbrey, K.R. Seddon, R. Wareing, Green Chem. 3 (2001) 33

[26] J.A. Dean, Lange's Handbook of Chemistry, Mcgraw-Hill Book Company, New York, 15th Edn. 1999, Sect. 8

[27] N. Nishi, N. Tsumagari, S. Terabe, Anal. Chem. 6 (1989) 12434.

[28] K.L. Rundlett, D.W. Armstrong, J. Chromatogr. A 721 (1996) 173

CHAPTER 3 IONIC LIQUID AS BACKGROUND CHROMOPHORE

3.1 Introduction

As we stated in eq (1-4) of Chapter 1, the limit of detection in indirect detection is determined by the BGE concentration, the transfer ratio (TR) and the dynamic reserve (DR). Low LOD can be obtained by applying low BGE concentration, high TR and DR. Nielen [1] proposed that the mobilities determine TR, while Foret and co-workers [2] further reported that a good-match between the effective mobilities of BGE and the analytes can offer high sensitivity. By its definition, TR can be expressed as

$$TR = \frac{C_{coion}^{buffer} - C_{coion}^{sample}}{C_{ana}^{sample}} \qquad (3\text{-}1)$$

Where, C_{ana}^{sample} is the concentration of analyte in the sample plug; C_{coion}^{sample} and C_{coion}^{buffer} are concentrations of background co-ion in sample plug and in background electrolyte, respectively. The background counterion in this experiment is UV inactive, and the absorbance change due to the replacement of background co-ion by the analyte is

$$\Delta A = \varepsilon l \Delta C = \varepsilon l (C_{coion}^{buffer} - C_{coion}^{sample}) = \varepsilon l C_{ana}^{sample} TR \qquad (3\text{-}2)$$

Where ε is the molar absorptivity of the background co-ion, and l is the path length of UV light, usually equal to the internal diameter of the capillary.

Derived from Kohlrausch's regulation function [3], TR can be expressed as [4,5]

$$TR = \frac{(\mu_{ana} + \mu_{counterion})\mu_{co-ion}}{(\mu_{co-ion} + \mu_{counterion})\mu_{ana}} = 1 + \frac{\dfrac{\mu_{co-ion}}{\mu_{ana}} - 1}{\dfrac{\mu_{co-ion}}{\mu_{counterion}} + 1} \qquad (3\text{-}3)$$

Eq (3-3) suggests that TR is not only determined by the mobility ratio of the background co-ion to the analyte, but also by the mobility ratio of co-ion over background counterion.

Fig. 3-1 shows that TR decreases with the increasing $\mu_{co\text{-}ion}/\mu_{ana}$ value. While the influence of $\mu_{co\text{-}ion}/\mu_{counterion}$ is a bit complicated: if $\mu_{co\text{-}ion}/\mu_{ana} < 1$, TR increases with $\mu_{co\text{-}ion}/\mu_{ana}$; if $\mu_{co\text{-}ion}/\mu_{ana} = 1$, TR equals 1 and is not influenced by $\mu_{co\text{-}ion}/\mu_{counterion}$; if $\mu_{co\text{-}ion}/\mu_{counterion} > 1$, TR decreases with the value. Compared with $\mu_{co\text{-}ion}/\mu_{ana}$, the influence of $\mu_{co\text{-}ion}/\mu_{counterion}$ on TR is smaller and hence not discussed so frequently when choosing background counterions. However, when more counterions are available, it is theoretically favorable to choose counterions which can offer high TR. It can be seen from **Fig. 3-1** that low $\mu_{co\text{-}ion}/\mu_{counterion}$ value and high $\mu_{co\text{-}ion}/\mu_{ana}$ favor high TR, while low $\mu_{co\text{-}ion}/\mu_{counterion}$ and low $\mu_{co\text{-}ion}/\mu_{ana}$ lead to low TR. That means in buffers containing counterion of high mobility, there exist both chances of advantages and risks for the TR of the analytes. In real analysis, the influence of electrodispersion caused by mobility-mismatch also should be considered for good peak shape and high separation efficiency. Empirically, the background co-ion for indirect detection is chosen at similar mobility as the analytes for the overall performance.
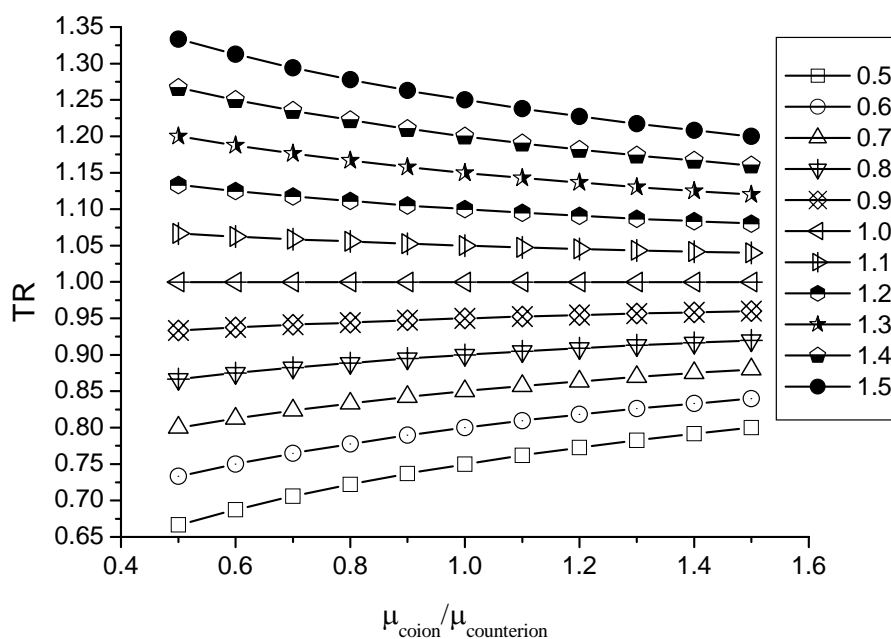
Fig. 3-1 Calculated value of TR versus different $\mu_{\text{co-ion}}/\mu_{\text{counterion}}$ and $\mu_{\text{co-ion}}/\mu_{\text{ana}}$
The values in the legend are the ratios of $\mu_{\text{co-ion}}/\mu_{\text{ana}}$

Another factor that should be considered is the applicable pH range of the background chromophore. The most often used chromophores for detection of cations are those N-heterocyclic compounds containing nitrogen atoms that have lone electron pairs to be shared by protons and thus they are positively charged in acidic buffer. They are widely used in the determination of metal ions, amines, etc. The main disadvantage of those kinds of chemicals are that they are prone to undergo deprotonation in alkaline buffer. The high buffer pH often leads to the reduced detection sensitivity due to the decreased concentration of the cationic chromophore available, and sometimes even no peaks obtained for the analytes.

Since EMIM is charged and has an imidazole ring which may have UV absorbance like imidazole, it may be a potential background chromophore for CE. To our best knowledge, however, there had been no report on this application until we reported this research.

Ammonium in urine comes chiefly from the decomposition of urea. Monitoring ammonium helps to understand the role of kidney in metabolism and to diagnose some diseases [6,7]. Methods determining NH_4^+ in water include a laborious Kjeldahl Titration method, electrochemical method in which K^+ is still an interfering ion to the electrode [8], a spectrophotometric method requiring expensive instruments, and CE with modifiers (such as 18-crown-6) which also have influences on the sensitivity of the analytes.

The purpose of this chapter is to study the CE-related property of EMIM based ILs and to explore their feasibility as chromophores for indirect detection in high pH buffers. The buffer developed was applied to analysis a real sample.

3.2 Experimental

3.2.1 Adjustment of pH and calculation of ionic strength

In order to study the mobilities of targets in wide pH range, NaH_2PO_4 solutions of known concentrations (the value was calculated according to eq (3-4) so that each solution was of same ionic strength; adjusted to different pH values by 4 M NaOH or 4 M phosphoric acid) were employed as buffer electrolytes. Because of the high concentration of NaOH and phosphoric acid, the volume change caused by the pH adjustment was very small and thus negligible. The ions in the buffer are $H_2PO_4^-$, HPO_4^{2-}, PO_4^{3-}, H^+, OH^- and Na^+. At any given pH and temperature, the concentrations

of $H_2PO_4^-$, HPO_4^{2-}, PO_4^{3-} and OH^- can be calculated from the fraction equation of phosphoric acid and ionization product of water. The concentration of sodium is governed by

$$[Na^+] = [H_2PO_4^-] + 2[HPO_4^{2-}] + 3[PO_4^{3-}] + [OH^-] - [H^+] \qquad (3\text{-}4)$$

The formula in square brackets represents the equilibrium concentration of that species in the buffer. The ionic strength can be calculated by $I = 0.5 \sum Z_i^2 C_i$, where, I, Z_i and C_i are ionic strength, charge and concentration of the ions concerned, respectively [9].

3.2.2 Treatment of urine specimen and stock solutions

About 100ml urine specimen was collected from a healthy person. The specimen was diluted to 20%(v/v) with deionized water and filtered with Millipore filter then store at 5°C. Each solution of K^+, Na^+ and NH_4^+ of ca. 1000 ppm was prepared preciously with deionized water and filtered and then stored at 5°C. Before analysis, the analytes were further diluted with running buffer to desired ratios.

3.3 Results and Discussion

3.3.1 UV absorbance of imidazolium

At 25°C, EMIMCl and imidazole water solutions ranged from 1×10^{-5}mol/L to 3.5×10^{-5}mol/L were prepared and scanned with a spectrometer. EMIM and imidazole shows similar absorbance character with absorpitivities of 5870 ± 62 $dm^3mol^{-1}cm^{-1}$ (n=3) at 209 nm and 5071 ± 41 $dm^3mol^{-1}cm^{-1}$ (n=3) at 207 nm, respectively (**Fig. 3-2**). We think

the slightly longer wavelength and high absorptivity of EMIM compared with that of imidazole may be attributed to the hyperconjugation of the alkyl groups attached on the N atoms of EMIM, which leads to a slight red shift of the spectrum.
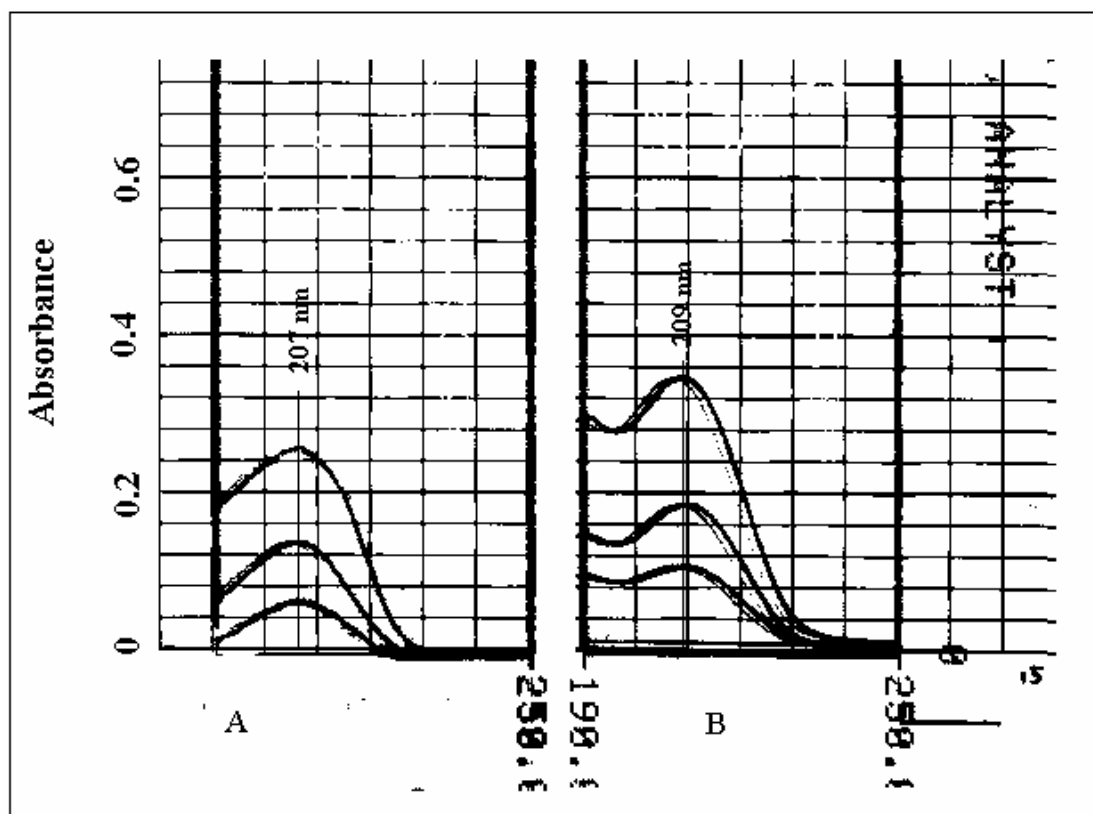
Fig. 3-2 UV absorbance of imidazole and EMIMCl
A, imidazole; B, EMIMCl. Concentrations: water solutions of 1,2, and 3.5 $\times 10^{-5}$ M, respectively.

3.3.2 Mobility of imidazoles and EMIM

The mobilities of species are affected by buffer concentration (ionic strength) and buffer viscosity. In order to eliminate these influences, phosphate buffers of different pH were prepared at equal ionic strength according to the method stated in 3.2.1. The viscosity of the buffers of different pH were measured and all the mobilities were adjusted against viscosity to pH 3 buffer by $\mu_i = \mu_3 \eta_3 / \eta_i$, where, μ_i, μ_3, η_i and η_3 are mobility of the metal

87

ion, mobility of this ion in pH 3 buffer, viscosity of the test buffer and viscosity of the

pH 3 buffer, respectively. Mobilities of EMIM based ILs composed of different anions,

namely, BF_4^-, Cl^-, PF_6^- and TFO, were measured to evaluate the influence of these

anions.

Table 3-1 shows that the effective mobilities of imidazole and 1,2-dimethylimidazole

decrease remarkably with the increasing pH and drop to zero at pH 9 and pH 10,

respectively, while the mobility of EMIM remains relatively stable over the entire pH

range studied.

Imidazole and 1,2-dimethylimidazole are weak bases that can be protonated in acidic or

weakly basic solutions. Their dissociation in water can be expressed by [10]:
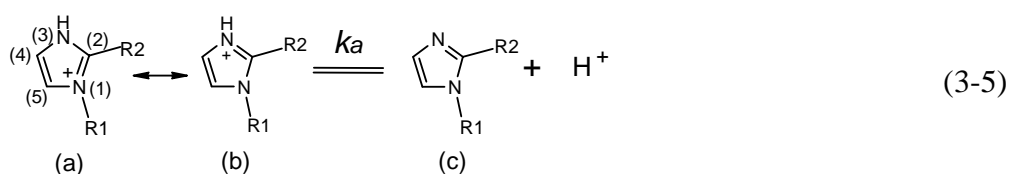
$$R1=R2=H: \text{imidazole}; \quad R1=R2=CH_3: \text{1,2-dimethylimidazole}$$

(3-5)

(a) and (b) in eq (3-5) are two of the resonance forms of imidazole and 1,2-

dimethylimidazole , and k_a is the equilibrium constant. The effective mobilities of

imidazole and 1,2-dimethylimidazole are governed by:

$$\mu_{ef}= \mu_0[H^+]/([H^+]+k_a) \tag{3-6}$$

Eq (3-6) suggests that change of pH will significantly affect the effective mobility of the

above weak acids and the compound with larger k_a will suffer more decrement at higher

pH.

Table 3-1 Adjusted mobility of imidazoles and EMIM in buffer of different pH

pH	Adjusted Mobility (10^{-4} cm^{2}V^{-1}s^{-1})					
			Anion binding to EMIM			
	Imidazole	dimi [b]	Cl$^-$	BF$_4^-$	PF$_6^-$	TFO$^-$
3	4.76	4.50	4.56	4.67	4.5	4.62
4	4.77	4.50	4.49	4.56	4.61	4.53
5	4.60	4.46	4.52	4.42	4.51	4.43
6	3.95	4.39	4.58	4.42	4.56	4.41
7	2.24	3.78	4.4	4.7	4.39	4.41
8	0.74	2.65	4.72	4.72	4.6	4.69
9	0.08	0.95	4.66	4.65	4.43	4.57
10	0.00	0.22	4.5	4.53	4.5	4.23
11	0.00	0.00	4.34	4.33	4.48	4.77
Ave ± SD [a]			4.53 ± 0.12	4.56 ± 0.14	4.51 ± 0.07	4.52 ± 0.17

[a] Average ± Standard deviation
[b] 1,2-dimethylimidazole

Both the imidazole and 1,2-dimethylimidazole rings contain 2 nitrogen atoms having lone electron pair. One nitrogen atom contributes its electron pair to the aromatic π system. Another one has its electron pair in an orbital directed away from the ring [10]. This nitrogen atom can be protonated and thus the imidazole can act as base. Moreover, in 1,2-dimethylimidazole, the hyperconjugation effect of the methyl on C(2) makes both the protonated form stable. In its resonance form (a), the induction effect of the methyl on N(1) tends to reduce the positive charge, which also contributes to the stability of its

protonated form. So 1,2-dimethylimidazole is more basic than imidazole and thus has lower K_a and higher protonation ratio accounting for its higher mobility in basic buffer in spite of its lower change-to-size ratio in structure.

Two factors may account for stable mobility of EMIM. First, there is no lone electron pair in any carbon or nitrogen atoms in the EMIM cation to be shared by a proton thus it cannot be protonated. Second, all hydrogen atoms combine with carbon atoms via covalent bonds; the dissociation constants of the most active hydrogen atoms, those combined to the sp^2 hybridized carbon atoms on the ring, are so small that change of pH cannot produce neutral 1,3-dialkylimidazole of detectable level to vary the mobility.

For EMIM with different anions, the Chi Square (x^2) distribution of the four sets of data is $x^2=0.535$, suggesting no difference among the mobilities according to the x^2 distribution table [11]. It may imply that these EMIM based ILs, although with different anion, are dissociated completely in water.

The mobilities of the two other permanent cationic chromophores, trimethyl(benzyl)ammonium and N-butylpyridinium, were measured to be 3.70 and 3.63×10^{-4} $cm^2V^{-1}s^{-1}$, respectively. Considering the mobility range of the metal ions are usually between 4.0 and 7.0×10^{-4} $cm^2V^{-1}s^{-1}$, EMIM may be the better choice as "permanent" cationic chromophores for their indirect detection.

3.3.3 Demonstration and application

The buffer pH is one of the most important factors affecting CE performance. As we discussed in Chapter 1, it influences effective mobilities of weak basic or acidic analytes, solubilities of some metal ions, and EOF which is a key parameter in CE. There will be more options to optimize the separation conditions if the BGE co-ion can work over wide pH range. The stable mobility of EMIM is advantageous for applications in CE, particularly for indirect UV detection of metal ions in high pH buffer since its mobility is closer to those of metal ions compared to the cationic chromophores reported [12].

3.3.3.1 Performance of the IL-containing buffer

In this experiment, EMIMCl and imidazole were employed separately as BGE in separating inorganic cations K^+, Na^+ and NH_4^+ in a standard solution. NH_4^+ is a weak acid whose pK_a is 9.24. At low pH, it will co-migrate with K^+ since they have almost the same mobility [13]. It can be seen from **Fig. 3-3** that BGEs composed of EMIM performances well between pH 3.5 and 11.5, and NH_4^+ and K^+ can be baseline separated in buffers of pH ≥ 8.5. However, no peaks can be obtained corresponding to the analyte cations when imidazole was employed as BGE in buffers of pH ≥ 8.5. This is because the pK_a of protonated imidazole is about 7.0 [14], and only about 3% of the species is protonated at pH 8.5. Consequently, the absorbance change due to the replacement of the protonated imidazole by the UV inactive analyte will be too small to be detected.
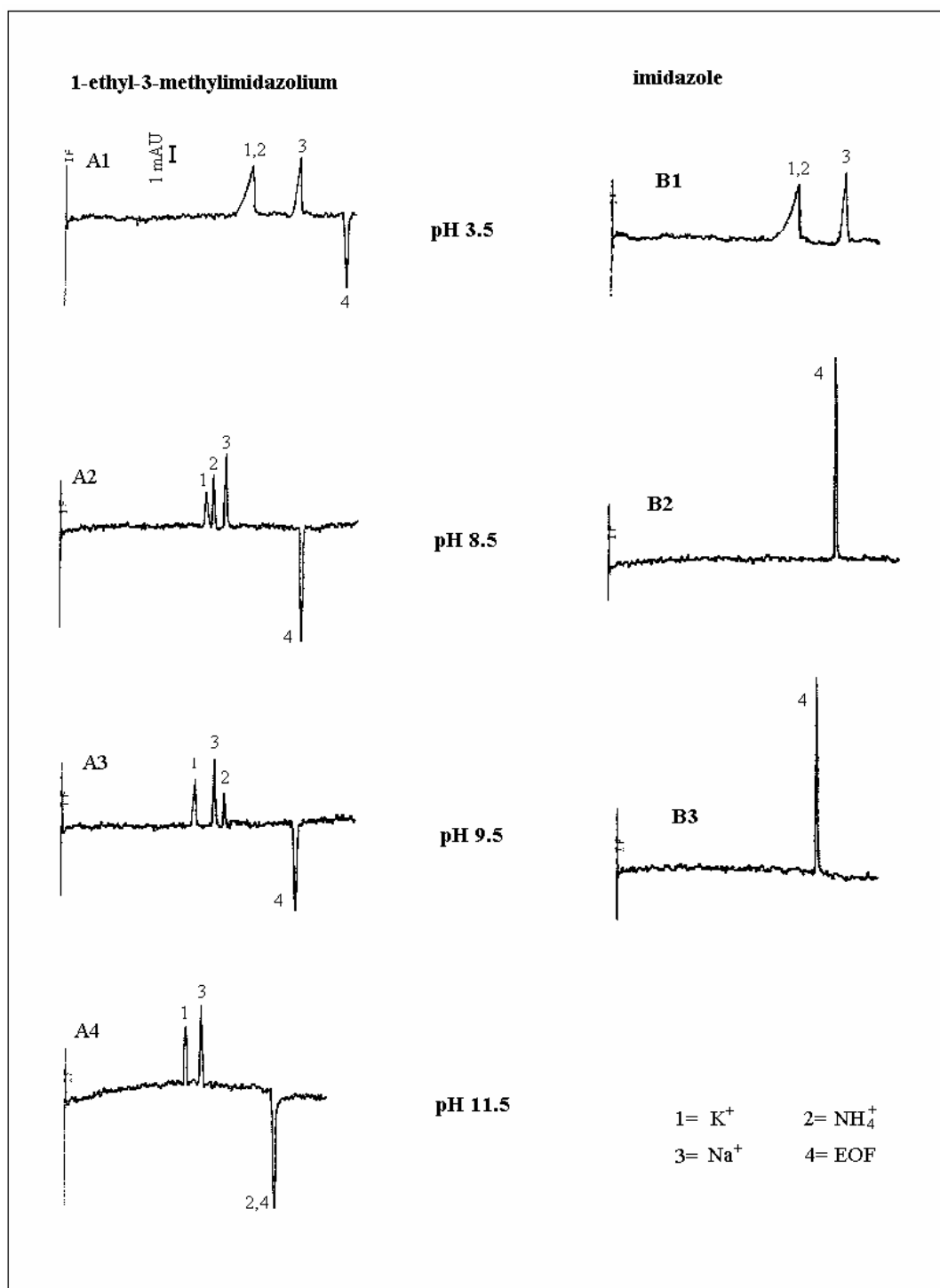
Fig. 3-3 Comparison of EMIM and imidazole as background chromophores

Experimental conditions: fused-silica capillary: 50µm I.D./ 360µm O.D., 43.5cm length/34.5 cm effective length; voltage: +6 kV; injection: 5s by gravity (8 cm height). Detection at 210 nm. Buffers: A, mixture of 3mM EMIMCl and 8 mM tetraethylammonium hydroxide adjusted to desired pH with 4 M phosphoric acid; B, mixture of 3mM imidazole and 8 mM tetraethylammonium hydroxide adjusted to desired pH with 4 M phosphoric acid.

It should be noted that the buffers for **Fig. 3-3** contain tetraethylammonium hydroxide, which is used to adjust the buffer pH but it also introduce co-ion (tetraethylammonium) into the buffer and hence reduce the TR value for the analytes. The experiment in this section is not designed to find optimal buffer conditions for imidazole and EMIM as background chromophores, but to compare their feasibilities as cationic chromophores under different pHs.

For the weak bases or acids, their mobilities change with buffer pH, and can be calculated using eq (3-6); hence, their migration orders can be predicted theoretically. The mobilities of potassium and sodium theoretically will not change with pH; while the pK_a of ammonium is 9.24, its mobility will not change noticeably in acidic buffers. In order for the accuracy of prediction, we did not take their reported mobilities as μ_0 in eq (3-6); their mobilities in buffer of pH 3.5 were measured and used as μ_0 in the calculation.

Fig. 3-4 shows that the theoretical and experimental values of mobilities have the same trend with pH, and they match well within experimental error. It can be found from the theoretical calculation that potassium and ammonium can be separated between pH 8 and 9, which was confirmed from our experiment.
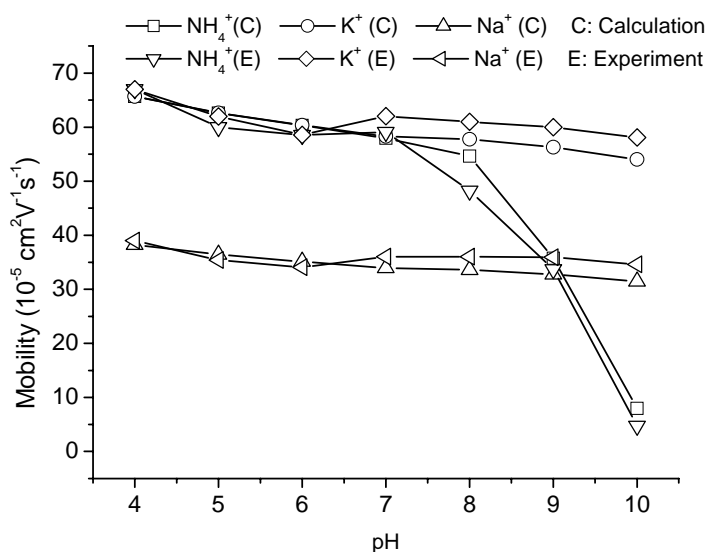
Fig. 3-4 Comparison of the calculated and measured mobilities of ions
Buffer: EMIMOH solution adjusted to the desired pH values by 4 M 4 M phosphoric acid; the ionic strength of the buffer was kept at 20 mM, the amount of EMIMOH used was calculated as described in 3.2.1. Capillary, applied voltage and detection are same as **Fig. 3-3**.

3.3.3.2 Detection of ammonium in human urine

The buffer of our method only consists of EMIMOH and phosphoric acid; thus, the conditions are easy to control. Additionally, fairly high sensitivity can also be expected because no modifier is added. The separation conditions were optimized before analyzing the real sample. The buffer was composed of 5 mM EMIMOH adjusted to pH 8.8 by phosphoric acid; the applied voltage was set to 10 kV. The detecting wavelength was 207 nm. Under the above conditions, NH_4^+ is baseline resolved from K^+ and consequently the concentration of K^+ can also be quantitatively determined (**Fig. 3-5**). The LOD for NH_4^+ is 2 µg/ml (S/N=3), the linear range is 5-500 µg/ml. Based on external standard method, the concentration of NH_4^+ in urine was determined to be 0.37% ± 0.012% (n=5) from its peak area. For comparison, it was detected to be 0.34% ± 0.014% (n=5) by Kjeldahl Titration.
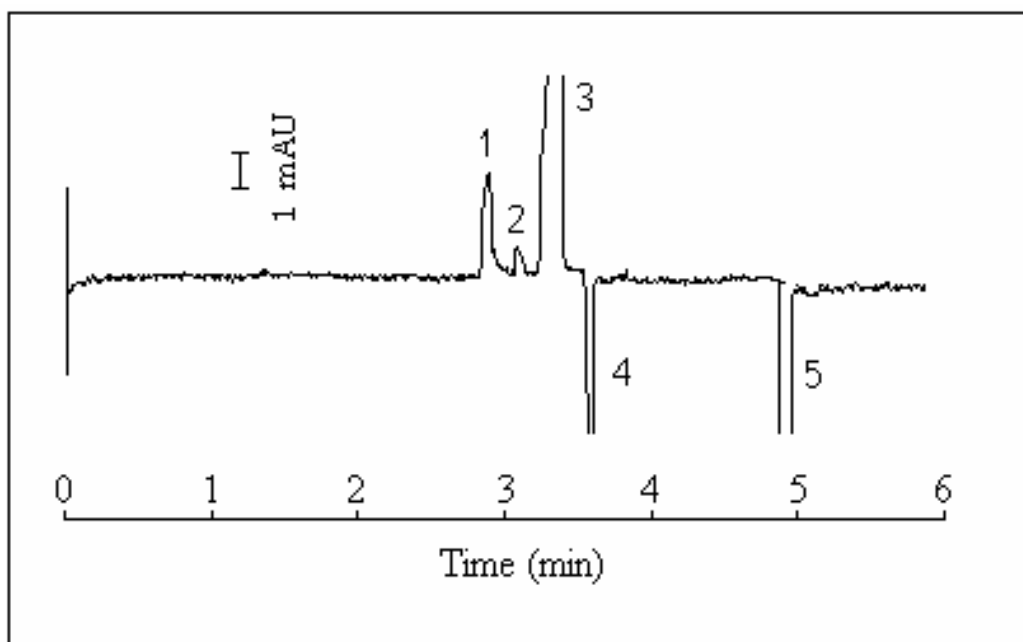
Fig. 3-5 Separation of K^+ and NH_4^+ in human urine

Buffer conditions are described in text. Peaks: 1, K^+; 2, NH_4^+; 3, Na^+ and Ca^{2+}; 4, system peak; 5, EOF.

3.4 Summary

TR value of an analyte is not only determined by the ratio of its mobility to that of background co-ion, but also is affected by the mobility of the background counterion. High TR can be obtained in the presence of high-mobility counterion. The EMIM cation has similar UV absorbance characters as imidazole but with a bit higher absorptivity and its mobility is independent on the pH of the buffer. Unlike the conventional chromophores for indirect detection, EMIM based ionic liquids performed well not only in acid buffer but also in buffers of very high pH. With the help of these ionic liquids, the pH range of the buffer in CE with indirect detection mode can be expanded and some analytes that cannot be separated in low pH buffers may be separated easily.

References

[1] M.W.F. Nielwn, J. Chromatogr. 588 (1991) 321

[2] F. Foret, S. Fanali, L. Ossicini, P. Bocek, J. Chromatogr. 470 (1989) 299

[3] F. Kohrlrausch, Ann. Phys. (Leipzig), 62 (1897) 209

[4] M.T. Ackermans, F.M. Everaerts,J.L. Beckers, J. Chromatogr. 549 (1991) 345

[5] F.E.P. Mikkers, Th.P.M. Verheggen, F.M. Everaerts, J. Chromatogr. 169 (1979) 1

[6] K.W. Joo, S.H. Chang, J.G. Lee, K.Y. Na, Y.S. Kim, C. Ahn, J.S. Han, S. Kim, J.S. Lee, J of Nephrology 13 (2000) 120

[7] B. Kirschbaum, D. Sica, F.P. Erson, J. Lab, Clinical Medicine 133 (1999) 597

[8] A. Merkoci, V. Cocoli, B. Baraj, S. Buzo, Acta Chim. Hung. 130 (1993) 9

[9] S.F.Y. Li, Capillary Electrophoresis: Principles, Practice, Applications, Elsevie, New York, 1992,

[10] T.M. Sorrel, In: Organic Chemistry, University Science Books, California, 1998, P.1235

[11] J. Murdoch, J.A. Barnes, In: Statistical Tables, Macmillan Education Ltd., Hongkong, 1989, P.17

[12] B. Lu, D. Westerlund, Electrophoresis 19 (1998) 1683

[13] J.A. Dean, Lange's Handbook of Chemistry, Mcgraw-Hill Book Company, New York, 1985, Pp5-14, Pp6-34

[14] X. Xiong, S.F.Y. Li, J. Chromatogr. A, 822 (1998) 125

CHAPTER 4 IONIC LIQUID AS COATING MATERIALS

It has been recognized that in order to approach ideal conditions for CE, EOF should be controlled and analyte adsorption to the capillary wall should be eliminated. In fused-silica capillary, the EOF driving force is the ionized silanol groups at the capillary surface. These groups are also responsible for the adsorption of analytes. In most cases, surface coating blocks these active sites; some times, for example, the cationic coating can even neutralize the surface charge. Thus the coating serves to eliminate or even reverse EOF and to reduce the adsorption of analytes, especially cationic analytes, to the capillary wall.

Coating can be physically adsorbed or chemically bonded to the surface. It was reported that physical coatings are likely result in poor detection limits [1]. Nowadays, chemical coatings are increasingly employed.

Buffer concentration and buffer pH are important parameters in CE. Buffer pH relate to the velocity of EOF and the resolution of analytes, while buffer concentration influences the separation of macromolecules.

In this work, the ionic liquids were tested as coating materials for the fused silica capillary. The IL-coated capillaries were employed in the separation of sildenafil from its metabolite; separation of DNA fragments was also investigated in IL-coated capillaries.

4.1 Materials

Acrylamide, γ-methacryloxypropyltrimethoxysilane, N,N,N',N'-tetramethylenediamine, 3-chloropropyl-trimethoxysilane (CPTMS), 3-chloropropyl-trichlorosilane (CPTCS), hydroxyethylcellulose (HEC, CAS number: 9004-62-0), and potassium persulphate were obtained from Fluka (Buchs, Switzerland). The 1-methylimidazole was from Aldrich (Milwaukee, WI, USA). Dimethyl sulfoxide (DMSO) was supplied by Merck (Darmstadt, Germany). The ΦX174 DNA-Hae III digest was purchased from Sigma (Saint Louis, MO, USA). The 36-mer (TTTTTTTTTTTTTTTTCAGATCCCCAAAGGACTCAA) and 7-mer (5'-FGGCGCL-3') oligonucleotides were bought from Operon (Alameda, CA, USA). Research samples of sildenafil and UK103,320 were kindly provided by Dr. Liu of the Institute of Molecular & Cell Biology (Singapore). HPLC grade ethyl acetate was a product of J. T. Baker (Phillipsburg, NJ, USA). HPLC grade methanol was obtained from Fisher Scientific (Fair Lawn, NJ, USA). Polyvinylpyrrolidone (PVP, average molecular mass: 1,000,000) was product of Polysciences (Warrington, PA, UAS). Tris-Boric acid-EDTA (TBE) solution containing 445 mM Tris, 445 mM boric acid and 10 mM EDTA at pH 8.3 was prepared and diluted to desired concentrations for use. Stock solutions of PVP and HEC of 10% (w/v) each were prepared by adding precisely weighted PVP or HEC to distilled water in a beaker, stirred in a water bath at 70°C. The homogeneous solution was then transferred to a conical flask, which was subsequently sonicated and connected to a vacuum pump for degassing. The stock solutions were kept at 5°C in a refrigerator. All solutions were prepared with deionized water from a MILLI-Q System (Millpore, MA, USA) and were filtered with 0.20μm Millipore filters before use.

4.2 Capillary coating

Capillary coating with linear polyacrylamide was carried out following the method proposed by Hjertén [1].

Coating of the capillary with ILs generally contains three steps. Step 1: bonding of the bifunctional compounds; step 2: introduction of imidazole ring; step 3: addition of alkyl group to the imidazole ring.

Two compounds, CPTMS and CPTCS, were studied in step one. During the reaction, Si-O-Si bonds were formed between the reagents and the surface silanol. From CE studies, it was found that the CPTMS provided a lower EOF, suggesting a more complete coverage of the silica silanols than was obtained with the CPTCS.

In the second step, the imidazole ring was covalently attached to the llinker. The solid imidazole was dissolved in organic solvents such as toluene before being introduced into capillary, while 1-methylimidazole was injected directly. The EOF of imidazole-coated capillary without further alkylation was lower than that of 1-methylimidazole due to the deprotonation of the imidazole under the pH of testing buffer. The EOF of the coated capillary could be controlled by varying the concentration of imidazole solutions [2]. In our experiment, the reaction time of this step was employed to control the magnitude of EOF.

In the third step, an alkyl group was added to the imidazole ring. This is only applicable to the imidazole-coated capillary. After reaction, the coating is cationic over a wide range of pH range. Meanwhile, with the attached alkyl chain of different lengths, the hydrophobicity of capillary surface is varied thus having different influences on separation.

Table 4-1 Reagents used in the coating procedure

A (for Step 1)	B (for Step 2)	C (for Step 3)
1: R1=methoxy, CPTMS	1: 1-methylimidazole	0: no reagents
2: R1=Cl, CPTCS	2: imidazole	1: 1-bromobutane
		2: chlorohexane
		3: 1-bromodecane

For convenience, the coatings are classified by the reagents used in each step (A, B, C) and noted as CT_{ABC}. For example, CT_{210} stands for the coating formed by CTPCS (step 1) and 1-methylimidazole (step 2) with no further alkyl-addition reactions. The structure is shown in **Fig. 4-1**.
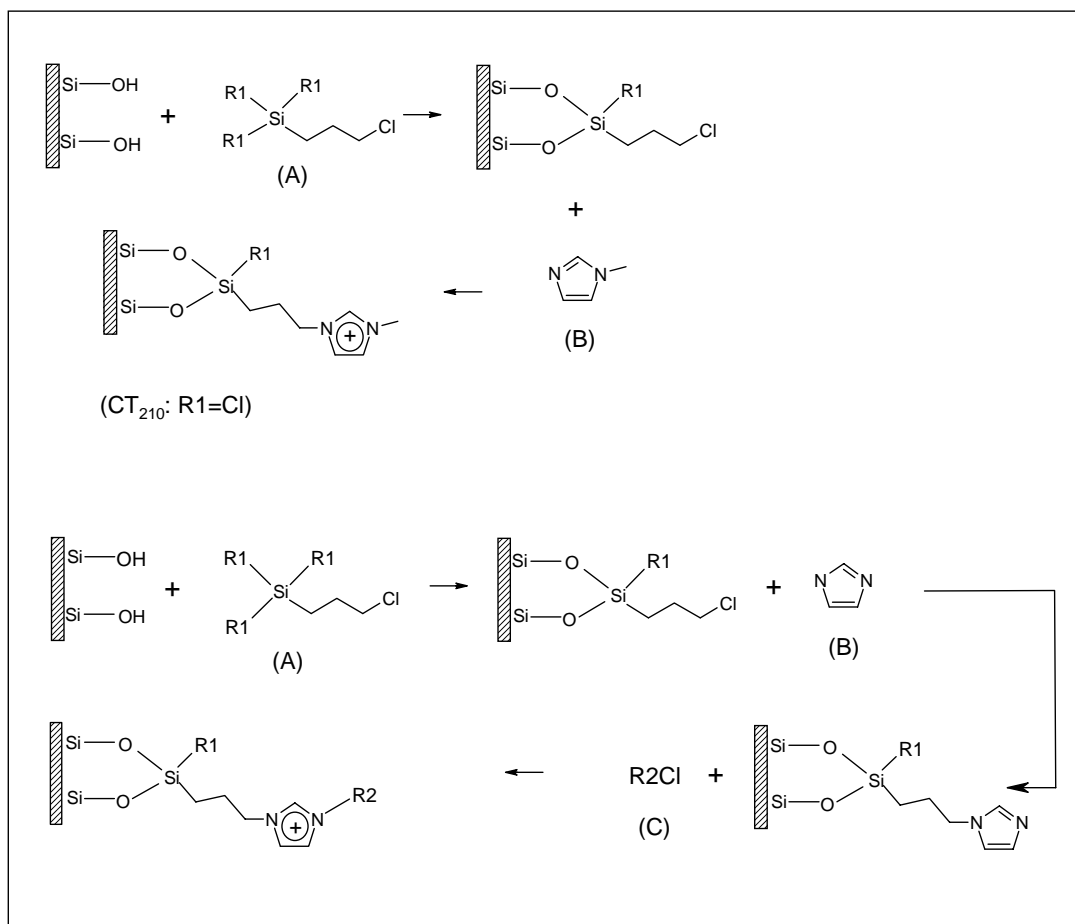
Fig. 4-1 Schematic representation of the IL coating procedure

The coating reaction is very straightforward. We describe here as an example the coating procedure for CT_{223}:

The fresh capillary was treated for two hours with 0.5 M sodium hydroxide, one hour with 1 M hydrochloric acid, 10 minutes with deionized water, and 10 minutes with methanol consecutively. It was then heated in a 120°C oven and flushed gently with pure nitrogen to drive out the residual water and methanol. The Si-O-Si bond was generated on the silica surface by filling the capillary with CPTCS followed by sealing both ends and keeping it at room temperature for two hours. After that the column was rinsed with toluene for 20 minutes. At room temperature, excess imidazole was

dissolved in toluene; the supernatant was filtered and introduced into the capillary by a positive pressure. After the column was heated at 90°C for 6 hours, the capillary was rinsed with toluene and dichloromethane successively and subsequently dried with nitrogen under 70°C for 2 hours. It was rinsed with 1-bromodecane for 10 minutes then sealed at both ends and heated in oven at 90°C for 10 hours. The pretreated capillary was rinsed successively for 10 minutes with toluene, 10 minutes with methanol and 30 minutes with deionized water before use.

4.3 EOF of the IL-coated capillary

Measuring the EOF is an effective way to evaluate the properties of the coating. The fast EOF was measured by the migration time of a neutral marker (DMSO solution) from inlet to detector under electric field. If the migration time was longer than 30 minutes, the procedure described by Williams and Vigh [3] was employed. Three consecutive runs were carried out on each capillary for the EOF measurement.

4.3.1 Influence of pH and reaction time

Fig. 4-2 shows that cationic EOF increases with pH for the bare-silica capillaries, while reversed EOF is observed for the IL-coated capillary (CT_{110}) due to the cationic surface-bonded imidazolium and the velocity decreases with increasing pH value. The cathodically increasing EOF of IL-coated capillary (ILCC) under alkaline conditions suggests incomplete coverage of IL-coating on the capillary surface; more uncovered silanols (**Fig. 4-3**) will deprotonate at higher pH thus the surface negative charge density increases. The coating procedure parameters also affect EOF; our experiments on

reaction time of the 1-methylimidazole alkylation indicated that the reversed EOF reached maximum after 8-hour reaction under 80°C (**Fig. 4-2**), which suggested the maximal coverage of the dialkylimidazolium on the capillary surface.
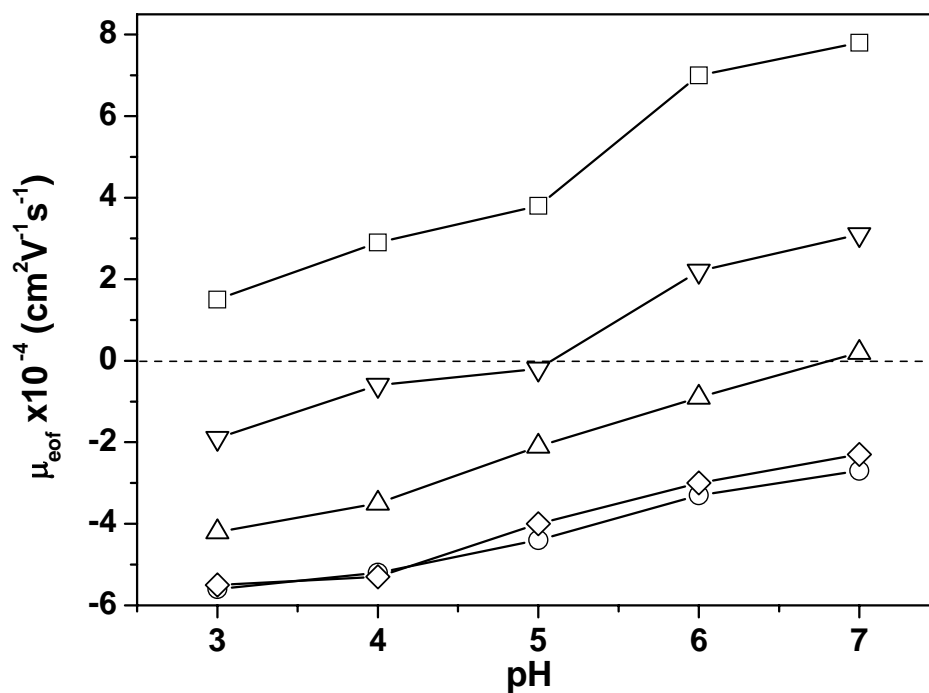
Fig. 4-2 Influence of alkylation time and buffer pH on the EOF of CT_{110}

Legend: (■) bare silica capillary; (▼) 2 hours; (▲) 4 hours; (✚) 6 hours; (O) 8 hours.

A = coated IL cation

B = uncovered silanol **C** = coated CPTCS
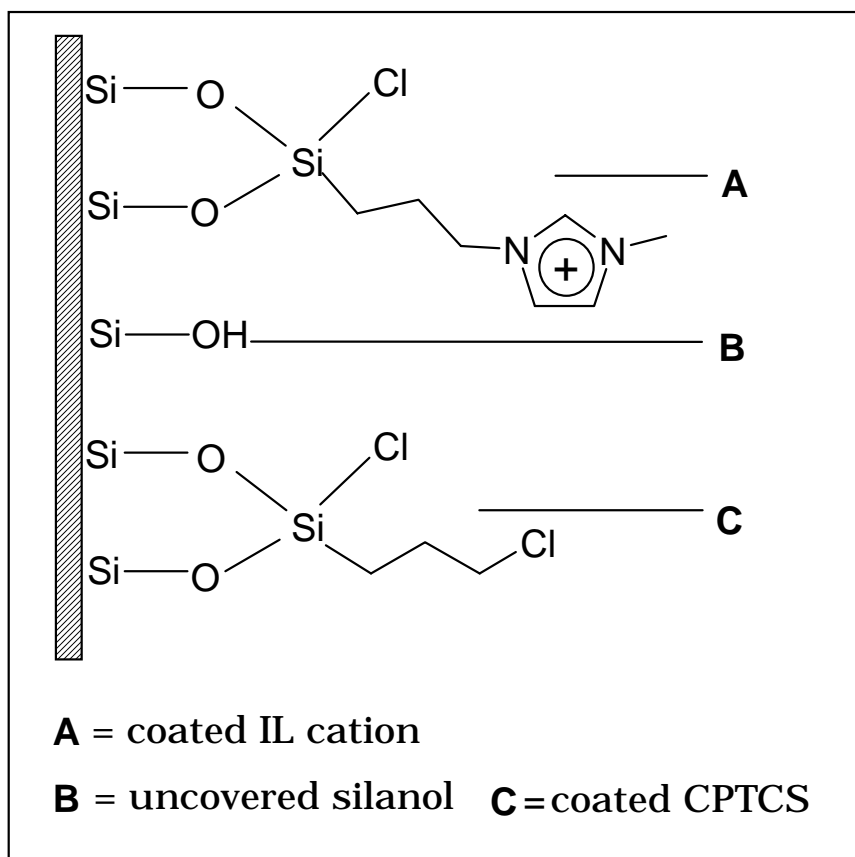
Fig. 4-3 Schematic representation of the CT_{210} Surface

4.4 Application 1: Separation of sildenafil and its metabolite

Sildenafil citrate (Viagra), used for the treatment of erectile dysfunction, has become one of the most popular and widely used drugs. Sildenafil (SL), 1-[4-ethoxy-3-(6,7-dihydro-1-methyl-7-oxo-3-propyl-1H-pyrazolo-[4,3-d]pyrimidin-5-yl)phenylsulphonyl]-4-methylpiperazine, is a potent inhibitor of the cyclic guanosine monophosphate (cGMP)-specific phosphodiesterase type 5 enzyme (PDE5) found predominantly in the penile corpus cavernosum [4]. After oral administration, it is absorbed and metabolized to UK-103,320 (UK), 1-[4-ethoxy-3-(6,7-dihydro-1-methyl-7-oxo-3-propyl-1H-pyrazolo[4,3-d]pyrimidin-5-yl)phenyl-sulphonylpiperazine, which

exhibits approximately 50% of the potency of the parent drug and contributes to the observed pharmacological effects [5]. Because of its increasing usage and potential side-effects [6,7], detection of both sildenafil and its metabolite in biological sample is becoming important.

There is only one methyl difference between the two compounds (**Fig. 4-4**A, B) and both have basic functional groups with a pKa value of ca. 8.7 [8]; hence their intrinsic mobilities will very close to each other under a wide pH range. Our experiments demonstrated that the electrophoretic mobilities of SL and UK in 10 mM ammonium acetate at pH 4.5 ranged from1.7 to 1.9×10^{-4} $cm^2V^{-1}s^{-1}$ and they could be only partially separated under capillary zone electrophoresis (CZE) mode in a 70 cm bared-silica capillary. High performance liquid chromatography (HPLC) was employed to determine the two drugs in human blood and urine, etc [9-11]. They were also separated by gas chromatography (GC) [12]. Nevado and co-workers [10] determined SL and UK in human serum by micellar electrokinetic capillary chromatography (MEKC).
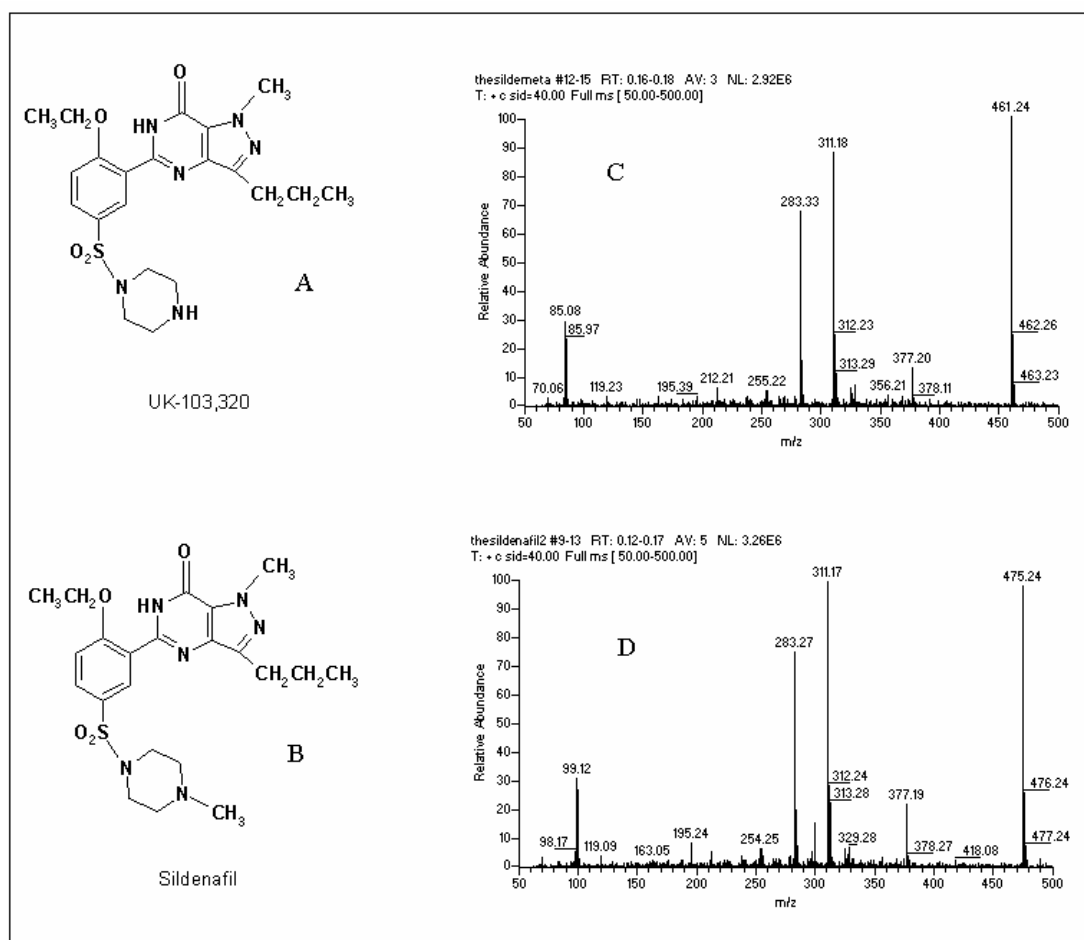
Fig. 4-4 Structure and mass spectra of SL and UK

C and D are mass spectra of UK and SL, respectively. The MS conditions: syringe infusion flow rate at 10 μl/min; capillary temperature at 270°C/; concentrations of SL and UK are 100ng/ml each.

A theoretical equation derived from eq (1-23) of Chapter 1 for resolution of two zones in CZE considering the effect of electroosmotic flow (EOF) can be expressed as [13]:

$$R = \frac{1}{4\sqrt{2}}\Delta\mu\sqrt{\frac{lV}{DL(\overline{\mu} + \mu_{eof})}} \qquad (4\text{-}1)$$

Where, R is the resolution of the neighboring peaks; $\Delta\mu$ the difference between electrophoretic mobilities of the analytes; V the separating voltage; l the migration length of the analytes, L the total length of the capillary, D the diffusion coefficient of

the analytes in the buffer; $\overline{\mu}$ the average electrophoretic mobility of the analytes; μ_{eof} the EOF.

Eq (4-1) suggests that EOF affects the separation of analytes: when EOF migrates in the same direction with targets, the resolution will decrease. When they migrate at opposite directions, there is a chance that the resolution between analytes can be improved. The enhancement of the resolution depends upon the difference between EOF and the electrophoretic mobility of the analyte; the highest resolution could be reached when $\mu_{eof} = -\overline{\mu}$, however the analysis time will be infinite. The EOF of the silica capillary can be reversed by dynamic or static coatings [2,14,15], in which cationic ions adsorb or covalently bond to the internal capillary surface.

At pH lower than 7, the drugs are positively charged and the interactions between the drugs and the cationic coating will be predominantly electrostatic repulsion, so the analytes may be separated under CZE mode rather than CEC. Since there is no involatile surfactant added in the buffer which is needed in dynamic coating, the analytes can be detected by mass spectrometer. MS has been coupled to various separation techniques including HPLC, GC and CE in gathering structural information of separated compounds. Targets in complicated matrices can be identified by techniques such as MS[n] scan or consecutive reaction monitoring (CRM) modes. In this section, a method was developed for determining SL and UK in human serum by solid-phase extraction followed by CZE-MS/MS conducted in an ionic liquid coated capillary.

4.4.1 Experimental

4.4.1.1 Serum sample and Solid-phase extraction procedure

Fresh serum obtained from volunteers was stored at −15°C and defrosted before use every time. Solid phase extraction (SPE) of SL and UK was performed on a 500mg Varian (Harbor City, CA, USA) octadecylsilane (C_{18}) bonded silica cartridge. The cartridge was first rinsed with 3 ml methanol, then with 3 ml of 20 mM NH_4HCO_3 solution. Care was taken not to dry the column prior to sample loading. Three milliliters of human serum spiked with desired concentration of drugs was loaded and slowly passed through the cartridge. The cartridge was then washed with 3 ml of the aforesaid NH_4HCO_3 solution, and dried with nitrogen for 10 minutes. The analytes were eluted from the cartridge with 3 ml ethyl acetate. The eluent was evaporated to dryness under 40°C by a stream of nitrogen gas. The residue was dissolved in 500 μl water-methanol (70:30, v/v) for analysis.

4.4.1.2 Drug recovery in CE

The method measuring protein recovery described by Regnier and Towns [16] was modified to determine recoveries of SL and UK. A bare or IL-coated capillary of 80 cm length was burned at 40 and 70 cm from the inlet to make detecting windows. CZE was conducted in 10mM acetic acid-ammonia buffer (pH 4.5) under 313 V/cm electric field. Only one UV detector (set to 230 nm) was used and the recovery of drug of interest was determined by areas in two consecutive runs, in which all the other experimental conditions were same except that the UV detector was put on different detecting windows. The capillary was rinsed progressively after each run to remove the adsorbed analytes (if any). For the bare capillary: 2 minutes with deionized water, 10 minutes

with 50 mM acetic acid-ammonia buffer at pH 9.5, 2 minutes with deionized water, 2 minutes with running buffer; for IL-coated capillary: 10 minutes with 50 mM acetic acid-ammonia buffer at pH 4.5, 2 minutes with deionized water, 2 minutes with running buffer. A lab-made cartridge was used to hold tightly the un-used detecting windows to avoid breakage.

4.4.1.3 CZE-MS/MS analysis

The CE separation voltage was set to -25 kV; a capillary of 70 cm × 75 μm I.D. was used for separation. The auxliary gas pressure was set to zero; sheath gas (N_2) pressure was at 20 arbitrary units and a mixture of methanol-water (70:30, v/v) containing 0.5% acetic acid at a flow rate of 2 μl/min was used as sheath liquid. The ion spray voltage was 3.8 kV; the temperature of the heated capillary was set to 230°C. The instrument was controlled by the Xcalibur 1.0 software (Finnigan). To optimize MS conditions for CZE analysis, the buffer solution of the analytes was injected into the mass spectrometer through the capillary by a positive pressure of 35 mbar, under which the migration velocity of the analyte was approximately same as that in the CZE procedure. The initial ionization evaluation of the analytes using both positive and negative ESI source indicated that the positive mode provided greater signal to noise ratios. The ESI conditions were optimized by auto tuning to the best signal of quasi-molecular ion of sildenafil ($[M+H]^+$ at m/z = 475.3). MS/MS was performed during the detection and the full spectra were used for identification and confirmation. Two unique fragments, at m/z=282.3 and 311.2, were found to have the highest abundance in MS/MS spectra of both SL and UK and they were summed for quantitation.

4.4.2 Results and discussion

4.4.2.1 Adsorption of the analytes onto the internal wall of the capillary

Adsorption of the drugs onto both the bare and coated capillaries were tested by first filling the capillary with drug standard solution and then rinsing it with run buffer at positive pressure of 100 mbar (corresponding to ca. 120 nl in volume). It was observed that SL and UK were prone to adsorb onto the bare capillary surface over pH range of 3.5 to7: the drug residues could be found from the mass spectrum even after 10-minute flush. For the IL-coated capillary, electrostatic repulsion between the coating and analytes results in no detectable analyte residue found after a 5-minute rinse with run buffer. To assess the adsorption quantitatively, their recoveries after passing through a 30-cm capillary were determined by three consecutive runs. For the bare capillary: SL, 79.2% ± 2.4%; UK, 77.9 ± 3.7%. For the IL-coated capillary: SL, 98.2% ± 1.9%; UK, 100.0 ± 2.7%.

4.4.2.2 Influence of pH

Buffer pH influences both mobilities of the analytes and the EOF of IL-coated capillary. In this study, the EOF migrated at higher velocity but in opposite direction to electrophoretic mobilities of the drugs, and the drugs were drawn to the detector by the EOF. Change of pH would affect the resolution between the analytes according to eq (4-1), and would substantially influence the analysis time. **Fig. 4-5** shows that both migration time and resolution increase with pH. The analytes can be baseline separated in the pH range investigated. However, at pH higher than 6, the repeatability of migration time was not good, which might due to the low buffer capacity of acetate

(pK_a of acetic acid is ca. 4.75). Additionally, analysis time increased significantly at higher pH; at pH 7, the migration time of UK was even longer than 30 minutes. Considering the above factors, a pH value of 4.5 was chosen.
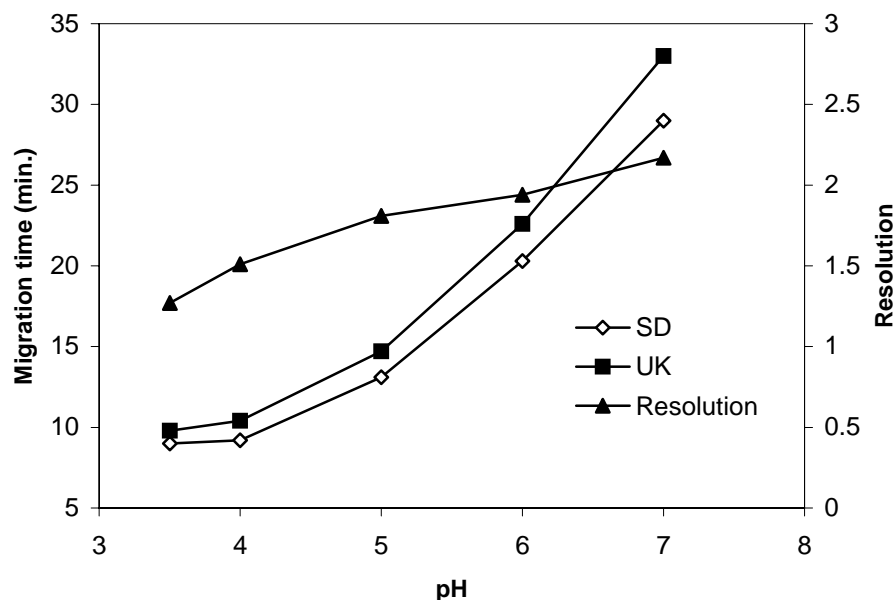
Fig. 4-5 Influence of pH on the CZE performance

The capillary: 75 μm I.D. × 70 cm. Applied voltage: -25 kV. The running buffer: 10 mM acetic acid adjusted to desired pH by 1 M ammonia. Other conditions are described in text.

4.4.2.3 Influence of injection time

The sample amount introduced into the capillary is proportional to the injection time in hydrodynamic injection; hence the detection limit decreases due to the stacking effect. However, both the separation efficiency and resolution decreased due to lengthened sample plug. Injection time of 12 seconds at 130 mbar (ca. 160 nl in volume) was optimal; when the injection time was longer than 15 sec, there showed obvious peak broadening (**Fig. 4-6**).
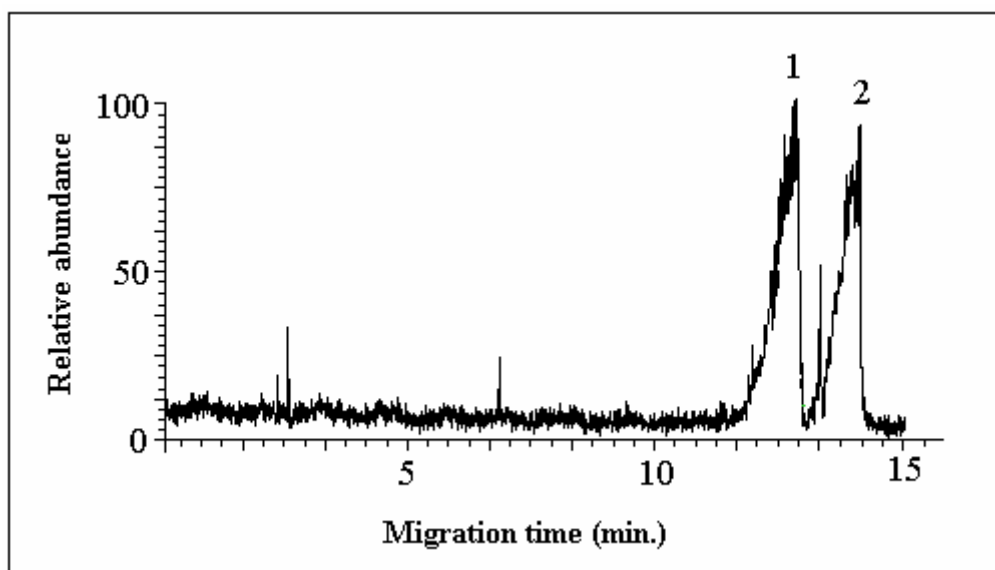
Fig. 4-6 Influence of injection time

The spiked concentrations before SPE are 100 ng/ml each. Injection time: 20 s at 130 mbar. Detected by TIC, the detecting m/z range is 50-500. Peaks: 1, SL; 2, UK. CE conditions as in **Fig. 4-5**.

4.4.2.4 Influence of separating voltage

The separating voltage is an important parameter to be considered in a CE system. The effect of separation voltages ranging from -10 to -30 kV was investigated. Although the two peaks could be separated at -10 kV, the analysis time was longer than 25 minutes. The analysis time decreased with increasing applied voltage, while the resolution of the analytes reached maximal at -20 kV and began to decrease from -25 kV. The separation voltage was set to -25 kV producing good resolution and short analysis time.

4.4.2.5 Validity of the method

Fig. 4-7 shows the representative electropherogram of SL and UK in human serum separated using the optimal parameters obtained and detected under both MS/MS and total ion chromatogram (TIC) modes. It can be seen that the signal/noise ratio in MS/MS is much higher than that under TIC mode due to the enhanced specificity by

monitoring the mother-daughter fragments reaction. The recovery of the SPE procedure and the run-run precision of CE analysis were studied and recorded in Table 4-2. It should be stated that all the concentrations in this section correspond to the spiked concentrations in human serum before SPE procedure. The linear dynamic range (LDR) of detection was determined by analysis of drug-spiked serum. The LDR of the calibration curves were 40-400 ng/ml for SL and 50-600 ng/ml for UK. Five concentration levels, namely 50, 100, 150, 200 and 300 ng/ml were used for linearity study. The calibration curve of peak area (after correcting against migration time) y vs. concentration x (ng/ml) for each drug was constructed and their regression equations and correlation coefficients r were calculated: SL, $y = 335.9x - 154.7$ ($r = 0.9994$); UK, $y = 318.3x - 190.0$ ($r = 0.9991$). In order to assess the reproducibility of the calibration curve, a three-day validation was carried out. In each day, all the five levels of standard solutions were measured three times. Each drug was evaluated with all the nine curves. The correlation coefficients for the linear best fit were better than 0.99, and the relative standard deviations (RSD) for the slopes were no more than 4.21%. The RSD of the migration times of the drugs within the three days were no more than 1.1%.

Fig. 4-7 Electropherogram of SL and UK in human serum

The spiked concentrations before SPE are 100 ng/ml each. A: detected by MS/MS, MS/MS conditions were described in the text; B: detected by TIC, the detecting m/z range is 50-500. Peaks: 1, SL; 2, UK. CE conditions as in **Fig. 4-5**.
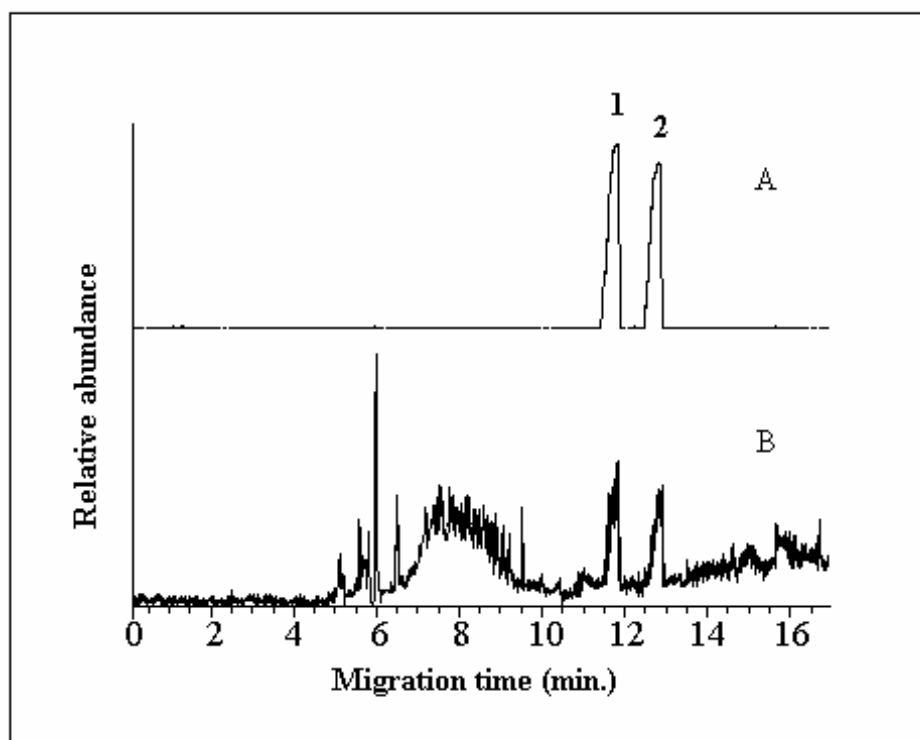
Table 4-2 Recovery, repeatability and LOD of the SPE-CZE-MS/MS method

	%Recovery ± %RSD (n=5)			RSD of t_m, %	RSD of A_p, %	LOD
	30 ng/ml	100ng/ml	300ng/ml	(n=5)	(n=5)[a]	(ng/ml)
SL	97.6 ± 7.1	100.5 ± 4.9	98.0 ± 4.2	0.69	2.5	14
UK	102.3 ± 6.7	98.3 ± 5.1	98.3 ± 4.6	0.76	3.4	17

[a] The spiking concentration was 100 ng/ml

4.5 Application 2: Separation of DNA in ILCC

4.5.1 Introduction

CE is increasingly used in the separation of DNA; in fact, it has been an attractive alternative to the conventional slab gel method. However, coating of the internal silica surface, either by covalent bonding or self-adsorption of the sieving polymer, is usually needed to suppress EOF and DNA-wall interaction [17] so that both recovery of the fragments and reproducibility of their migration times can be improved. Polymers such as linear polyacrylamide (PA) and its derivatives [18-20], polyvinylpyrrolidone [21], cellulose and its derivatives [22-24] and poly(ethylene oxide) (PEO)[25-27] have been used as sieving matrices, and some of them were also employed as self-coating reagents. Self-coating is compelling because of its simplicity. But for capillaries coated by static adsorption, performance deteriorates with multiple runs and rinsing with the coating polymer between runs is usually required. The covalent coating exhibits longer lifetime than the dynamic coating and needs less maintenance [28]. Since Hjerten proposed silanization of the capillary surface [1], a number of new materials or methods have been reported for the covalent bonding [29-45].

PEO and HEC, the weak self-coating polymers, are often-used sieving matrices for DNA separation and are efficient for large-size fragments. However, the large DNA fragments migrate at very low speed due to the sieving effect of the matrix and their migration times are usually very long in the presence of the large opposite residual EOF; sometimes, the fragments do not even reach the detector. In order to improve the separation speed, the silica surface is usually covalently coated to reduce the EOF. But as we observed in our experiment and as reported by other authors, there is still residual

EOF after the coating procedure. Another approach for fast analysis is separating DNA fragments in the presence of EOF [23,46,47] in which the analytes were drawn to the detector by the high-velocity EOF. Detection of the large-fragment DNA will not be a problem because they are drawn out first, but the migration times for the small fragments will be long. Due to the low concentration of sieving matrix used to obtain high residual EOF, the separation was only fast and better for large DNA fragments under normal polarity mode [46].

For the capillary coated with charged materials, the coating may act as both stationary phase and ion exchanger. The (small) oppositely charged species are separated under a different mode from conventional CZE and it was termed as ion-exchange open tubular capillary electrochromatography (IE-OTCEC). The technique was studied theoretically and experimentally in the past couple of years [48]. Generally, cationic coating is not chosen for DNA separation because the negatively charged DNA fragments will strongly interact with or even adsorb onto the wall. But adsorption of macromolecule onto the oppositely charged wall does not occur in all circumstances. It was reported that proteins, which are more prone to suffer adsorption during electrophoresis, would not be adsorbed onto a surface when the association constant of the protein-surface interaction was smaller than 10^3 dm^3mol^{-1} [49]. If the silica surface is covered with cationic coating, the EOF will be reversed so that it moves codirectionally with the DNA fragments and there exists a chance that the analysis times of the fragments are shortened provided that the electrostatic interaction between DNA fragments and the cationic coating is efficiently controlled. We think such coating may be an alternative approach for fast separation of these multivalent macromolecules.

In the work of Valkenberg et al [50], one IL was coated onto the silica powder surface for catalysis study. Although IL-cation also contains an imidazole ring, it remains cationic in alkaline buffer for DNA separation; moreover it is transparent at the DNA detection wavelength. Studies were carried out in this work on preparation of ILCC (CT_{223}) and assessment of its properties relating to DNA separation.

4.5.2 Results and discussion

4.5.2.1 Electrophoresis of DNA fragments in free TBE buffer

4.5.2.1.1 dsDNA

When the ΦX174 DNA-Hae III digest was electrophoresed in free TBE buffer (without sieving polymer), the mixture comigrated in both ILCC and PACC, and the peak heights increased with buffer concentration. All peaks in **Fig. 4-8** show peak tailing, extenuating with increasing buffer concentration, due to DNA-wall interaction. The electrophoretic behavior of DNA fragments varied dramatically in different coatings. In ILCC, the migration time of the DNA fragments was longer, and it decreased with increasing buffer concentration, from 33.3 min in 1× TBE to 18.3 min in 3× TBE. While in PACC DNA migration was in the range of 8-10 min and slightly increased with buffer concentration. Moreover, the peaks in ILCC were more asymmetric due to the electrostatic interaction between DNA and the positive IL-coating. The above experiments suggest that DNA interacts with both IL- and PA-coated capillaries, while the electrostatic DNA-IL interaction is stronger and is the predominant factor determining the migration time of the fragments in ILCC. The cations in TBE buffer compete with the coating for the negatively charged DNA, so the higher the

concentration, the weaker the adsorption of DNA onto the IL-coating and hence the shorter the migration time. The behavior of DNA fragments in the ILCC is similar to that described in capillary electrochromatography (CEC) [51]. The interaction between DNA and the residual siloxane or the coated PA in the PACC may be attributed to hydrogen bonding or hydrophobic adsorption, which is weaker compared with that in the ILCC. Although increasing concentration of the buffer can help to elute it from the surface (which can be confirmed from the increasing peak height), the increasing ionic strength leads to the reduced the double layer thickness and increased buffer viscosity which will cause decreased migration rates of the fragments in the buffer. So the behavior of DNA fragments in PACC is more CZE-characterized in free solution.
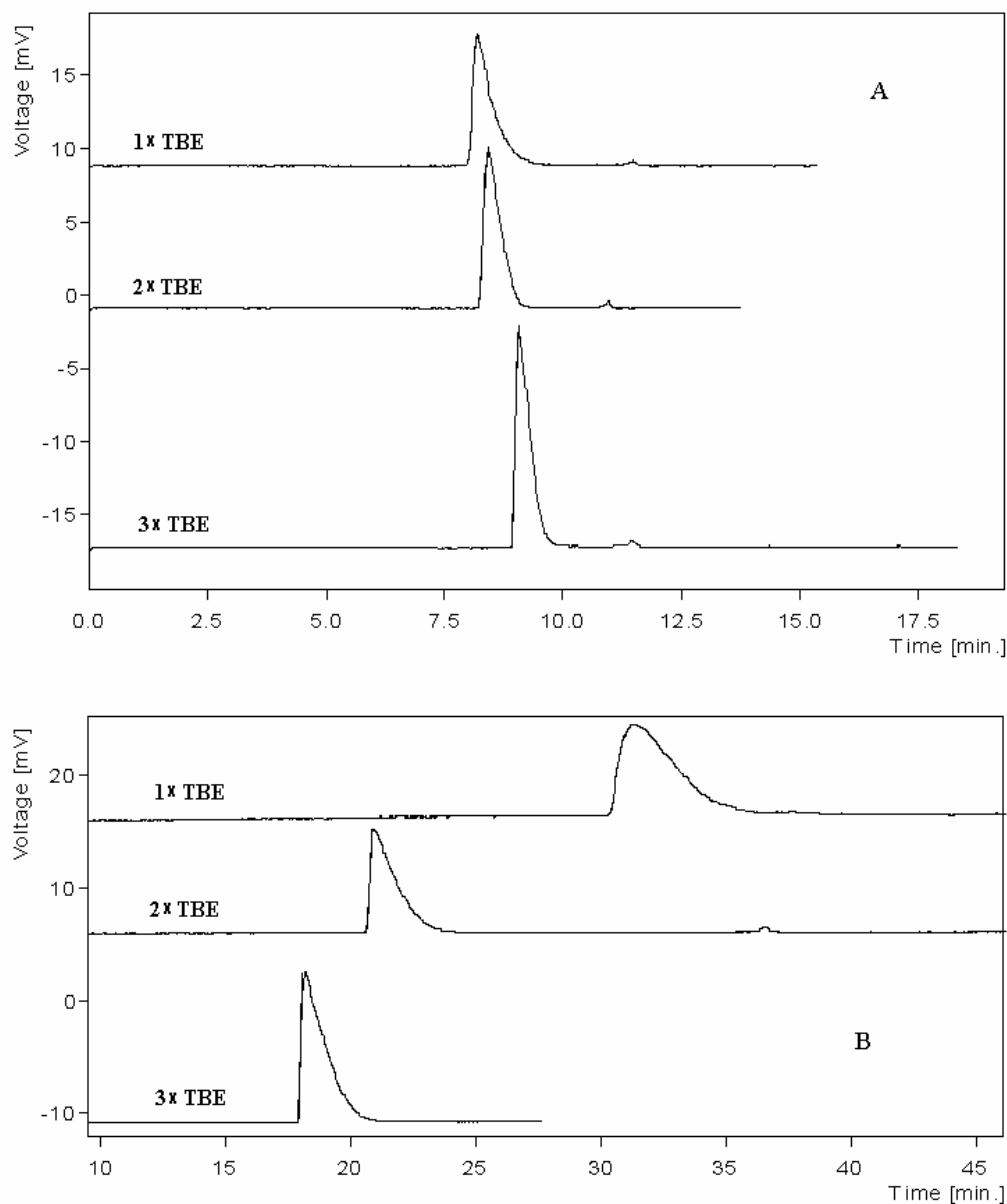
Fig. 4-8 Electropherograms of DNA in ILCC (CT$_{223}$) and PACC

A: PACC; B:ILCC. Running buffer: TBE with concentrations stated in the figure. Length of ILCC and PACC: 50/38.5 cm (total/effect length). Concentration of the DNA: ΦX174 DNA-Hae III digest diluted to 40.4 µg/ml. Sample injection: 3 kV × 3 s. The Applied voltage: -15 kV. UV detection was set at 266 nm.

4.5.2.1.2 ssDNA

CE results were also obtained with ssDNA (**Fig. 4-9**). It was observed that the mobility of

the 39-mer ssDNA was not always higher than that of the 7-mer in the PACC; in buffer

119

concentration higher than 0.5× TBE, the 7-mer was higher. But may be due to the influence from the cationic coating, the mobility of the 39-mer DNA was higher in the ILCC over the investigated buffer range.
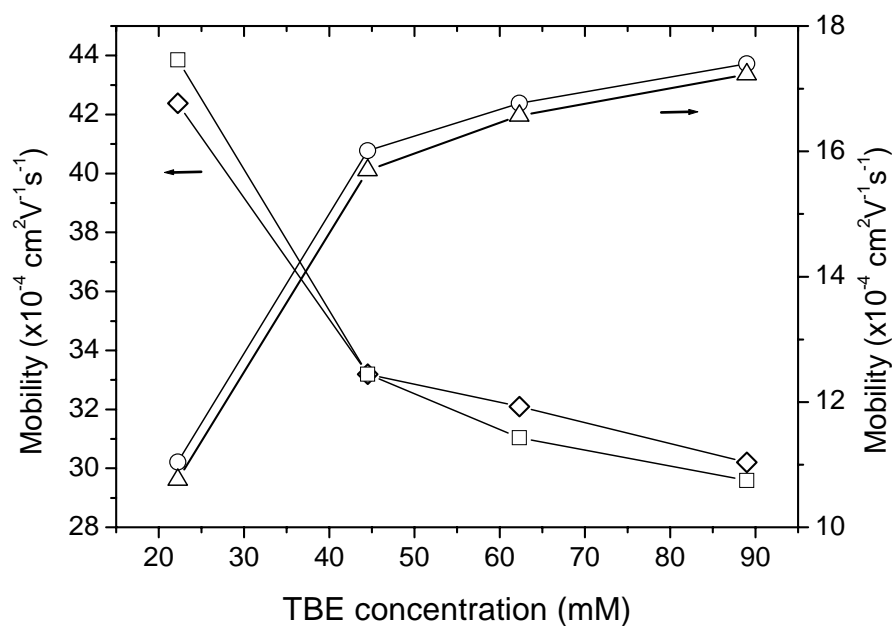
Fig. 4-9 Mobility differences of ssDNA in ILCC (CT$_{223}$) and PACC

The electric field strength was 200 V/cm. O: 39-mer in ILCC; Δ: 7-mer in ILCC; □: 39-mer in PACC; : 7-mer in PACC. Other conditions were same as in **Fig. 4-8**

4.5.2.2 Electrophoresis of DNA fragments in the presence of sieving matrix

4.5.2.2.1 *Dependence of EOF on sieving matrix*

Both HEC and PVP added into buffer suppress EOF by adsorbing onto the silica surface and by increasing the buffer viscosity as well. However, PVP was found to be more

efficient in suppressing EOF. The residual EOFs in the above two capillaries were negligible in the presence of 1% PVP. While in buffer consisting of 1 ×TBE and 1% HEC, anodic and cathodic EOFs were observed in ILCC and PACC respectively. PVP is more efficient in suppressing EOF than HEC because it is more hydrophobic [52,53]. It was reported that even in a bare silica capillary, the interaction between the hydrophobic PVP and the hydrophobic siloxane on the silica surface favors its adsorption [54]; also, as pointed out by Chiari et al [55], hydrogen bonding between the surface silanol and PVP plays a role in the adsorption and stability of the coating.

4.5.2.2.2 *Dependence of DNA-IL interaction on fragment size*

HEC is not a strong self-coating polymer and it was employed to obtain high residual EOF rate for DNA separation [23]. In our experiments, the anodic EOF of ILCC in the presence of 1% HEC suggests that the coated IL-cations are not completely shielded by the polymer. Although there exists interactions between DNA and the PA coating, the free mobility of DNA fragment is virtually unchanged [19]. So it may be possible to investigate DNA-IL interaction by plotting the mobility difference of the fragment between the PACC and IL coated capillaries vs. the fragment size. (**Fig. 4-10**) shows that the mobility of a given DNA fragment in ILCC is lower than that in PACC. The mobility difference, within experimental error, is obviously size-dependent; it increases with fragment size and becomes constant at a certain number of base pairs (near 900 bp). Since the electrophoretic conditions were identical for the two capillaries, the low mobilities of the DNA fragments in ILCC may be the direct consequence of the electrostatic DNA-IL interaction, which increases with charge density of DNA fragments. The above experiments suggest that the charge density of DNA fragments increase with fragment size till 900 bp; the result is similar to a previous report stating

that the charge density of DNA fragment increases with size and become constant from 400 onwards [19]. But such interaction does not lead to resolution of the corresponding fragments in buffer free of sieving polymer, their peaks merged as shown in **Fig. 4-8**B.

Fig. 4-10 also illustrates that the mobility difference decreases with increasing concentration of sieving matrix, which suggests that the capillary wall was further covered by the increasing amount of HEC added into the buffer; thus the interaction between DNA fragments and IL cations became weaker. Moreover, the collision frequency between DNA and the wall decreased in the presence of high concentration sieving polymer [56]
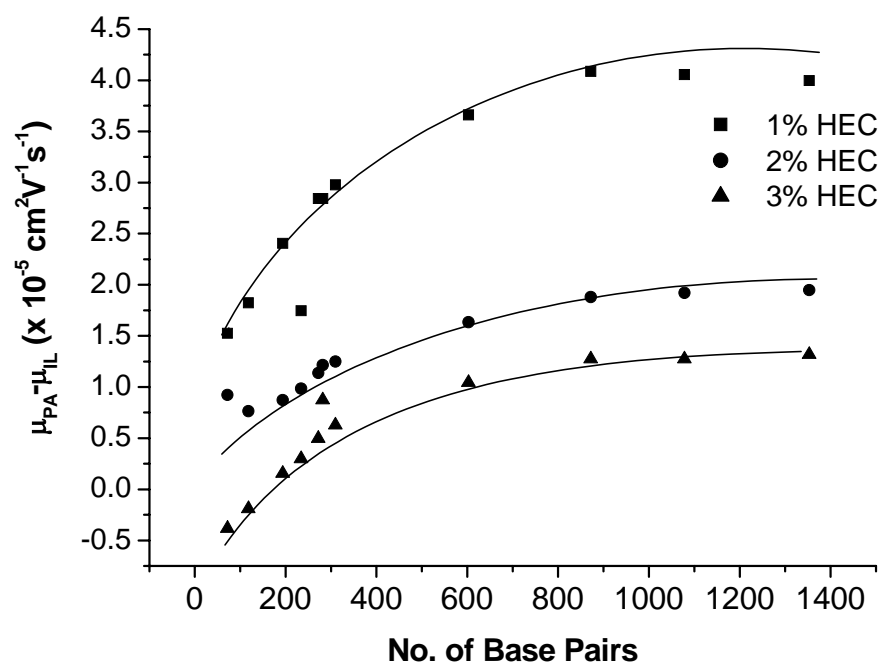
Fig. 4-10 Dependence of DNA-IL interaction on No. of base pairs

Buffer: 2× TBE plus desired concentration of HEC as stated in the figure. Other conditions as in **Fig. 4-8**.

4.5.2.2.3 *Influence of buffer concentration*

Buffer concentration is another important parameter in DNA separation. The electropherograms obtained in ILCC and PACC were similar (**Fig. 4-11**), and resolution of the peaks improved in both capillaries due to solvent-fragment interaction [57]. Peak heights enhanced from low to high buffer concentration in both capillaries mainly due to the increasing stacking factor during electrokinetic injection, but less due to the increasing elution ability of the high concentration buffer - in the buffer containing sieving polymer PVP, the adsorption of DNA fragments onto the internal capillary surface was significantly suppressed because it was effectively covered
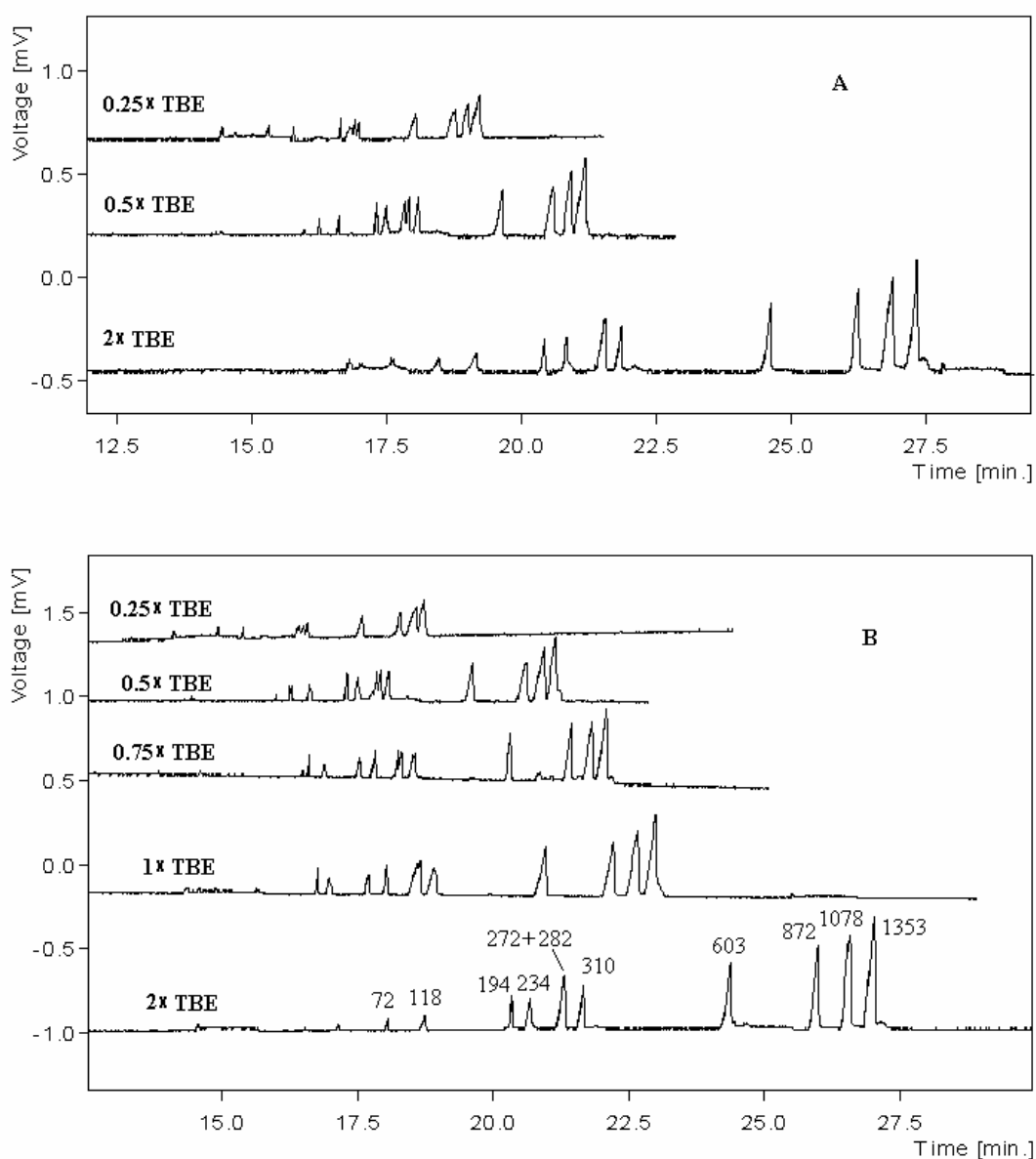
Fig. 4-11 Influence of buffer concentration on DNA separation

Buffer: desired concentration of TBE mixed with 2% PVP. Capillaries: A, PACC; B, ILCC. Other conditions as in **Fig. 4-8**.

4.5.2.2.4 *Influence of electric field strength*

Electric field strength affects the mobility of DNA migrating in a porous matrix [58] (both HEC and PVP were entangled at the concentrations in the experiment). Generally,

124

the separation is improved in lower field strength because of the longer interaction time of DNA with the sieving polymer. **Fig. 4-12** shows that the influence of separation voltage on the migration of DNA fragments depends on polymer concentration and species. In 1% HEC sieving matrix, apparent mobilities of all the fragments in ILCC and PACC were obviously changed (top right panel of Fig 4A) with applying voltage; the migrations of large fragments were more retarded under the low electric field strength and the resolution corresponding peaks was notably improved, from partially merging to baseline separation. But for the separation in 2% PVP matrix in ILCC, although migration times of the fragments changed with the electric field strength, the migration patterns of the DNA fragments under different separation field strengths were almost same and there was no significant improvement in peak resolution in lower electric field strength. The experiments in PACC showed similar results (electropherograms not shown).
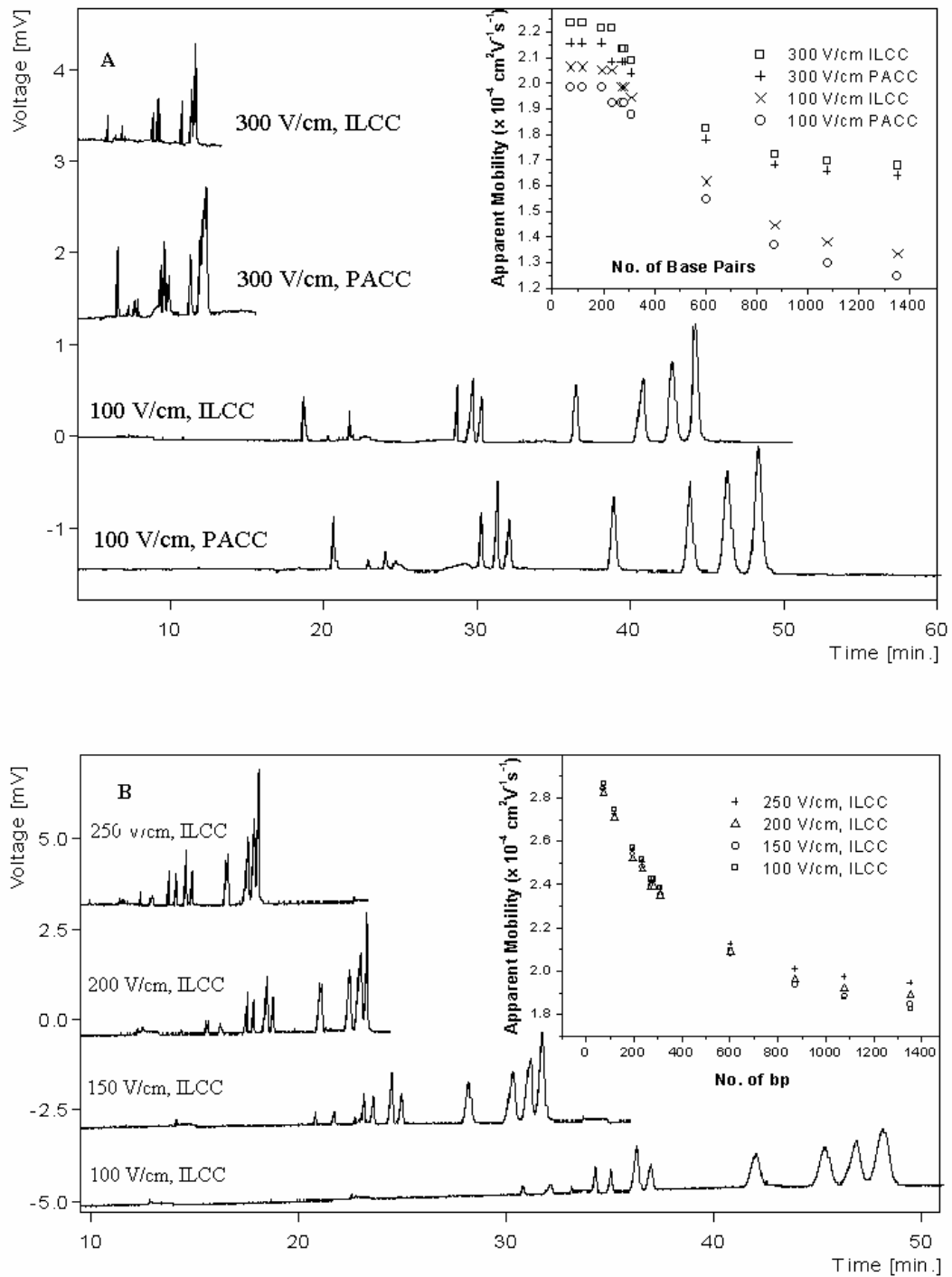
Fig. 4-12 Influence of electric field strength

Buffer: A, 2× TBE + 2% HEC; B, 2× TBE + 2% PVP. The experiments were conducted in ILCC.

4.5.2.2.5   Influence of sieving polymers

Although resolution between fragments generally improves with the increasing matrix concentration, HEC and PVP showed different influences on DNA fragments. When the running buffer contained PVP, there showed little difference between PACC and ILCC in terms of analysis time and resolution of the fragments (**Fig. 4-12**A). The coating difference was almost eliminated by the strongly adsorbed PVP. In the presence of 2% HEC, DNA fragments migrated in similar patterns in the two capillaries (**Fig. 4-11**). But the fragments of 72 and 118 bp, separated in PACC, comigrated in ILCC probably due to the influence from the IL coating. They were baseline resolved in 4% HEC (electropherogram not shown). From HEC concentration of 2% onward, the analysis times in the ILCC were shorter.

4.5.2.3 Stability of the IL coating

The stability of the IL- and PA-coating was investigated in a 4-day period with two runs a day. 2% HEC was chosen as sieving matrix because it could separate the DNA fragments (although partially, but enough for performance assessment) and did not completely cover the coating surface. Every day in the morning, the ΦX174 standard was electrophoresed in the fresh buffer; eight hours later, another run was carried out. The buffer was left in the capillary over night. The migration times of the fragments showed detectable trends in the two capillaries, which suggests the gradual hydrolysis of the Si-O-Si bond. But the change was very slow and the maximum relative errors in migration time were 4.78% for ILCC and 3.71% for PACC (Table 4-3). While plate number and resolution between peaks did not decrease significantly, suggesting that the deterioration of the capillary coating was not so serious. Considering the capillary effective length, the separation efficiencies were all more than 10^5 plates/meter. The

ILCC can be used with the separation buffer for at least 96 hours without substantial deterioration in performance.

Table 4-3 Comparison of stability and reproducibility of ILCC with PACC

| No. of bp | Migration time (min.) | | | | Plate number ($\times 10^4$) | | | | Resolution | | | |
| | ILCC | | PACC | | ILCC | | PACC | | ILCC | | PACC | |
	1st	96th	1st	96th	1st	96th	1st	96th	1st	96th	1st	96th
72			22.89	23.69			11.4	19.7				
118	21.77 [a]	22.81	23.96	24.71	33.0	38.8	12.4	11.4			3.9	3.8
194 + 234	28.85	29.52	30.22	31.07	22.0	20.5	14.5	11.6	46.3	47.9	21.3	22.5
271+281	29.81	30.50	31.23	31.91	8.6	7.9	9.4	10.2	3.1	2.7	2.8	2.8
310	30.46	31.21	31.99	32.71	13.8	10.7	9.9	13.2	1.8	2.1	1.9	2.0
603	36.65	37.71	38.84	39.80	6.7	7.0	7.0	6.9	13.8	13.6	13.7	13.4
872	40.93	42.30	43.77	44.94	4.3	4.5	5.0	5.9	6.3	7.0	7.2	7.4
1078	42.93	44.51	46.21	47.52	4.6	4.1	4.6	6.1	2.5	2.5	3.0	3.1
1353	44.37	46.20	48.19	49.98	6.8	7.3	4.8	4.2	1.9	1.8	2.3	2.5

[a] in ILCC, the peaks of 72 bp and 118 bp merged

4.6 Summary

The EOF of capillary was reversed with covalently bonded IL-coating; the rate of the EOF was influenced by the buffer conditions and the coating parameters as well. The ILCC (CT_{223} as example) could be used for at least 96 hours with relatively stable EOF.

The resolution between SL and UK was enhanced in the ILCC due to the modified EOF. Additionally, the adsorption of the drugs onto the internal capillary surface which occurred in bare capillary was eliminated due to the electric repulsion between the positively charged analytes and the coating. The SPE-CZE-MS/MS method developed in this study is of good recovery, high sensitivity and selectivity; it can detect SL and UK in human serum at concentrations as low as 14 and 17 ng/ml, respectively.

When it was employed in separation of DNA fragments, ILCC showed strong interactions with DNA fragments in buffers of low ionic strength because of their opposite charges. The interaction between DNA and the IL-coating in buffer containing sieving matrix is determined by the electrostatic attraction that increases with fragment charge density; the DNA fragment with higher charge density is more retarded. With introduction of sieving polymer, DNA fragments can also be separated in ILCC in similar patterns as that of PACC. In TBE buffers containing HEC higher than 2%, the analysis time is shorter in ILCC. Our experiments showed that the ILCC exhibits comparable long-term stability as the PACC in DNA separation.

This chapter demonstrates applications of IL-coated capillary in separation of both cationic and anionic species. The results suggest that the ILCC can offer good performance.

References

[1] S. Hjerten, J. Chromatogr. 347 (1985) 191

[2] C.Y. Liu, Y.W. Ho, Y.F. Pai, J. Chromatogr. A. 897 (2000) 383

[3] B.A. Williams, G. Vigh, Anal. Chem. 68 (1996) 1174

[4] J. Henion, E. Brewer, G. Rule, Anal. Chem. 70 (1998) 650a

[5] Pfizer Inc., Viagra: Compound Data Sheet, Pfizer Inc. 1998

[6] A. Burls, L. Gold, W. Clark, Brit. J. Gen. Pract. 51 (2001) 1004

[7] S.G. Moreira, R.E. Brannigan, A. Spitz, F.J. Orejuela, L.I. Lipshultz, E.D. Kim,
Urology 56 (2000) 474

[8] J.J.B. Nevado, J.R. Flores, G.C. Penalvo, N.R. Farinas, Electrophoresis
22 (2001) 2004

[9] B.H. Jung, D. Moon, B.C.Chung, Can. J. Anal. Sci. Spect. 46 (2001) 40

[10] J.D.H. Cooper, D.C. Muirhead, J.E. Taylor, P.R. Baker, J. Chromatogr. B 701
(1997) 87

[11] A. Eerkes T. Addison, N.D. Weng J. Chromatogr. B. 768 (2002) 277

[12] K. Saisho, K.S. Scott, S. Morimoto, Y. Nakahara, Biol. Pharm. Bull. 24 (2001)
1384

[13] S.F.Y. Li, Capillary Electrophoresis: Principles, Practice,, Applications, Elsevie,
New York, 1992, pp.15

[14] J.E. Melanson, N.E Baryla,. C.A. Lucy, Trac-Trend Anal. Chem. 20 (2001) 365

[15] Q.C. Liu, F.M. Lin, R.A Hartwick,. J. Chromatogr. Sci. 35 (1997) 126

[16] J.K. Towns, F.E. Regnier, Anal. Chem. 63 (1991) 1126

[17] M. Chiari, M. Cretich, J. Horvath, Electrophoresis 21 (2000) 1521

[18] D.N. Heiger, A.S. Cohen, B.L. Karger, J. Chromatogr. 516 (1990) 33

[19] N.C. Stellwagen, C. Gelfi, P.G. Righetti, Biopolymers 42 (1997) 687

[20] M. Chiari, S. Riva, A. Gelain, A. Vitale, E. Turati, J. Chromatogr. A 781 (1997) 347

[21] H.M. Pang, V. Pavski, E.S. Yeung, J. Biocem. Biophys. Methods 41 (1999) 121

[22] A.E. Barron, W.M. Sunada, H.W. Blanch, Electrophoresis 17 (1996) 744.

[23] D.T. Mao, J.D. Levin, L.Y. Yu, R.M.A. Lautamo, J. Chromatogr. B 714 (1998) 21

[24] F.T. Han, B.H. Huynh, Y.F. Ma, B.C. Lin, Anal. Chem. 71 (1999) 2385

[25] R.S. Madabhushi, M. Vainer, V. Dolnik, S. Enad, D.L. Barker, D.W. Harris, E.S. Mansfield, Electrophoresis 18 (1997) 104

[26] C.H. Wu, T.B. Liu, B. Chu, Electrophoresis 19 (1998) 231

[27] H.S. Chen, H.T. Chang, Anal. Chem. 71 (1999) 2033

[28] J. Horvath, V. Dolnik, Electrophoresis 22 (2001) 644

[29] S. Hjerten, K. Kubo, Electrophoresis 14 (1993) 390

[30] A. Cifuentes, M. Defrutos, J.M. Santos, J.C. Diezmasa, J. Chromatogr. 655 (1993) 63

[31] M.A. Strege, A.L. Lagu, J. Chromatogr. 630 (1993) 337

[32] J.K. Towns, J.M. Bao, F.E. Regnier, J. Chromatogr. 599 (1992) 227

[33] W. Nashabeh, Z. Elrassi, J. Chromatogr. 559 (1991) 367

[34] K.A. Cobb, V. Dolnik, M. Novotny, Anal. Chem. 62 (1990) 2478

[35] H.J. Jung, Y.C. Bae, J. Polym. Sci. Pol. Chem. 40 (2002) 1405

[36] Z.X. Zhao, A. Malik, A. L. Lee, Anal. Chem., 65 (1993) 2747

[37] D. Schmalzing, C.A. Piggee, F. Foret, E. Carrilho, B.L. Karger, J. Chromatogr. A 652 (1993) 149

[38] J.T. Smith, Z. Elrassi, Electrophoresis 14 (1993) 396

[39] M. Chiari, M. Nesi, J.E. Sandoval, J.J. Pesek, J. Chromatogr. 717 (1995) 1

[40] M.X. Huang, J. Plocek, M.V. Novotny, Electrophoresis 16 (1995) 396

[41] C. Gelfi, M. Curcio, P.G. Righetti, R. Sebastiano, A. Citterio, H. Ahmadzadeh,

[42] N.J. Munro, A.F.R. Huhmer, J.P. Landers, Anal. Chem. 73 (2001) 1784

[43] M. Nakatani, A. Shibukawa, T. Nakagawa, Electrophoresis 16 (1995) 1451

[44] K. Srinivasan, C. Pohl, N. Avdalovic, Anal. Chem. 69 (1997) 2798

[45] H.J. Tian, L.C. Brody, D. Mao, J.P. Landers, Anal. Chem. 72 (2000) 5483

   N. J. Dovichi, Electrophoresis 19 (1998) 1677

[46] M.F. Huang, C.E. Hsu, W.L. Tseng, Y.C. Lin, H.T. Chang, Electrophoresis 22

   (2001) 2281

[47] H.S. Chen, H.T. Chang, J. Chromatogr. A 853 (1999) 337

[48] R. Xiang, C. Horváth, Anal. Chem. 74 (2002) 762

[49] C.J. van Oss, Colloid Surface A 78 (1993) 1

[50] M.H. Valkenberg, C. Decastro, W.F. Holderich, Top Catal. 14 (2001) 139

[51] M.C. Breadmore, E.F. Hilder, M. Macka, N. Avdalovic, P.R. Haddad,

   Electrophoresis 22 (2001) 503

[52] M.N. Albarghouthi, B.A. Buchholz, P.J. Huiberts, T.M. Stein, A.E. Barron,

   Electrophoresis 23 (2002) 1429

[53] R.S. Madabhushi, Electrophoresis 19 (1998) 224

[54] T. Tanahashi, M. Kawaguchi, T. Honda, A. Takahashi, Macromolecules 27 (1994)

   606

[55] M. Chiari, M. Cretich, F. Damin, L. Ceriotti, R. Consonni, Electrophoresis 21

   (2000) 909

[56] Y. Jin, B.C. Lin, Y.S. Fung, Electrophoresis 22 (2001) 2150

[57] N.C. Stellwagen, A. Bossi, C. Gelfi, P. G. Righetti, Anal. Biochem. 287 (2000) 167

[58] C. Heller, Electrophoresis 19 (1998) 3114

CHAPTER 5 IONIC LIQUIDS AS BACKGROUND ELECTROLYTE AND COATING MATERIAL

5.1 Introduction

CZE is an increasingly used technique in the separation of ionic species because of its high resolution, short analysis time, little buffer consumption and simplicity in operation [1]. Separation of alkali and alkaline-earth metals, and ammonium ion by CZE has been actively studied due to the real-world requirements [2-9]. The chelating reagents such as lactic acid, melonic acid and tartaric acid can be added into the separation buffer to modify the mobilities of alkaline-earth metal ions, while inclusion complex reagents such as 18-crown-6 ether [5-8] and poly(ethylene glycol) [10] were used to separate the co-migrated ammonium and potassium ions, and to improve the resolution between some alkaline-earth metal ions.

Optical detection is the most commonly used detection method in CE. Because most metal ions are UV and fluorescence inactive, the ions have to be detected by indirect mode in which imidazole, nicotinamide, pyridine, benzylamine and benzimidazole have been used as background visualization ions [11-13]. However, indirect detection usually results in lower sensitivity than the direct modes [14,15]. Furthermore, optical detection presents a disadvantage for CE because the optical path length (diameter of the capillary) is generally less than 100 μm in order to favor better dissipation of Joule heat during the separation process. Potential gradient detection (PGD), one of the electrochemical detection methods, is based on the changes of the electric field strength during electrophoresis. Because the electric field strength is inversely proportional to

the ionic mobility, a change in signal will be generated when the sample zone of different mobility than the buffer passes through the detecting electrodes. It is a universal detecting method for charge-carrying species. Like the optical method, the direct PGD method, in which the mobility of the analyte is higher than that of the background co-ion, offers higher detection sensitivity than the indirect mode. Although PGD is the most straightforward method and simple to be applied [14], it is not widely used possibly due to difficulties in achieving high sensitivity so far.

As stated in eq (1-23) of Chapter 1, resolution (*Rs*) of CZE is the function of the column efficiency (N) and the relative mobility. It is obvious that besides the column efficiency, relative mobility is another factor which should be considered in optimizing resolution. The apparent mobility of a species is the sum of its intrinsic mobility and the EOF. Cations in bare silica capillary move codirectionally with EOF and hence their relative mobilities are low. There are several ways to control the relative mobility of the analytes. One is to alter, or better to reverse, the EOF of capillary so that apparent mobilities of the analytes can be lowered. Another approach is addition of organic solvents into the running buffer [16-19]. Besides changing the mobilities of the analytes, organic solvents added into the running buffer also suppress EOF, but they normally do not result in reversed EOF. As reported [18], the electrophoretic mobilities of the analytes decreased almost linearly as the percentage of the methanol in the background electrolyte increased, and hence the separation of metal ions having adjacent migration times was improved. However, there were also reports stating that addition of methanol changes the selectivity of separation by solvating cations through ion-solvent dipole interaction [3,4] and therefore crossover of the peaks might occur. Introduction of organic solvent into the buffer also brings a disadvantage, e.g., some of

the organic solvents in the buffer may evaporate gradually during storage and such evaporation may become faster during the electrophoresis process due to Joule heating generated, and consequently leads to poor reproducibility.

Generally, EOF can be reversed by three approaches: a) adding cationic surfactant directly into the run buffer; b) making the surfactant adsorb onto the internal capillary surface by rinsing the capillary with cationic surfactant solution before run, while the running buffer containing no surfactant; c) covalently bonding the cationic surfactant onto the capillary surface [20]. However, problems were often encountered with the non-covalent coatings. In method a), the surfactant added is likely to form ion pairs with background electrolytes and sometimes may lead to precipitation [21]; while reconditioning steps of the polymeric coating are usually required between each run for method b) [22,23]. The covalent bond coating showed a strong beneficial influence on the CE performance. It is more efficient in suppressing EOF and can show great stability at high pH [24].

Our experiments in Chapter 2 showed that some 1,3-dialkylimidazolium cations could complex with α-CD and resulted in very low mobilities [25]. Thus it is possible to improve the detection sensitivity if such α-CD-complexed dialkylimidazolium is employed as background co-ion in PGD.
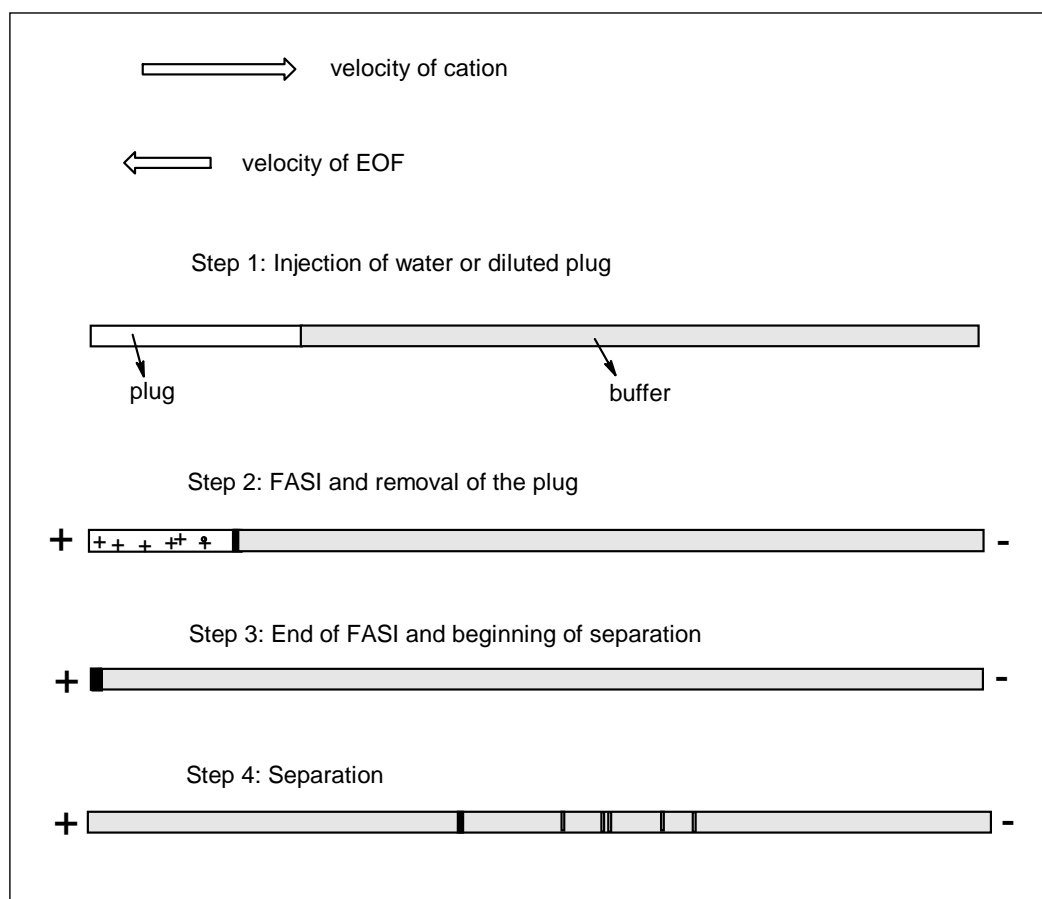
Fig. 5-1 Schematic diagrams illustrating the procedures of FASI

Field-amplified sample injection (FASI) is an effective way for on-column preconcentration of charged species [26-29]. This technique requires analytes migrating oppositely with EOF. To perform FASI, the samples are prepared in a low-conductivity solution, sometimes in water. A field enhancement can be achieved at the injection point during electrokinetic injection. Because the analytes migrate oppositely with EOF, it is possible to push the injected water plug out of the capillary by EOF during injection. The technique employed in this research generally contains four steps as shown in **Fig. 5-1**. During Step 1, a plug of low-conductive solution is hydrodynamically injected into the capillary. During step 2, the inlet end of the capillary is transferred to the sample solution and a voltage is applied to inject metal ions to the capillary. The ions would experience a field-amplified enrichment and concentrate at the boundary of

plug and buffer. Meanwhile, the plug moves out of the capillary from the injection end under the effect of anionic EOF. During this period, the signal from the potential gradient detector will increase due to the increasing conductivity in the capillary. At the end of sample injection, the inlet is transferred to the run buffer (Step 3) and then a separation voltage is applied across the capillary (Step 4). Because the potential changes measured by the PGD detector reflects the process of water plug removal, the procedure can be conveniently and precisely monitored. Also because no polarity switching is needed between injection and separation, high reproducibility may be obtained [27].

There are usually a number of factors affecting the experiment results. Experiments are often carried out firstly to determine the relationship between performance (response) and some set of factors (variables) of interest, usually by constructing a curve that describes the response over an appropriate range of these variables. These curves may be referred to as response surfaces which can in turn be useful in characterizing the response for optimization purposes. The face-centered composite design is one of the often-used methods in optimizing experimental conditions. There are three trials for each variable, two for extreme level settings and one at the midpoint of the study range. It provides information on both direct effects and curvilinear variable effects. For the three-dimension (three variables), only 15 runs are needed for optimization.

In this study, the separation behavior of alkali and alkaline-earth metal, ammonium and heavy metal cations by CZE was investigated. Four IL cations, 1-hexyl-3-methylimidazolium (HMIM), 1-decyl-3-methylimidazolium (DMIM), 1-butyl-3-methylimidazolium (BMIM) and 1-(4-hydroxy-butyl)-3-methylimidazolium (HBMIM) were compared as background co-ion; and lactic acid 18-crown-6 ether were used as

chelating reagent and inclusive complex reagent respectively for the analytes in an ILCC. With addition of α-CD into run buffer, the mobility of the background electrolyte decreases and is lower than the analytes. So, the direct PGD method was employed in this experiment. Under optimized conditions, baseline separation of the 11 analytes (Li^+, Na^+, K^+, Cs^+, Mg^{2+}, Ca^{2+}, Sr^{2+}, Ba^{2+}, NH_4^+, Ni^{2+}, Pb^{2+}) were accomplished within 14 minutes with detection limits as low as sub-ppb level using the FASI technique.

5.2 Experimental

5.2.1 Synthesis of ionic liquids and coating

Four ILs, namely, 1-decyl-3-methylimidazolium chloride (DMIMCl), 1-hexyl-3-methylimidazolium bromide (HMIMBr), 1-butyl-3-methylimidazolium chloride (BMIMCl), 1-(4-hydroxy-butyl)-3-methylimidazolium bromide (HBMIMBr), were synthesized and converted to the hydroxide forms by the methods described in Chapter 2. The capillary was coated by CT_{122} (please refer to Section 4.2 of Chapter 4 for details).

5.2.2 Sample injection

For the hydrodynamic injection, the metal ions dissolved in run buffer were injected into the capillary by 50 mbar $\times$ 5 s. For ILCC coupled with PGD, FASI was employed. The targets were dissolved in 50-fold diluted run buffer. Ultrapure water or run buffer diluted to different ratios (1/50, 1/100, 1/200 or 1/300) was injected into the capillary by 50 mbar for different durations (20, 50, 100, 150 or 200s) as the "water plug" that would be removed by EOF during FASI. The injection end was then dipped into the

sample vial and a voltage of 4 kV was applied to electrokinetically inject the sample into the capillary. The injection procedure was monitored by the PGD detector (CE-P1, CE Resources, Singapore, Republic of Singapore). The signal from the detector was collected by CSW software, the signal would increase with the pushing out of the plug of low conductivity and introduction of the sample. When the signal reached 90% of the maximum, the voltage was increased to 8 kV till all the analytes had been detected. For the same sample and procedure, the time passed before the baseline reached 90% of the maximum was recorded and the quantitative runs were time-controlled.

5.3 Results and discussion

5.3.1 Background co-ion

Detection of analytes in PGD is based on the mobility difference between the analyte and the background co-ion; the larger the difference, the higher the signal. In order to obtain high sensitivity, the mobility of the selected IL-cation should be lowered. Our previous study [25] suggested that the mobilities of BMIM could be modified by complexation with α-CD, while the mobility of imidazole was not affected even in the presence of the high concentration complex reagent. In this work, ionic liquids composed of BMIM, HBMIM, HMIM and DMIM were tested for the feasibility as co-ions. Their mobility variations with α-CD concentrations were measured and plotted in **Fig. 5-2**. It can be seen that the mobilities of BMIM, HMIM and DMIM decrease with increasing α-CD concentration; the mobility of BMIM keeps dropping in the whole range investigated, while the mobilities of HMIM and DMIM drop and level off at ca. 5 and 7 mM, respectively. Using the method described in the literature [25] and

employing imidazole as internal standard, the complexation constants of BMIM, HMIM and DMIM with α-CD were calculated to be 23, 80 and 117 respectively. The larger complexation constant of the cation with longer alkyl chain may be attributed to the higher hydrophobicity corresponding to the alkyl chain. It is strange for the mobility of HBMIM to remain unchanged because the only difference between HBMIM and BMIM is the group connecting to the terminal carbon of butyl: it is hydrogen for BMIM and hydroxy for HBMIM. One possible reason could be that the hydroxy group decreases the hydrophobicity of HBMIM.

BMIM, HMIM and DMIM were tested as background co-ions in separation and detection of the analytes; the buffers were added to desired concentrations of α-CD. Our experiments showed that amongst the three IL cations, BMIM offered the lowest sensitivity for the analytes; while DMIM showed interaction with some of the targets such as lithium, which resulted in low sensitivity and bad-shape peaks. HMIM could offer desirable detection limits of the analytes with acceptable peak shape.
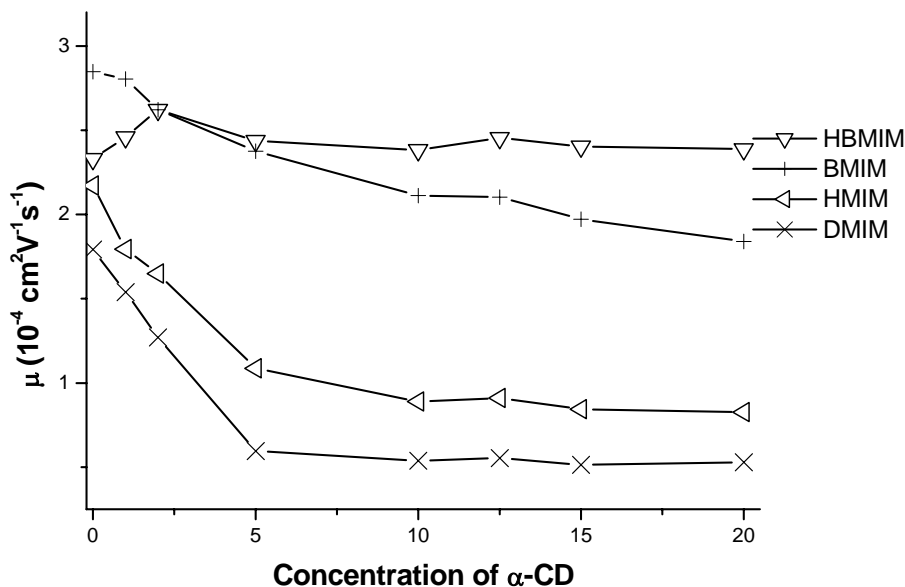
**Fig. 5-2** Effect of α-CD on mobilities of IL cations
Buffer: 20 mM sodium dihydrogen phosphate adjusted to pH 7.0 by 4 N sodium hydroxide.
Capillary: 40/50 cm of effective/total length. Applied voltage: 14 kV. Detection: UV at 210 nm.
Injection: 50 mbar × 5 s.

5.3.2 Influence of IL coating

Reversed EOF was observed because the internal capillary surface was covered with

CT_{122}. The reversed EOF enhanced resolutions of the cationic analytes, but it also

lengthened analysis time.

Fig. 5-3 shows that the shoulder-merging peaks of magnesium and lead in the bare silica

capillary was baseline separated in the CT_{122} coated capillry. It was also determined that

the separation efficiency, in terms of plate number, increased from 8.70 –37.3 × 10^4

plates/m with bare capillary (excluding the peaks of magnesium and lead) to 12.7-47.3×

10^4 plates/m with the IL-coated capillary, which might be due to the repulsive force

between the cations and the positively charged capillary surface [20]. The increased

efficiency observed with the IL coated column is significant because the analyte-wall

interaction which can seriously degrade separation efficiency in bare capillary is alleviated. The baseline, although still showed drifting, was more stable than that of uncoated capillary, favoring a low detection limit.
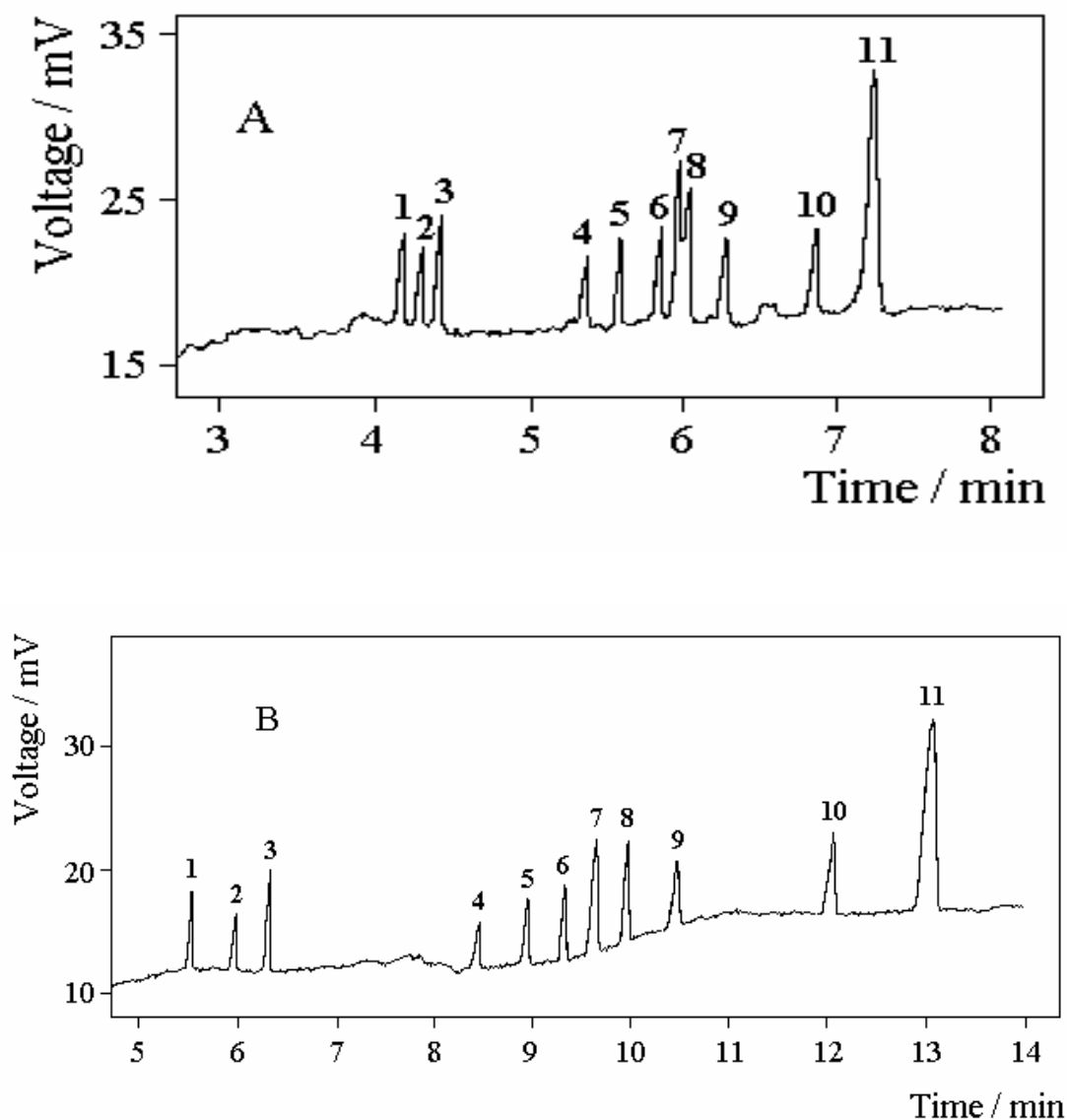

Fig. 5-3 Comparison of bare and ILCC (CT_{122})

Capillaries: A) Bare silica; B) IL-coated (CT_{122}). Buffer: 7.5 mM lactic acid, 0.6 mM 18-crown-6, 12 mM α-CD, adjusted to pH 4.0 by 100 mM HMIM hydroxide. Peak (concentration in μg/ml): 1, Cs^+ (2.5); 2, NH_4^+ (0.1); 3, K^+ (0.5); 4, Ca^{2+} (0.5); 5, Sr^{2+} (1); 6, Na^+ (0.5); 7, Pb^{2+} (5); 8, Mg^{2+} (0.5); 9, Ba^{2+} (2.5); 10, Ni^{2+} (2.5); 11, Li^+ (0.5). Others as **Fig. 5-2**.

5.3.3 Effect of buffer pH

Lactic acid is a weak complex reagent to the divalent and some of the monovalent ions such as lithium with a pK_a value of 3.86 [30], thus change of pH should influence the degree of complexation of the metal ions. **Fig. 5-4** shows variation of mobilities of the analytes with buffer pH. As expected, magnesium, calcium, barium, lead and nickel ions move at lower speed with the increasing buffer pH owning to the ion-lactate complex formed. Increase in pH would change the migration orders of some analytes, for example, sodium, calcium and lead: at pH 3.3, calcium and lead comigrated followed by sodium; from 3.5 to 4.3, they migrated in the order of calcium, lead and sodium; as pH further increased, sodium migrated out between the other two cations; at pH 4.8, the order changes to be sodium and calcium (merged) followed by lead. The best resolution of the analytes could be obtained between pH 3.75-4.25.
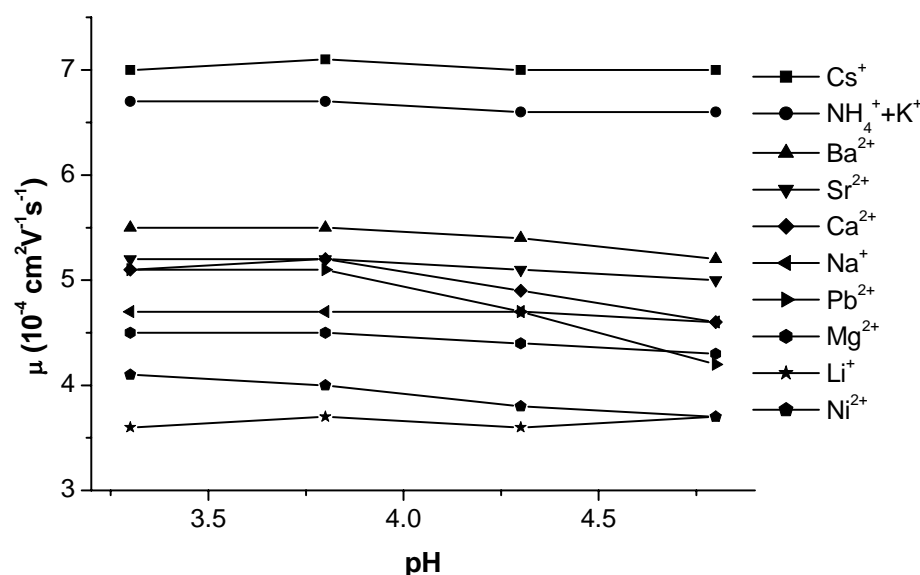

Fig. 5-4 Influence of buffer pH on mobilities of ions
Buffer: 7.5 mM lactic acid adjusted to desired pH by 100 mM HMIM hydroxide. Capillary: 40 cm. Applied voltage: 8 kV. Injection: 50 mbar × 15 s. Detection: PGD

5.3.4 Effect of 18-crown-6

18-Crown-6 binds metal ions through its inside oxygen atoms which carry unshared pairs of electrons and thus can form inclusive complexes with some ions (**Fig. 5-5**) [31]. The binding leads to a new and bulky cation and therefore the migration velocity of the bound species is lowered in the electric field. It has a cavity diameter of 0.27 nm [3] and its selectivity to the ions is dependent on the size-fit between the cavity and the targets. The diameters of the target ions studied generally have the following order: $Ni^{2+} < Mg^{2+} < Li^{+} < Ca^{2+} < Na^{+} < Sr^{2+} < Pb^{2+} < K^{+} < Ba^{2+} < Cs^{+}$. It should be noticed that there is inconsistency in the reported diameters of K^{+} and Ba^{2+}. In reference [3], $K^{+} < Ba^{2+}$; while in reference [32], $K^{+} > Ba^{2+}$. However their diameters are very close. Of the above ions, Sr^{2+}, Pb^{2+}, K^{+} and Ba^{2+} have ion diameters close to that of 18-crown-6. The diameter of barium is 0.268 [3], nearest to cavity size of the crown ether, thus it is expected to have highest complexation constant which can be confirmed from **Fig. 5-6** in which mobility of barium reaches its minimum at 0.5 mM 18-crown-6 and keeps constant with further addition. The mobility of potassium decreases over the whole 18-crown-6 concentration range studied; while the mobilities of lead and strontium decreased then leveled off at 1.0 and 1.5 mM, respectively.
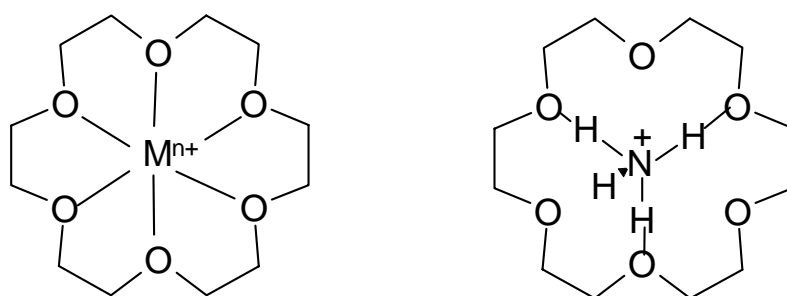
Fig. 5-5 Complexing of 18-crown-6 with metal ions and ammonium
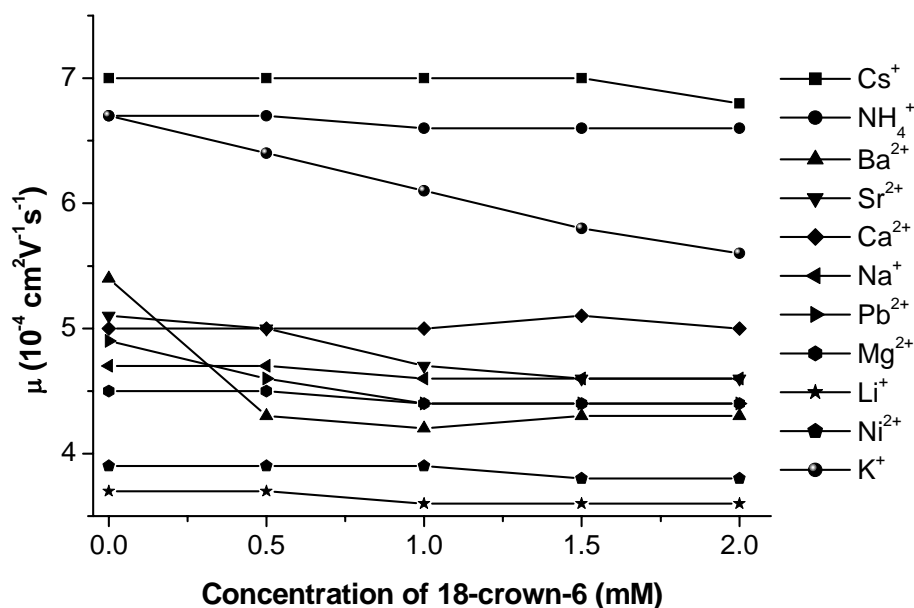
Fig. 5-6 Effect of 18-crown-6 on the mobilities of ions

Buffer: 7.5 mM lactic acid added by desired concentration of 18-crown-6 and adjusted to pH 4.0 by 100 mM HMIM hydroxide. Others as **Fig. 5-4**.

5.3.5 Effect of α-CD

The detection sensitivity for the analytes should be enhanced with addition of α-CD due to the increasing mobility difference between the background co-ion and the analytes. **Fig. 5-7** illustrates the variation of peak height ratios (of analyte in the α-CD containing buffer over that in non-α-CD buffer) versus concentration of α-CD. The peak height ratios increase significantly with α-CD concentration till 12 mM; from concentration of 15 mM, there was no notable amplification of the peak heights (not shown). Introduction of α-CD did not bring obvious influence on the mobilities or migration order of the metal ions. α-CD does not form complex with 18-crown-6 or metal ion [33]. We also found that peak symmetry deteriorated with increasing α-CD concentration due to the increasing mobility mismatch between analytes and co-ion,

however, all the peaks were baseline resolved in the ILCC. Also, the analysis time

slightly increased from ca 12.8 minutes of unmodified buffer to ca 13.1 minutes in

buffer containing 12 mM α-CD. It should be pointed out that the signal intensity (peak

height) is not only governed by the mobility difference (between the analyte and the

background coion), but also determined by the mobility of background counterion and

the TR value. The theoretical study can be found elsewhere [34].
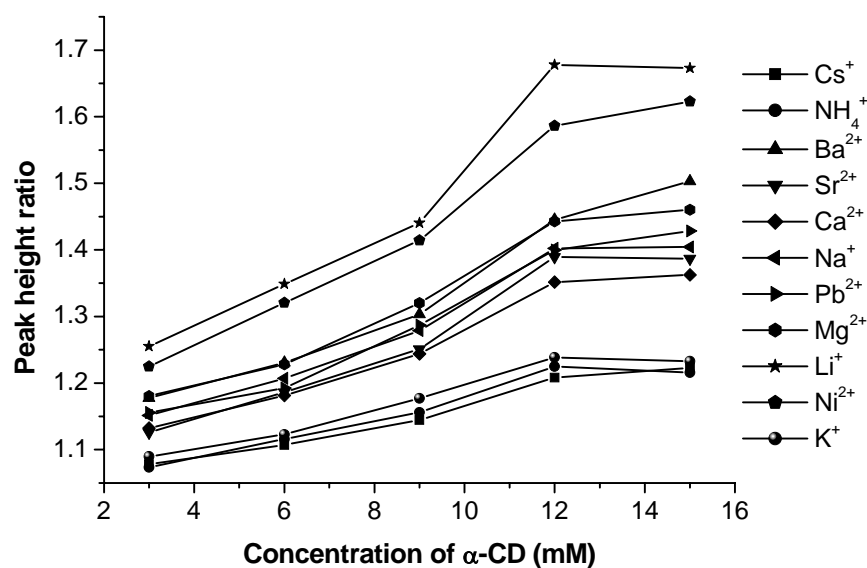
Fig. 5-7 Influence of α-CD on detection sensitivity of ions

Buffer: 7.5 mM lactic acid, 0.6 mM 18-crown-6, added by desired concentration of α-CD and adjusted to pH 4.0 by 100 mM HMIM hydroxide. Others as **Fig. 5-4**.

5.3.6 Effect of FASI

Compared with **Fig. 5-3**B, the resolution of the ions changed after FASI-CZE process

(**Fig. 5-8**). Plug length plays an important role in FASI. Generally, the longer the plug the

higher the stacking ratio. However, the longer plug leads to not only long stacking time

but also decreased resolution of the peaks. With injection of 200 seconds of water, the

peaks of magnesium and lead partially merged. Although the diluted plug will favor stacking of the analytes, we did not observe more significant stacking with solution of concentration lower than 1/300 of the run buffer; moreover, the reproducibility of both stacking factors and migration times of the analytes were notably improved when the plug concentration was changed to 1/200 of run buffer. Further dilution of the sample resulted in higher stacking factors; e.g., cesium of 1/200 of the original concentration (5 μg/ml) would produce 270-fold stacking (in terms of detection limit) after FASI. But it was at the price of poor reproducibility and narrow linear range. There are two factors restricting stacking in this experiment: a) low buffer concentration and, b) the existed conductivity of the plug hydrodynamically injected. High buffer concentration is not favorable in PGD method because it will cause high background noise and a plug of moderate conductivity could offer good reproducibility, which is also favorable in CE. In our work, the plug was formed by 50 mbar × 100 s injection of 1/200 buffer.
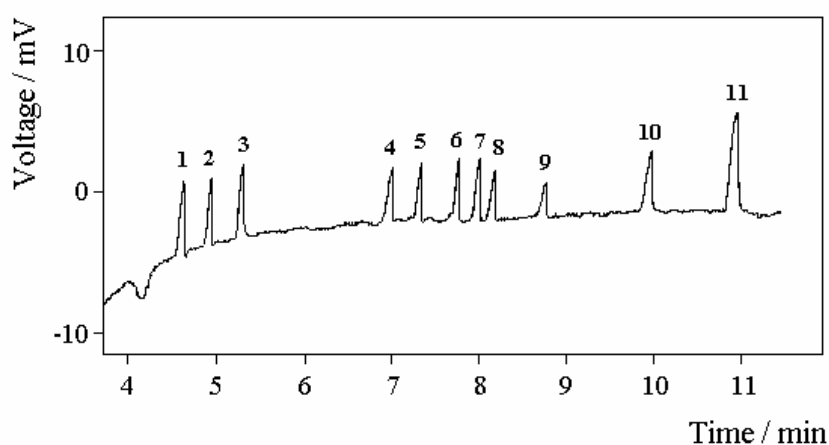
Fig. 5-8 Electropherogram of ions under FASI mode

FASI conditions: solution of 1/200 run buffer in concentration was hydrodynamically injected into capillary by 50 mbar × 100 s; the sample ions (diluted to 100-fold of **Fig. 5-3**) in 1/50 run buffer was injected into the capillary by 4 kV ×4.3 min.; the separation voltage was set to 8 kV. The buffer contains 7.23 mM lactic acid, 0.67 mM 18-crown-6, 12 mM α-CD adjusted to pH 4.1.

5.3.7 Optimization of the experimental conditions

In this experiment, the buffer pH, buffer concentration and concentration of 18-crown-6 are the main factors influencing the resolution and analysis time. Although α-CD also has influence on resolution, it does not change the migration order of the analytes and both sensitivity and resolution vary monotonically with its concentration; so it was not considered in the model. A three-factor, three-level, face-centered central composite design [35] coupled with multicriteria approach was employed in optimizing the operational conditions for simultaneous separation of the targets.
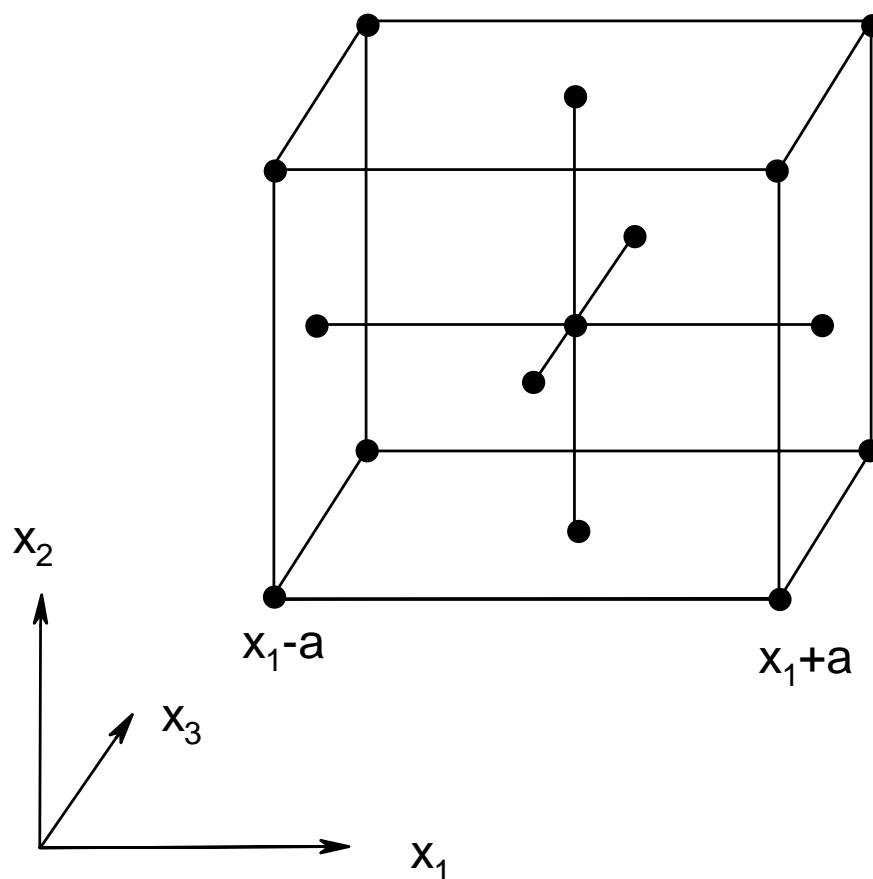
Fig. 5-9 Experimental domain of the face-centered composite design

Suppose there are three variables x_1, x_2 and x_3, whose optimal values are in the ranges of (x_1-a, x_1+a), (x_2-b, x_2+b) and (x_3-c, x_3+c), respectively. The experimental design of the three variables is shown in **Fig. 5-9**. Three testing points are chosen for each variable, for example, x_1-a, x, x_1+a are selected for x_1. Theoretically, only 15 experiments in the central point (as dotted in **Fig. 5-9**) are needed to estimate the effects and the various factors on the select response.

The value of *y* from experimental data for each peak were then fitted into a polynomial equation:

$$y = a_0 + a_1 x_1 + a_2 x_2 + a_3 x_3 + a_{11} x_1^2 + a_{22} x_2^2 + a_{33} x_3^2 + a_{12} x_1 x_2 + a_{13} x_1 x_3 + a_{23} x_2 x_3 \quad \text{(5-1)}$$

The individual responses functions (RF) in present work were analysis time (*t*) and resolution (*R*, which was chosen as the smallest in a single run). We define for this experiment, the resolution and analysis time of same significance, and the combined responses functions (CRF) for a single run can be expressed as [36]

$$y_i = CRF_i = 0.5 \times \frac{R_i}{R_{\max}} + 0.5 \times \left(1 - \frac{t_i}{t_{\max}}\right) \quad \text{(5-2)}$$

Where, R_{max} is the maximum value from the 15 minimum resolutions obtained in each run; and t_{max} is the maximum analysis time observed in the 15 runs. From the primary runs above, we can choose the testing points of the criteria corresponding to that in **Fig. 5-9** as: pH (x_1): 3.5, 4.0, 4.5; concentration of 18-crown-6 (x_2, mM): 0.4, 0.6, 0.8; concentration of lactic acid in the buffer (x_3, mM): 7.0, 7.5, 8.0. The 15 sets of data were obtained from different criteria from the face-centered composite design as indicated in **Fig. 5-9**. The constants in eq (5-1), from a_0 to a_{23} were obtained by resolving the multi-equations, and the maximum response surfaces (example as **Fig. 5-10**) were

located by differentiating the fitted second-degree polynomial with respect to each factor and equating derivatives to zero. The optimal values were: pH, 4.10; concentration of 18-crown-6: 0.67 mM; concentration of lactic acid: 7.23 mM. They have been used in experiment combined with FASI as shown in **Fig. 5-8**. The pherogram we obtained with the calculated optimal criteria was similar to the one we got by rule of thumb because the parameters are very close (the empirical values were: pH 4.0; concentration of 18-crown-6, 0.60 mM; concentration of lactic acid, 7.5 mM. Please refer to **Fig. 5-3**B which was obtained under the hydrodynamic injection mode.). But the face-centered composite design is more useful when there are multiple factors (e.g., analysis time, resolution, number of peaks, etc.) of different significance (in our experiment, we consider the two criteria of same significance) should be considered for performance. The design can provide different criteria within a unified mathematical framework.
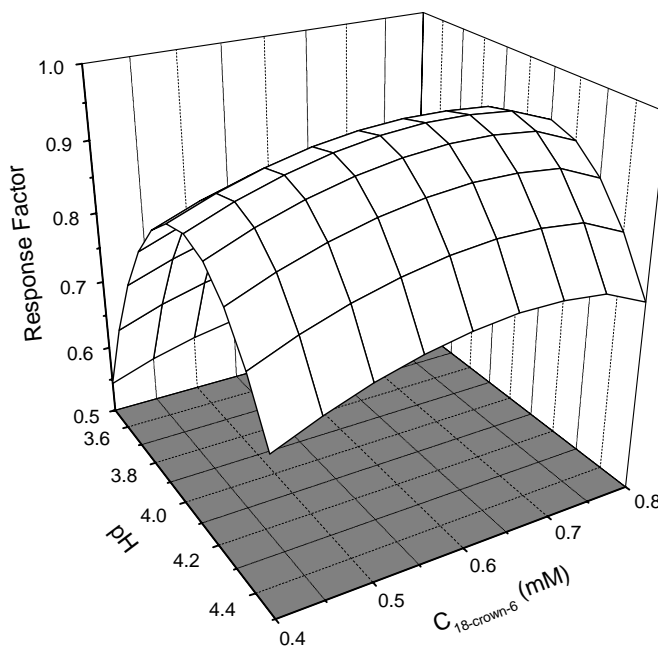
Fig. 5-10 Three-dimensional plots of the response function against pH and concentration of 18-crown-6
The concentration of lactic acid was set to 7.5 mM

5.3.8 Quantitations

Experiments were carried out on the analytes for evaluating LOD (defined as S/N=3 from peak height) and run-to-run repeatability. The day-to-day reproducibility of the migration time was assessed from a 10-day validation (five runs a day). The method showed good run-to-run repeatability and day-to-day reproducibility (Table 5-1). The calibration curve of peak area (mV·s) *vs.* concentration (ng/ml) for each analyte in the range of 10 to 80-fold LOD was constructed based on 5 concentrations, namely, 10, 20, 40, 60 and 80-fold of the LOD. The correlation coefficients of the calibration curves were between 0.992-0.998. LODs of analytes under hydrodynamic injection were also measured for comparison. It can be found that stacking factors of ions are different: Lithium has lowest mobility among the ions studied, its detection limit in FASI

decreased by a factor of 56, while the fastest ion cesium decreased by a factor of 122. Moreover, comparison of PGD with indirect UV method in terms of detection limits shows that PGD is generally more sensitive.

Table 5-1 Quantification factors of the CZE-PGD method

	Slope ± SD	Intercept ± SD	RSD% of t_m		LOD (ng/ml)		
	$(\times 10^2)$	$(\times 10^2)$	Run-run	Day-day	FASI	HD [a]	Literature (UV)
			(n=5)	(n=10)			
Cs^+	37.5 ± 1.1	1.6 ± 0.12	0.34	1.13	1.8	220	
NH_4^+	278 ± 17.5	14.4 ± 0.76	0.88	1.01	0.27	32	148 [37]
K^+	129 ± 3.0	3.8 ± 0.47	0.61	0.98	0.64	90	100 [38], 150 [39]
Ca^{2+}	128 ± 4.9	5.6 ± 0.05	0.58	1.18	1.2	86	92 [38]
Sr^{2+}	58.4 ± 2.2	-2.5 ± 0.17	0.77	1.18	2.6	210	133 [38], 180 [39]
Pb^{2+}	24.8 ± 1.4	0.06 ± 0.02	0.75	1.65	7.3	560	364 [38]
Ba^{2+}	37.8 ± 3.9	-2.0 ± 0.51	0.53	1.16	5.9	400	300 [38], 150 [39]
Na^+	224 ± 9.1	6.8 ± 0.40	0.37	0.77	0.82	60	114 [38], 140 [39]
Mg^{2+}	216 ± 6.8	-4.4 ± 0.28	0.51	1.09	1.0	64	105 [38], 80 [39]
Ni^{2+}	88 ± 5.6	-2.6 ± 0.17	0.90	1.34	3.5	190	261 [38]
Li^+	754 ± 12.4	39.4 ± 1.52	0.49	0.90	0.45	25	100 [38]

[a] Hydrodynamic injection

5.4 Summary

The resolution of the metal ions was greatly improved in the ILCC in which the EOF was reversed. With the buffer employed, ammonium and metal ions can be baseline separated. The FASI-CZE-PGD method developed can separate and detect the 11 ions with lower LOD than the conventional indirect optical detection method and with acceptable reproducibility.

References

[1] K. Ito, T. Hirokawa, J. Chromatogr. A 742 (1996) 281

[2] Y.C. Shi, J.S. Fritz, J. Chromatogr. 640 (1993) 473

[3] Q. Yang, J. Smeyersverbeke, W. Wu, M.S. Khots, D.L. Massart, J. Chromatogr. A. 688 (1994) 339

[4] Q. Yang, Y. Zhuang, J. Smeyersverbeke, D.L. Massart, J. Chromatogr. A 706 (1995) 503

[5] A. Weston, P.R. Brown, P. Jandik, W. Jones, A.L. Henckenberg, J. Chromatogr. 593 (1992) 289

[6] Y.H. Lee, T.I. Lin, J. Chromatogr. A 675(1994) 227

[7] M. Chen, R.M. Cassidy, J Chromatogr. 640(1993) 425

[8] E. Simunicova, D. Kaniansky, K. Loksikova, J. Chromatogr. A 665 (1994) 203

[9] J.M. Riviello, M.P. Harrold, J. Chromatogr. A 652 (1993) 385

[10] C. Stathakis, R.M. Cassidy, Analyst 121 (1996) 839

[11] W. Beck, H. Engelhardt, Chromatographia 33 (1992) 313

[12] C. Francois, P. Morin, M. Drenx, J. Chromatogr. A 706(1995) 535

[13] N. Cohen, E. Grushka, J. Chromatogr. A 678 (1994) 167

[14] T. Kappes, P. Hauser, Electroanalysis 12 (2000) 165

[15] T. Kappes, P.C. Hauser, Anal. Chem. 70 (1998) 2487

[16] S. Fujiwara, S. Honda, Anal. Chem. 59 (1987) 487

[17] B.B. Van Orman, G.G. Liversidge, G. L. Mcintire, T. M. Olefirowicz, A.G. Ewing, J. Microcol. Sep. 2 (1990) 176

[18] Y.C. Shi, J. S. Fritz, J. Chromatogr. A 671 (1994) 429

[19] C. Schwer, E. Kenndler, Anal. Chem. 63 (1991) 1801

[20] K.Z. Chang, Z.X. Zhao, R. Garrick, F.R. Nordmayer, M.L. Lee, J.D. Lamb, J. Chromatogr. A 706 (1995) 517

[21] C. Finkler, H. Charrel, H. Engelhardt, J. Chromatogr. A 822 (1998) 101

[22] P.J. Oefner, Electrophoresis 16 (1995) 46

[23] C. Stathakis,, R.M. Cassidy, Anal. Chem. 66 (1994) 2110

[24] M. Chiari, M. Cretich, M. Stastna, S.P. Radko, A. Chrambach, Electrophoresis 22 (2001) 656

[25] W.D. Qin, H.P. Wei, S.F.Y. Li, Analyst 127 (2002) 490

[26] D.S. Burgi, Anal. Chem. 65(1993) 3726

[27] L. Zhu, H.K. Lee, Anal. Chem. 73 (2001) 3065

[28] M. Albert, L. Debusschere, C. Demesmay, J.L. Rocca, J. Chromatogr. A 757 (1997) 291

[29] Y. He, H.K. Lee, Anal. Chem. 71 (1999) 995

[30] T.I. Lin, Y.H. Lee, Y.C. Chen, J. Chromatogr. A 654 (1993) 167

[31] G.W. Gokel, Crown Ethers and Cryptands, The Royal Chemical Society of Chemistry, Cambridge, 1991, pp 83-105

[32] J.A. Dean (Editor), Lange's Handbook of Chemistry, Mcgraw-Hill, New York, 1999, P. 4.30

[33] H.J. Buschmann, E. Cleve, K. Jansen, A. Wego, E. Schollmeyer, Mat. Sci. Eng. C 14 (2001) 35

[34] M.U. Katzmayr, C.W. Klampl, W. Buchberger, J. Chromatogr. A *850* (1999) 355

[35] D.L. Massart, B.G.M. Vandeginste, L.M.C. Buydens, S. De Jong, P.J. Lewi, J. Smeyers-Verbeke, Handbook of Chemometrics and Qualimetrics: Part A, Elsevier, Amsterdam, 1997

[36] M.D. Valle, J. Alonso, M. Poch, J. Bartroli, J. Chemom. 3 (1998) 285

[37] J. Havel, P. Janos, P. Jandik, J. Chromatogr. A 745 (1996) 127

[38] N. Shakulashvili, T. Faller, H. Engelhardt, J. Chromatogr. A 895 (2000) 205

[39] A. Tangen, W. Lund, R.B. Frederiksen, J. Chromatogr. A 767 (1997) 311

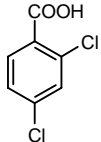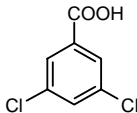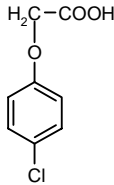# CHAPTER 6 IONIC LIQUIDS AS ADDITIVES
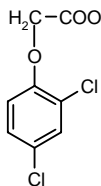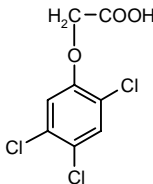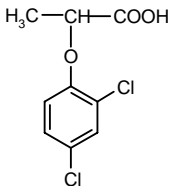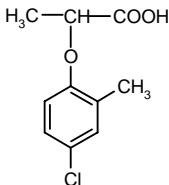
6.1 Introduction

Herbicides are widely used for controlling weeds or fungi in many agricultural and non-agricultural areas. Because most of them are readily dissolved in water, they can easily enter into surface or ground waters through natural drainage or filtration [1]; and their relatively slow degradation rates exacerbate their influences on the environment [2]. With the rapid development of herbicides and their increasing usage, careful monitoring of residue levels needs to be performed on crops, soil and water, etc, and there have been increasing needs for rapid and reliable detection of these herbicides [3]. A variety of analytical methods have been used for analysis of the targets in water including gas chromatography/mass spectrometry (GC/MS), gas chromatography/electron capture detection (GC/ECD) and high performance liquid chromatography (HPLC). Among these approaches, GC method is reliable for the analysis of herbicides in water and was adopted by US Environmental Protection Agency (EPA, Method 515.1). The disadvantage of the GC method is that derivatization of the carboxylic acid herbicides is usually needed before separation because some of them are not volatile or stable under the operating temperature [4], thus it is time consuming. Moreover, the sophisticated equipment is required which makes it expensive to operate [5].

The most commonly used mode for separation of herbicides in CE is known as micellar electrokinetic chromatography (MEKC) [6-11]. Because of the high concentration of the running buffer (including the surfactant) and the opposite migration directions between the micelle (also the acidic herbicides) and the EOF, the analysis time is

usually in the range of 10-25 minutes. For the charged species such as acidic herbicides, CZE is usually employed. Under cathodic EOF, fast separation can be obtained in alkaline buffer [12,13]; or with longer analysis time in the acidic buffer while the resolution of the analytes could be further adjusted by operating at a pH value near to the pKa of the analytes [14]. Nowadays, quite a number of separations are conducted in capillaries with modified internal surfaces. With reversed EOF, keeping high EOF velocity is not a crucial requirement under the CZE mode; hence, there is wider range for varying buffer pH in order for the optimal resolution, and the analysis time for the acids may be shortened. In the work of Marriott and coworkers [15], EOF was reversed by adding 0.001% hexamethrine bromide into the run buffer. The analytes, five chlorophenoxy acids and three neutral chlorophenols were nearly baseline separated within 17 minutes; but the charged phenoxy acids migrate out in less than 9 minutes.

Table 6-1 List of the analytes

No.	Name	Formula	Structure	pKa [16-18]
1	2,4-dichlorobenzoic acid (2,4-DCBA)	$C_7H_4Cl_2O_2$		2.68
2	3,5-dichlorobenzoic acid (3,5-DCBA)	$C_7H_4Cl_2O_2$		3.54
3	4-chlorophenoxyacetic acid (4-CPA)	$C_8H_7ClO_3$		3.56
4	2,4-Dichlorophenoxyacetic acid (2,4-D)	$C_8H_6Cl_2O_3$		2.87
5	2,4,5-Trichlorophenoxyacetic acid (2,4,5-T)	$C_8H_5Cl_3O_3$		2.83
6	2-(2,4-dichlorophenoxy)propionic acid (Dichlorprop)	$C_9H_8Cl_2O_3$		3.0
7	2-(2-Methyl-4-chlorophenoxy)propanoic acid (Mecoprop)	$C_{10}H_{10}ClO_3$		3.78

The concentrations of the herbicides in environment are usually very low, and extraction procedure is needed in order for the quantitative detection. Among these

methods, solid-phase extraction (SPE) is a widely used approach in preconcentration. Compared with liquid-liquid extraction, it consumes less organic solvent and is easy to operate. Recently, it has been combined with HPLC and CE in herbicide determination [19-25]. However, several different SPE columns are needed to clean up the sample solutions for HPLC analysis because the matrices of the real sample water such as humic and fulvic acids could interfere with the target analytes, which makes the operation complicated. Furthermore, the HPLC method was reported to lack adequate resolution for the acidic herbicides [26]. Because the separation mechanism in CZE is based on mass/charge ratios of the species, the neutral and positively charged compounds in surface water will not interfere with the determination of the negatively charged herbicides. This advantage of CZE makes pretreatment of sample solutions by a single SPE column possible. Several workers have studied the use of CZE in separation of acidic herbicides in standard mixtures [27,28] and in spiked lake water samples [10].

In this chapter, ILs were tested as additives in CE buffer and SPE-CZE method was developed for enrichment and separation of chlorophenoxy and chlorobenzoic acids (Table 6-1). The method was also applied to real sample analysis.

6.2 Experimental

6.2.1 Chemicals and stock solutions

All the chlorophenoxy and benzoic acid standards studied in this experiment were products of Aldrich (Milwaukee, WI, USA). Individual solutions of 1 mg/ml each were prepared by dissolving individual standards in pure acetonitrile, which were further diluted with deionized water to desired concentrations for the working standards. The

solutions were stored at 5 °C and the working standards were re-prepared every 5 days to avoid the potential errors from decomposition of the targets.

6.2.2 SPE procedure

The following procedures were employed in the SPE experiment unless otherwise stated.

Stock solution of the herbicides of 20 ppm each were prepared daily. For the ppb-level standard solutions, Milli-Q water and surface water were spiked to desired concentrations with the stock solutions. All solutions were added to sodium sulphate (2% w/w) and acidified to pH 2 by 4 M hydrochloric acid. Solid phase extraction was performed on a 500mg Varian (Harbor City, CA, USA) octadecylsilane (C_{18}) bonded silica cartridge. The cartridge was first cleaned by passing through 5 ml methanol and consequently dried with ultrapure nitrogen for five minutes, then it was rinsed with another 3 ml methanol followed by 10 ml deionized water. After being preconditioned, the sorbent was not allowed to dry until the sample loading procedure was completed.

Herbicide solution was loaded and passed through the SPE cartridge at a flow rate of 10-20 ml/min under positive pressure. After the cartridge was dried with nitrogen for about 2 minutes, the adsorbates were eluted using 2 ml of organic solvent (ethyl acetate, methanol, or acetonitrile as stated). The effluent was then heated to 50 °C and evaporated to dryness using a gentle stream of nitrogen. In order to avoid unexpected particles blown into the solution, the nitrogen delivery cable was connected to a filter

(0.22 μm). The residue was dissolved in 0.1 ml mixture of water and acetonitrile (50:50, v/v) before the CZE analysis.

6.3 CZE method development

6.3.1 Influence of buffer concentration

Phosphate, borate and their mixtures were reported as good background electrolytes for separation of herbicide acids which were analyzed under CZE [14,15,29] or MEKC [6-11] mode. Our preliminary runs without adding IL showed that the targets were not baseline resolved in 20 mM phosphate-borate at pH 8.5 (**Fig. 6-1**). Although reducing EOF enhances the resolution of the analytes, it also leads to longer analysis time. Furthermore, the two isomers presented in the mixture, 2,4-DCBA and 3,5-DCBA, were only partially separated and addition of resolving reagents were required, which will further extend the analysis duration. The phosphate-acetate buffer was employed as running buffer and 1,3-dialkylimidazolium was employed as additive in this study. Broaden peaks were obtained in low concentration phosphate-acetate; moreover, it was observed that high buffer concentration accelerated the adsorption of imidazolium onto the silica wall, which changed the capillary EOF (**Fig. 6-2**). In our experiments, 40 mM phosphate adjusted to desired pH by acetic acid was employed.
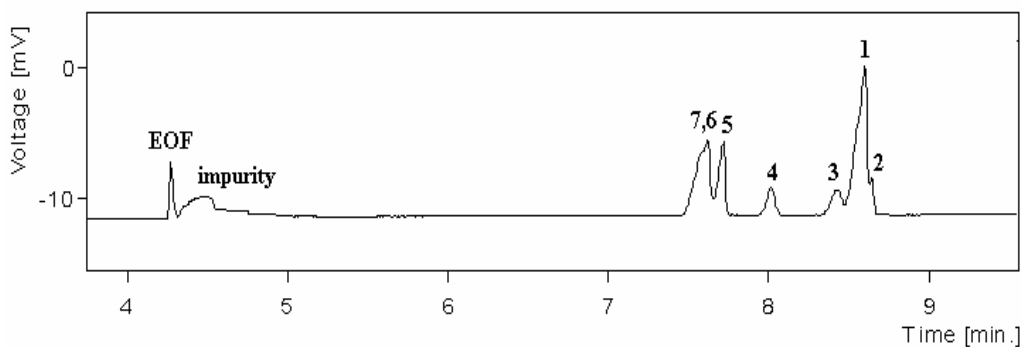
Fig. 6-1 Electrophoresis of standard mixtures in buffer without IL

The buffer: 20 mM sodium borate adjusted to pH 8.5 by 1 M sodium dihydrogen phosphate. The capillary: 50 μm I.D. and 360 μm O.D. with effective and total length of 45.7 and 56.4 cm, respectively. Applied voltage: 20 kV. UV detection wavelength: 230 nm. The analytes corresponding to individual peak numbers are described in Table 6-1; the concentrations (in μg/ml): 1, 10.0; 2, 3.0; 3, 3.0; 4, 5.0; 5, 5.0; 6, 3.0; 7, 5.0
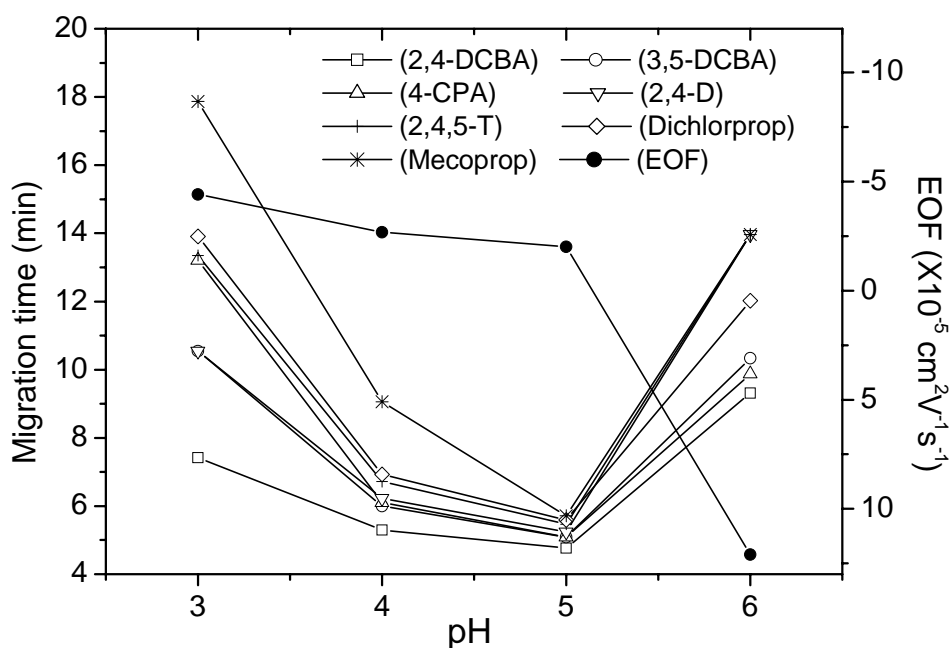
6.3.2 Influence of pH

The pH affects both EOF of the capillary and the electrophoretic mobility of the analytes. High pH leads to the high migration velocity of the acids due to the high anionic fraction of the analytes. However, it also causes increase of EOF towards the cathode due to the further deprotonation of the silanols on the silica surface. Migration time of the analyte in the capillary is determined by the combined effects of the above factors. **Fig. 6-3** depicts the variation of migration times of the analytes and velocity of EOF with change of pH. The analysis time decreases from 18 minutes at pH 3 to 5.7 minutes at pH 5, then increase to 14 minutes at pH 6. At lower pH, the reversed EOF rate is high, while the mobilities of the analytes are low due to the low mole fraction of the deprotonated portion of the herbicides. At higher pH, although analytes are fully deprotonated, their apparent mobilities are lower after compensating for the cathodic EOF, and hence the analysis time is prolonged. In fact when we tried to separate the

164

mixture at pH 7, the migration of the analytes in the capillary was so slow that we did not see the first peak after 25 minutes.
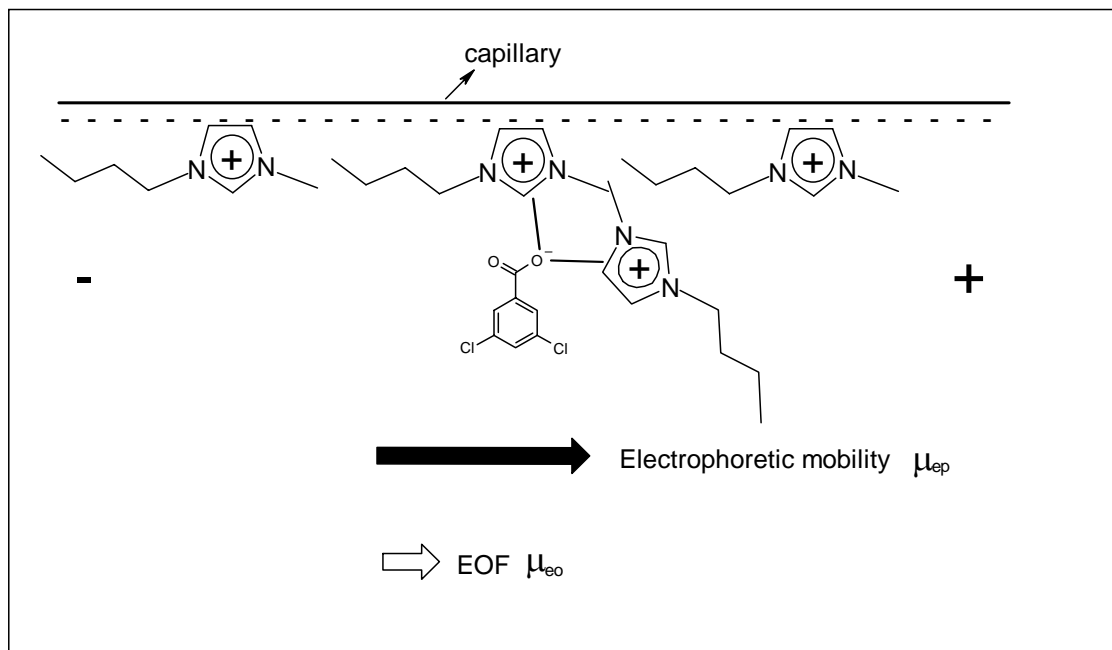
Fig. 6-2 Representative scheme of the electrophoresis of the analytes under the influence of the IL additive
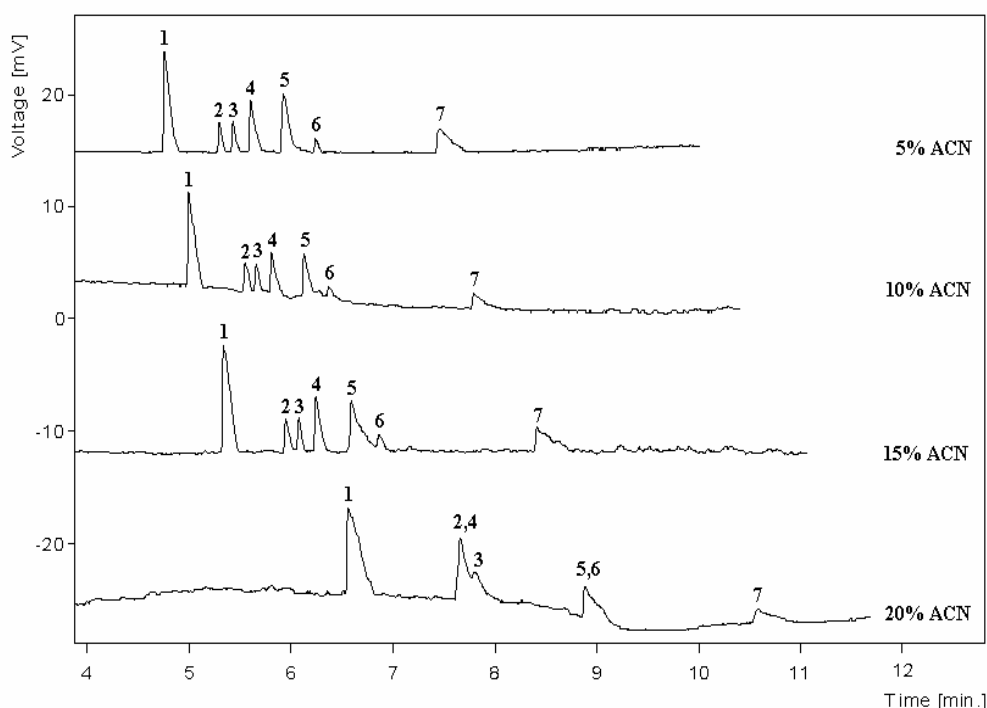
Fig. 6-3 Influence of pH

The buffer: 40 mM disodium hydrogen phosphate adjusted to desired pH by 10% (v/v) acetic acid. The buffer contains 10% acetonitrile and 10 mM BMIMPF$_6$. Applied voltage: -30 kV. Other conditions are same as **Fig. 6-1**.

6.3.3 Influence of organic solvents

Organic solvents added into the buffer will have influence on analysis time and sometimes even on resolution of the analytes. There is a decrease of EOF with addition of the organic solvent because it will lead to changes in viscosity [30], and dielectric constant of the buffer solution that will affect both EOF of the capillary and the electrophoretic mobility of the analytes [31]. It was also reported that the pK_a value of the silanol group of the capillary surface is increased when an increasing amount of organic solvent is added [32], so the surface density of protonated silanol groups will be decreased and hence resulting in low EOF. The introduction of organic solvent will also bring about changes in hydrophobicity of the buffer and pK_a of the analytes [30],

and variations in mobilities of the analytes and their migration orders may occur. **Fig. 6-4** shows that with addition of acetonitrile, the analysis time increases; all the analytes can be baseline resolved in the concentration range between 5% and 15%. At a concentration of 20%, 3,5-DCBA and 4-CPA comigrated with 2,4-D, also peaks of Dichlorprop and 2,4,5-T merged.

Fig. 6-4 Influence of acetonitrile concentration

The buffer containing 40 mM disodium hydrogen phosphate and 10 mM $BMIMPF_6$ was added to desired concentration (v/v) of acetonitrile, then was adjusted to pH 4.5 by acetic acid solution. Other conditions are same as **Fig. 6-3**.

6.3.4 Influence of additive concentration

As reported by other authors [33,34] and observed in our experiments, IL-cations in buffer adsorb onto the internal silica wall, causing changes in EOF. To the buffer containing 40 mM phosphate-acetate at pH 4.5, the EOF began to reverse with addition

of 5 mM BMIMPF$_6$, and the intensity increased with further addition. The velocity of

the reversed EOF was not very high, e.g., -4.4×10^{-5} cm^{2}V^{-1}s^{-1} with 20 mM BMIMPF$_6$.

Equilibrium of IL-cation adsorbed onto the silica wall is not instantaneous; the EOF rate

was observed to increase slowly from run to run and reach a relatively stable value after

a period of time (usually tens of minutes, depending on the concentration added). The

EOF rates in **Fig. 6-5** were measured after 20-minute electrophoresis using the fresh

buffers, so they should be considered as relative intensities rather than the equilibrated
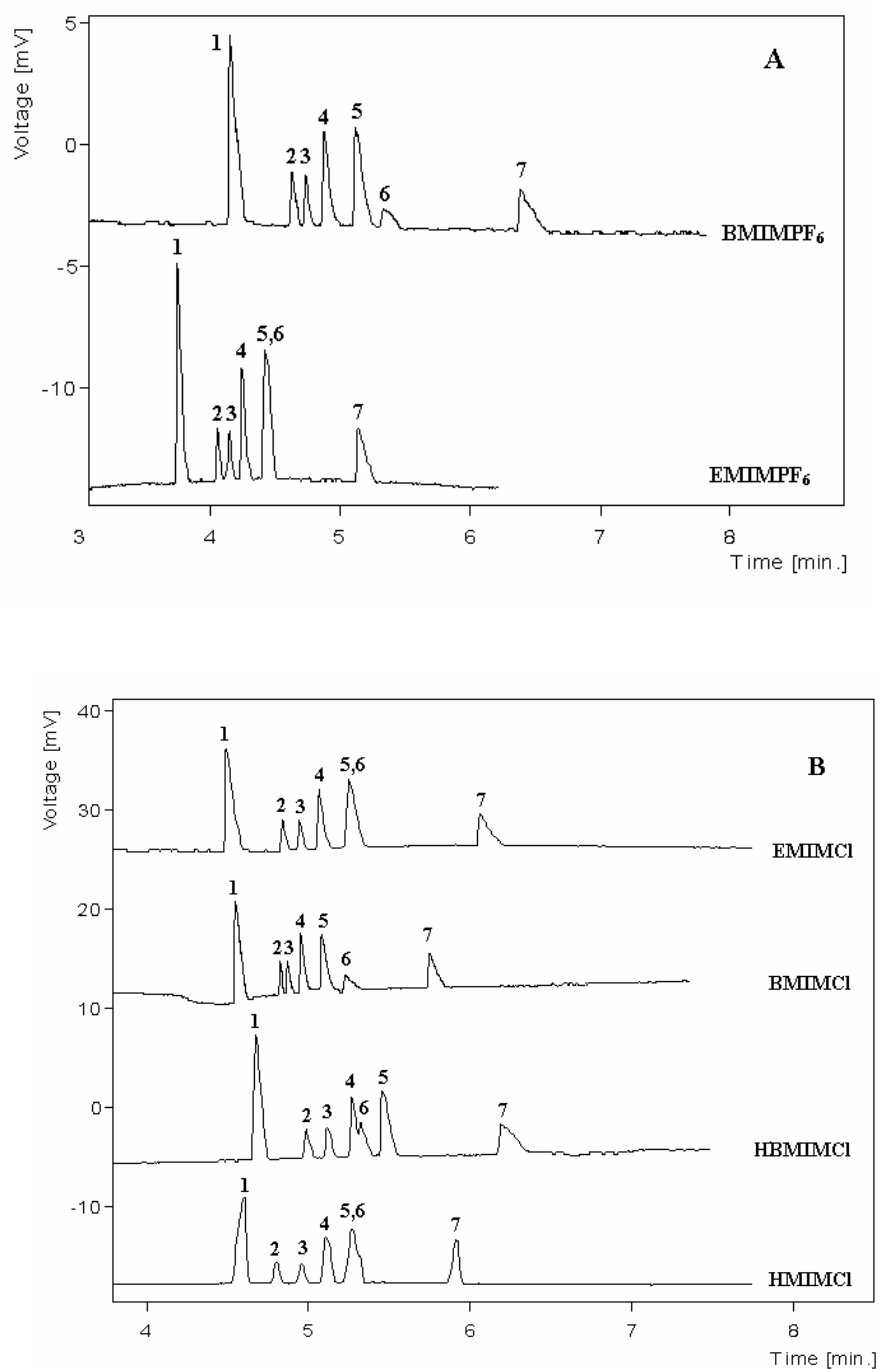
EOFs.
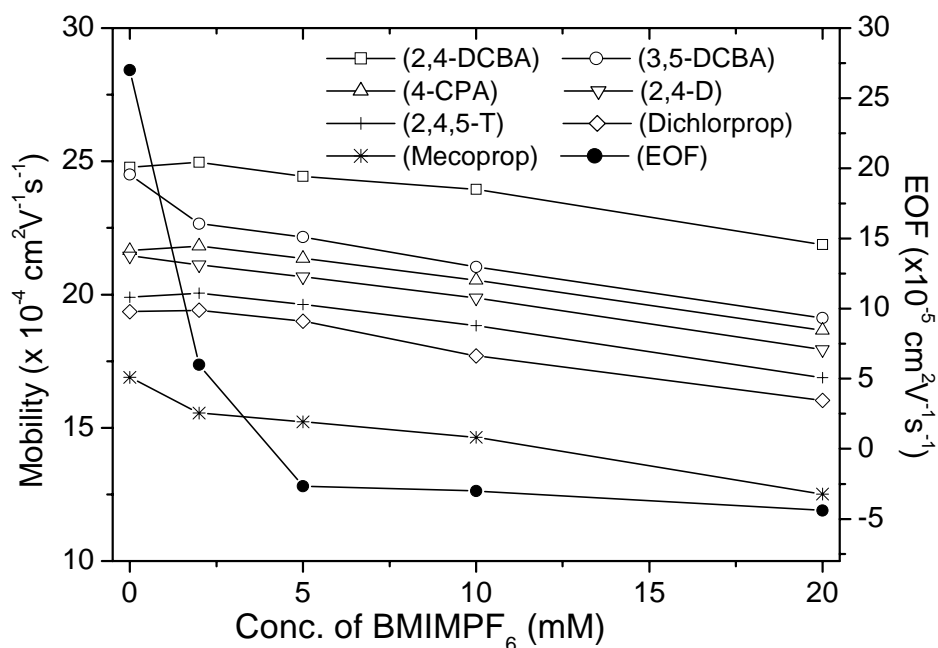
Fig. 6-5 Influence of BMIMPF$_6$

The buffer containing 40 mM disodium hydrogen phosphate and 10% (v/v) acetonitrile was added
to desired concentration of BMIMPF$_6$, then was adjusted to pH 4.5 by acetic acid solution. The
mobilities of the analytes in buffer containing 2 mM IL were measured by the method described in
reference [35]. Other conditions are same as **Fig. 6-3**.

The IL-cation is also UV-active. Its maximal absorbance wavelength was measured to be ca. 210 nm; the absorbance at 230 nm (the detection wavelength in this experiment) from the spectrum was so low compared to the maximum that it could be ignored. The influence of the IL concentration on the detection of the analytes was evaluated by measuring the peak heights of the individual standards in different concentrations of IL, showing no detectable decreasing trend of the peak heights with increasing IL concentration in range of 5-20 mM.

BMIM also exhibited selectivity to some analytes (3,5-DCBA and Mecoprop), which helped to resolve 3,5-DCBA from 2,4-DCBA: without BMIMPF$_6$, the peaks of the two compounds showed splitting but were not baseline separated; after addition of IL, mobility of 3,5-DCBA was reduced and was resolved from 2,4-DCBA, but no further separation was observed beyond 5 mM BMIM introduced. There was a report [33] on the resolution of positional isomer of phenols by ILs, in which it was believed to be caused by the heteroconjugation between the IL-anion with the analytes.

For the buffer containing 10 mM BMIMPF$_6$ and 10% acetonitrile, the analytes could be separated within 7 minutes after adsorption of BMIM onto the silica surface reaching equilibrium. The detection limits (in μg/ml, defined as S/N=3) of the analytes were: 2,4-DCBA, 0.99; 3,5-DCBA, 0.99; 4-CPA, 1.0; 2,4-D, 0.94; 2,4,5-T, 1.10; Dichlorprop, 3.5; Mecoprop, 2.2.

Fig. 6-6 Influence of different ILs

The buffer containing 40 mM disodium hydrogen phosphate and 10% (v/v) acetonitrile was added to 10 mM IL labeled in corresponding electropherogram, then was adjusted to pH 4.5 by acetic acid solution. Other conditions are same as **Fig. 6-3**.

6.3.5 Influence of the IL-cation and IL-anion

Influence of different IL-cations on the migration of the analytes was investigated and the electropherograms are shown in **Fig. 6-6**B. It can be seen that the cations generally have similar effects on the analytes due to the interaction between IL-cation and the anions. 3,5-DCBA was baseline resolved from 2,4-DCBA by all IL-cations. However, the cations showed different influence on the migration of Dichlorprop. With 10 mM BMIM, all the seven acids were separated; while Dichlorprop completely merged with 2,4,5-T in the presence of 10 mM EMIM; it was partially resolved in HMIM. It is interesting that with addition of 10 mM HBMIM the migration order of 2,4,5-T and Dichlorprop changed; the Dichlorprop migrated faster and baseline separated from 2,4,5-T, but shoulder-merged with 2,4-D. There does not seem to be a correlation between the length of the alkyl group connected to the dialkylimidazolium and the intensity of the cation-analyte interaction; amongst the cations studied, BMIM exhibits the strongest interaction with 3,5-DCBA. Comparison of electropherograms of ILs with different anions (EMIMCl and BMIMCl to EMIMPF$_6$ and BMIMPF$_6$) suggests that the IL anions, at least chloride and hexafluorophosphate, do not play as important a role as cations in influencing the migrations of the analytes.

6.4 SPE of the herbicides

6.4.1 Eluent and its influence on analysis

Methanol, acetonitrile and ethyl acetate are commonly used in SPE and they were tested for the feasibilities as eluents for the analytes and the results are tabulated in Table 6-2. The recoveries of herbicides were above 90% (n=5) for all the solvents when each

eluent was spiked with the herbicides to 0.2 ppm each. However, precipitation was observed when mixture of water-acetonitrile (10:90, v/v) was added to herbicides of 20 ppm each and it disappeared when water was added to the ratio of 40:60. Methanol showed slightly higher solubility for the acidic herbicides than ethyl acetate (on average *ca.* 2% in recovery); but it was also observed to be a good solvent for humic acid. Humic and fulvic acids are the main interfering matrix for determination of trace herbicides in real water samples. It was pointed out by other workers [36] and was also observed in our experiment that ethyl acetate, while used as eluent, was effective in reducing the concentration of humic acids in the effluent. Although it was reported that addition of methylene dichloride into ethyl acetate could enhance the recoveries of the polar extractants, there was, to our observation, little improvement of recoveries of the analytes in ethyl acetate after 10-30% (v/v) methylene dichloride was added. Pure ethyl acetate was used as eluent in our experiment because it could offer satisfactory recoveries without addition of methylene dichloride which might be potentially more harmful to human body.

Table 6-2 Recoveries of herbicides with different eluents

| | %Recovery ± %RSD (n=5) [a] | | | |
| | | | | EA + MD [b] |
	Methanol	Acetonitrile	Ethyl acetate	
2,4-DCBA	109.7 ± 2.7	93.2 ± 6.4	97.4 ± 4.0	98.7 ± 6.5
3,5-DCBA	104.2 ± 4.9	96.1 ± 4.9	96.6 ± 6.9	96.1 ± 5.6
4-CPA	96.8 ± 3.1	98.0 ± 4.5	102.1 ± 5.0	99.4 ± 7.3
2,4-D	99.1 ± 7.4	91.2 ± 5.3	99.2 ± 4.6	99.6 ± 6.0
2,4,5-T	100.0 ± 4.0	93.5 ± 4.7	95.3 ± 4.0	107.1 ± 3.4
Dichlorprop	98.5 ± 4.8	97.4 ± 3.8	98.1 ± 3.9	101.0 ± 4.4

| Mecoprop | 99.9 ± 5.5 | 104.7 ± 6.8 | 97.0 ± 6.4 | 98.2 ± 4.2 |

[a] eluent was spiked with herbicides to 0.2 ppm each
[b] ethyl acetate containing 30% (v/v) methylene dichloride

Since CZE employs a different separation mechanism from HPLC, GC, or MEKC, the concentration of humic acid may affect the detection of the phenoxy acids to different extents. We found that acidic herbicides spiked to 5 ppb each in real samples could be detected by CZE without elimination of humic acids during the extraction procedure. For real samples containing sub-ppb level of targets, ethyl acetate should be used because of the high matrix concentration.

Highest recoveries of all the analytes could be obtained with elution volume larger than 1.5 ml, thus 2 ml eluent was used in the experiments.

6.4.2 Salt-out effect and concentration of sodium sulphate
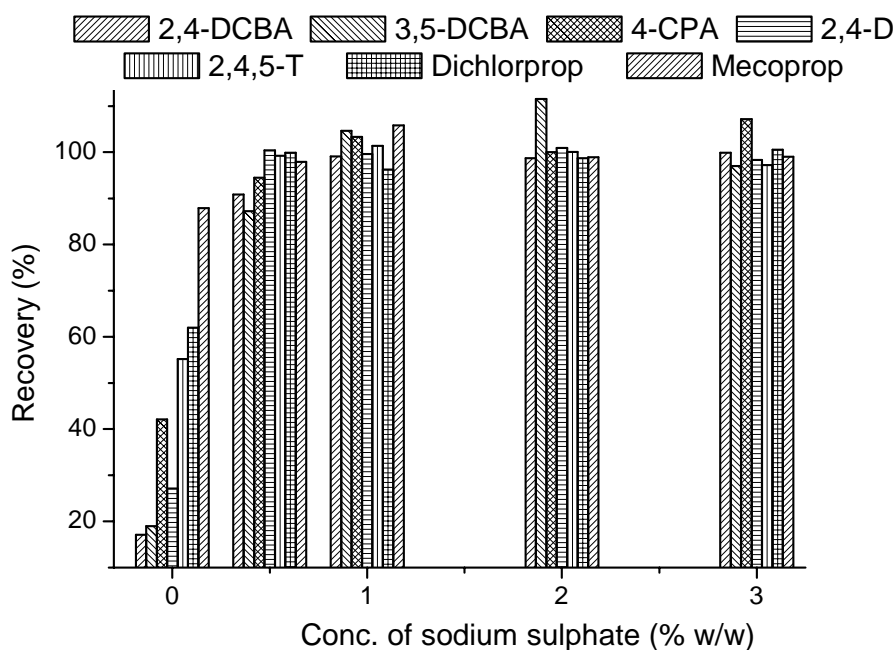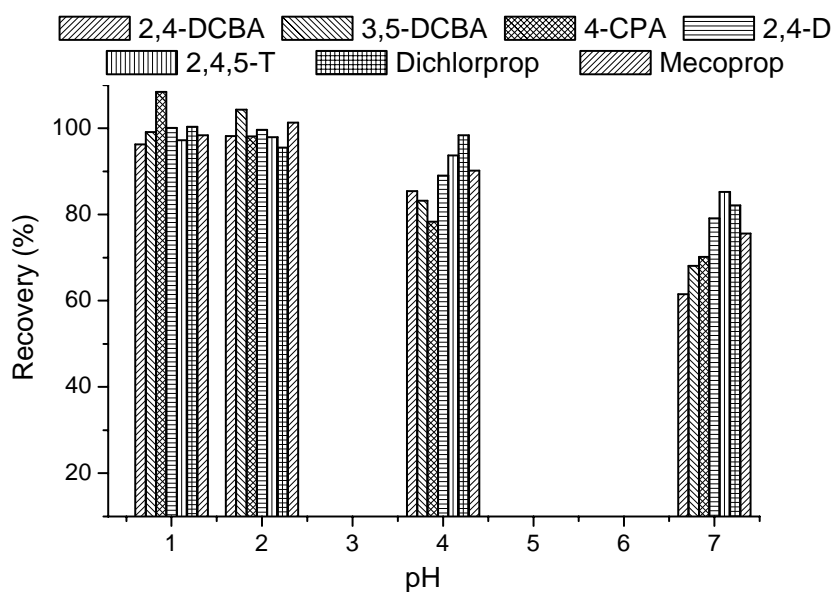

Fig. 6-7 Influence of concentration of sodium sulphate on the recovery of herbicides

Conditions: 400 ml 0.5 ppb standard solution, pH 2. Eluent: ethyl acetate. The dried residue was dissolved in 0.1 ml water-methanol (50:50, v/v) mixture.

The recoveries of the herbicides were not satisfactory even after the sample was acidified to pH 1 with 27.1% for 2,4-D, 55.3% for 2,4,5-T and 71.7% for 2,4-DB. Some inorganic salts such as potassium chloride or sodium chloride [37] were added to the sample solution to improve the retention of the polar analytes onto the solid phase so as to increase the recoveries of the herbicide. In this work, sodium sulphate was added to the sample and influence of concentration on the recoveries of the three targets was studied. Sodium sulphate of concentration higher than 0.5% (w/w) could offer maximum recoveries (higher than 95%) for all the analytes. In view of the complexity of the real samples, solutions were added by sodium sulphate to 2% (w/w) before passing through the cartridge.

6.4.3 Influence of pH

The pK_a values of the analytes are in the range of 2.6-3.6 and acidic environment will theoretically favor their adsorption on the C_{18} sorbent. Although not as significant as that of salt addition, the pH value did have some effects on the adsorption of the acids (**Fig. 6-8**). However, we did not find the obvious elimination of the humic / fulvic acids under neutral conditions as observed by other authors [24]. The sample solution was acidified to pH 1.5 before extraction because further acidification may cause hydrolysis of the Si-O-C bond of the sorbent.

Fig. 6-8 Influence of pH on the recovery
Experimental conditions: 400 ml 0.5 ppb standard solution; concentration of sodium sulphate was 2%. Other conditions are same as in **Fig. 6-7**.

6.5 Validation of SPE-CE method

A three-day validation was carried out in which all the freshly prepared standard solutions were measured three times. Each herbicide was evaluated with all the nine curves. The correlation coefficients for the linear best fit were no less than 0.992, and the relative standard deviation (RSD) for the slope and the intercepts were no more than 4.21% and 5.17%, respectively.

Table 6-3 Validation of the SPE-CZE method

	%Recovery $\pm$ %RSD (n=5)[a]			RSD of A_p, %	LOD (ppb)
	0.5ppb	5ppb	10ppb	(n=5)[c]	
2,4-DCBA	96.7 ± 7.0	100.7 ± 5.3	98.0 ± 4.6	2.4	0.25
3,5-DCBA	99.0 ± 4.8	98.2 ± 5.4	100.0 ± 3.3	1.7	0.25
4-CPA	95.9 ± 6.5	97.9 ± 5.3	96.2 ± 5.1	2.0	0.25
2,4-D	97.8 ± 5.9	101.4 ± 4.8	98.5 ± 3.6	1.9	0.23
2,4,5-T	98.8 ± 6.9	95.6 ± 4.7	99.4 ± 6.0	1.9	0.27
Dichlorprop	98.7 ± 5.4[b]	97.4 ± 2.8	97.5 ± 4.1	3.4	0.87
Mecoprop	107.4 ± 3.6[b]	99.1 ± 2.7	96.9 ± 4.0	1.0	0.55

[a] evaluated based on 400 ml deionized water spiked to concentrations stated below
[b] the spiking concentration was 1.0 ppb
[c] For the 5 ppb extracts

400 ml herbicide solutions of different concentrations were employed to evaluate the recoveries in SPE procedure, RSD of migration time (t_m) and peak area (A_p) in CZE. Table 6-3 shows that the SPE-CZE method is of good repeatability and high sensitivity; it can be used in analyzing herbicides of sub-ppb levels. The method may be used in detecting herbicides of lower concentration because the sample volume can be as high

as 1000 ml without significant decrease in % recoveries. It was also assessed for the feasibility of detecting herbicides in real water sample. Compared to the unspiked real sample water as control, the recoveries between 86.1% and 107.0% were obtained from 400 ml samples spiked with 0.2-2.0 ppb herbicide each.

6.6 Real Sample Analysis

The SPE-CZE method was applied to the determination of the concentrations of acidic herbicides in local pond surface water (Normanton Park, Singapore). Although the baseline after EOF was not very stable due to the high concentration of the interfering matrix, the species present could still be qualitatively identified by migration times (also by spiking in our experiment) and quantitatively determined by peak areas (**Fig. 6-9**). Two herbicides were identified by spiking method. One was 2,4-D; its concentration was determined to be 0.46 ± 0.06 ppb (n=3). Another was found to be 2,4-DB by spiking with the standards available in out laboratory. The concentration of 2,4-DB, considering its recovery in our previous work in SPE procedure [38], was estimated to be 0.33 ± 0.08 ppb (n=3). The extract eluted by ethyl acetate was also analyzed by a Waters HPLC system (chromatogram in **Fig. 6-10**) whose working conditions were similar to those in a previous publication [39]. Before analysis, the system was calibrated with standard solutions, and the linearity for each herbicide was determined from the peak areas of different concentrations over the range of 0.4 to 6 ppm (equal to 0.1 to 1.5 ppb in 400 ml water before the SPE procedure). The relative coefficient values were all better than 0.99. The concentrations of 2,4-DB and 2,4-D were found to be 0.52 ± 0.13 ppb (n=3) and 0.31 ± 0.05 ppb (n=3), respectively. It can be seen that the baseline of the HPLC chromatogram was worse than that in the CZE electropherogram;

the poor baseline might be attributed to the interference from humic/ fulvic acids. Both HPLC and CZE methods do not require derivatization of the acidic herbicides. However, compared with SPE-HPLC, the SPE-CZE method here may be a better alternative/complement to Method 515.1 since interferences can be more easily alleviated.
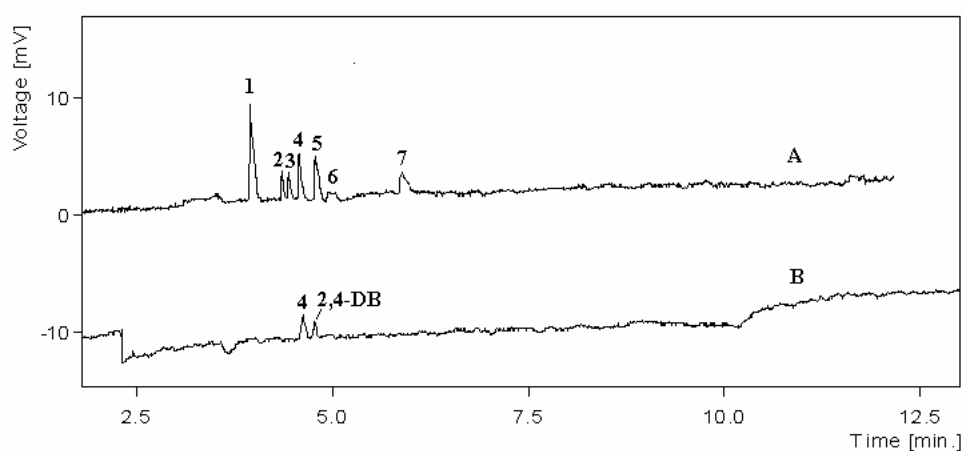
Fig. 6-9 Electropherogram of real sample
A: the sampled was spiked by adding 1.5 ml mixture standards as used in **Fig. 6-6** into 400 ml local surface water, eluted by methanol, the dried residue was dissolved in 2 ml water-acetonitrile (50:50, v/v). B: The sample: 400 ml local surface water, eluted by ethyl acetate, the dried residue was dissolved in 0.1 ml water-acetonitrile (50:50, v/v). The buffer: 40 mM phosphate-acetate containing 10 mM BMIMPF$_6$ and 10% (v/v) acetonitrile at pH 4.5. Other conditions are same as in **Fig. 6-6**.
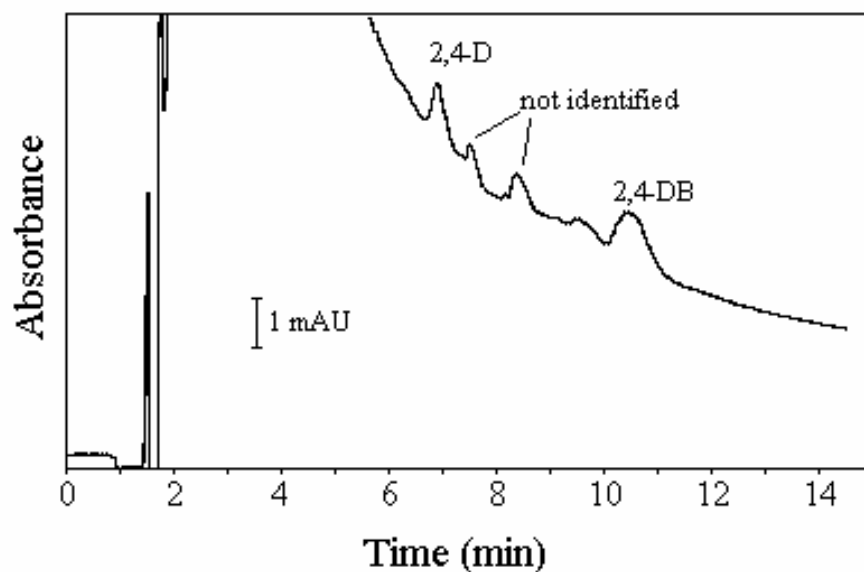
Fig. 6-10 Analysis of the real sample by HPLC
The sample is same as in **Fig. 6-9**B. HPLC conditions: column: Spherisorb ODS1 (150×4.6mm); eluent: 6 mM nitric acid in 60:40 (v/v) methanol-water mixture; flow rate: 0.6 ml/min). UV detector was set to 230 nm.

6.7 Summary

Accompanying with high concentration buffer, ILs of considerably low concentration can effectively reduce or reverse the capillary EOF. The interactions between IL-cations and phenoxy /benzoic acids are complicated and further investigation is needed in order to quantitatively explain some of the phenomena. However, IL showed promising performance as additive in the separation of phenoxy and benzoic acids: compared to the conventional CZE or MEKC, it offers relatively short analysis time and potential ability in resolving positional isomers. Moreover, the acidic working environment, which is near pK_a of the acids, renders a possibility for optimal separation. SPE-CZE is potentially a useful approach to determine acidic herbicides in the environment. Some advances, such as well matched SPE eluent and CZE buffer and improvement in detection sensitivity, will help to extend its application in routine analysis.

References

[1] R. Schuster, A. Gratzfeldhusgen, Analusis 19 (1991) I45

[2] C. Spagone, C. D'orazio, M. Rossi, D. Rotilio, J. High Resol. Chromatogr. 19 (1996) 647

[3] D.T. Eash, R.J. Bushway, J. Chromatogr. A 880 (2000) 281

[4] N.Q. Li, H.K. Lee, Anal. Chem. 72 (2000) 5272

[5] K.V. Penmetsa, R.B. Leidy, D. Shea, J. Chromatogr. A 745 (1996) 201

[6] M.Jung, W.C. Brumley, J. Chromatogr. A 717 (1995) 299

[7] Y. Mechref, Z. El Rassi, Anal. Chem. 68 (1996) 1771

[8] Y. Mechref, Z. El Rassi, J. Chromatogr. A 757 (1997) 263

[9] Y. Mechref, J.T. Smith, Z. El Rassi, J. Liq. Chromatogr. 18 (1995) 3769

[10] Y.Z. Hsieh, H.Y. Huang, J. Chromatogr. A 745 (1996) 217

[11] M.W.F. Nielen, Trends Anal. Chem. 12 (1993) 345

[12] M. Aguilar, A. Farran, V. Marti, Sci. Total Environ. 132 (1993) 133

[13] W.D. Qin, H.P. Wei, S.F.Y. Li, J. Chromatogr. Sci. 40 (2002) 387

[14] A.W. Garrison, P. Schmitt, A. Kettrup, J. Chromatogr. A 688 (1994) 317

[15] J. Kruaysawat, P.J. Marriott, J. Hughes, C. Trenerry, Electrophoresis 22 (2001) 2179

[16] C. Crescenzi, A. Di Corcia, S. Marchese, R. Samperi, Anal. Chem. 67 (1995) 1968

[17] P.H. Howard, W.M. Meylan, Handbook of Physical Properties of Organic Chemicals, Lewis Publisher, Boca Raton, 1997, pp. 6

[18] C.D.S. Tomlin, The Pesticide Manual: A World Compendium, 11th Ed., British Crop Protection Council, Surrey, 1997, pp. 224, 337

[19] D. Volmer, K. Levsen, G. Wunsch, J. Chromatogr. A. 660 (1994) 231

[20] E.A. Hogendoorn, E. Dijkman, B. Baumann, C. Hidalgo, J.V. Sancho, F. Hernandez, Anal. Chem. 71 (1999) 1111

[21] A. Balinova, J. Chromatogr. 643 (1993) 203

[22] J. Hodgeson, J. Collins, W. Bashe, J. Chromatogr A. 659 (1994) 395

[23] T.D. Bucheli, F.C. Gruebler, S.R. Muller, Anal. Chem. 69 (1997) 1569

[24] C.W. Thorstensen, O. Lode, A.L. Christiansen, J. Agr. Food Chem. 48 (2000) 5829

[25] J.P. Quirino, N. Inoue, S.Terabe, J. Chromatogr. A. 892 (2000) 187

[26] I.S. Kim, F.I. Sasinos, R.D. Stephens, J. Wang, M.A. Brown, Anal. Chem. 63 (1991) 819

[27] S.K. Yeo, H.K. Lee, S.F.Y. Li, J. Chromatogr. 594 (1992) 335

[28] G. Dinelli, A. Vicari, P. Catizone, J. Chromatogr. A. 733 (1996) 337

[29] X.B. Song, W.L. Budde, J. Chromatogr. A 829 (1998) 327

[30] Y.J. Lee, W.W. Price, M.M. Sheil, Analyst 20 (1995) 2689

[31] R.J. Hunter, Zeta Potential In Colloid Science, Academic Press, London 1981, pp. 70

[32] W. Schutzner, E. Kenndler, Anal. Chem. 64 (1992) 1991

[33] M. Vaher, M. Koel, M. Kaljurand, Electrophoresis 23 (2002) 426

[34] E.G. Yanes, S.R. Gratz, M.J. Baldwin, S.E. Robison, A.M. Stalcup, Anal. Chem. 73 (2001) 3838

[35] B.A. Williams, G. Vigh, Anal. Chem. 68 (1996) 1174

[36] M.S. Mills, E. M.Thurman, Ana. Chem. 64 (1992) 1985

[37] L. Sarrazin, W. Wafo, P. Rebouillon, J. Liq. Chromatogr. R. T. 22 (1999) 2511

[38] W.D. Qin, H.P. Wei, S.F.Y. Li, J. Chromatogr. Sci. 40 (2002) 387

[39] M.A. Hernandez-Mateos, L.V. Perez-Arribas, F. Navarro-Villoslada, M.E. Leon-
Gonzalez, L.M. Polo-Diez, J. Liq. Chromatogr. R. T. 22 (1999) 695

CHAPTER 7   CONCLUSION AND FUTURE WORK

7.1 Conclusion

ILs are a family of materials that shows promising properties for CE. They are easy to synthesize with high yields and are stable both in water and air. The impurities in the products can be detected by a α-CD-modified CZE method with low detection limit and good reproducibility. The fragmentation behaviors of ILs in organic solvent imply variations of their association patterns, which may partially correspond to their different performances in CE when they are used as background electrolytes. The lower charged anions tend to form larger aggregates, while higher charged anions form small aggregates. The large aggregates are stable in low polar media, while only small aggregates can exist in polar solvents such as water. So ILs can be important additives for CE in separation of neutral compounds, especially in NACE, in which the solvents are weak proton donors or acceptors compared with water.

The IL-cations are ideal background chromophores for indirect detection of cationic analytes. The chain length of alkyl group connecting to the imidazole ring can be trimmed and thereby their mobilities can be finely tuned, rendering well-matched mobilities between the chromophore and the analytes with consequently high TR and symmetric peaks. IL cations have stable mobilities over wide pH range, the buffers employing ILs as background chromophores for indirect detection can easily visualize and separate some analytes that cannot be separated and visualized in conventional

buffer. The inclusion complexation of the IL-cation with α-CD enables it to be an excellent background electrolyte for direct PGD detection.

Coating of the capillary with IL-cations leads to reversed EOF and alleviation in interaction between cationic analytes and the silica surface. Significant enhancement in resolution and recovery of the cationic ions can be obtained. Compared with the imidazole-coated capillary, the IL-coating can be cationic over a wide pH range, especially in alkaline buffer, which not only offers relative stable EOF and hence the reproducibility of the experiment, but also high ion-exchange capacity for anionic analytes in high pH buffer, making it possible in separation of weak acids under IC-OTCEC mode. Adsorption of DNA fragments onto the IL-coating due to the electrostatic attraction, increasing with electric density of the DNA fragments, can be controlled by addition of sieving matrices. The DNA fragments can be separated with shorter analysis time in ILCC than in PACC owing to the reversed EOF which moves codirectionally with the DNA fragments. The ILCC is a potential attractive alternative for the widely used PACC in separation of large-sized DNA fragments in consideration of analysis time.

In the presence of high concentration background electrolyte, relatively low concentration of IL-cation can be significantly and quickly adsorbed onto the negative capillary wall, leading to reversed EOF, although the magnitude is very low. Moreover, IL-additives showed discrimination effects on positional isomers, making the shoulder-merged peaks baseline resolved for some analytes.

7.2 Future work

The use of ILs in CE is still at its beginning stages and more work is needed to take full advantage of these new materials. For example, separation of anionic organics and neutral compounds in NACE using ILs as BGEs has been reported by several workers (Reference 18, 19 and 20, Chapter 1 and the work in Chapter 6); it may be an alternative or complement to the conventional MEKC method. However, due to the lack of precise data describing the behaviors of these materials in organic solvents, experiments conducted so far were restricted to empirically positive or negative results obtained after individual ILs added in the buffer. As reported in Chapter 2, there may exist relations between the mass spectra of the ILs and their performances as BGEs or additives in CE. MS is a tool for investigating the association patterns between the IL-cation and IL-anion and it is helpful in finding the potential candidates as background electrolytes or additives in CE. One can chose the ILs purposefully with the aid of the mass spectra. Moreover, since ILs have different influences on the targets, satisfactory separation of the targets may be obtained with combination of several ILs; The mass spectrometry as tool in this case may be important in quickly finding the appropriate candidates and in efficiently design the buffer system.

Our experiments showed that the IL-coated capillaries are efficient for separation of metal ions and DNA fragments as well. Stability of the coating is an important criterion in CE. Generally the thicker the coating, the higher resistance it possesses against the hydrolysis effect from the buffer and therefore the longer the duration. Furthermore, the thick coating may offer high ion-exchange capacity for the analytes when the capillary is operated under IC-OTCEC mode. There has been a report (M. Hirao, K. Ito, H. Ohno, Electrochim. Acta, 45, 2000, 1291) on polymerization of N-vinylimidazolium

tetrafluoroborate. The method can be applied to the polymerization of the IL-cation on capillary surface. By polymerization, the surface properties may be changed and new effects on the analytes may be expected.

LIST OF PUBLICATIONS

Journal paper

1. Weidong Qin, Hongping Wei, Sam Fong Yau Li, Separation of ionic liquid cations and related imidazole derivatives by α-cyclodextrin modified capillary zone electrophoresis, *Analyst*, 127 (2002) 490

2. Weidong Qin, Hongping Wei, Sam Fong Yau Li, Determination of acidic herbicides in surface water by solid-phase extraction followed by capillary zone electrophoresis, *Journal of Chromatographic Science*, 40 (2002) 387

3. Weidong Qin, Hongping Wei, Sam F. Y. Li, 1,3-Dialkylimidazolium based room-temperature ionic liquids as background-electrolyte and coating material in aqueous capillary electrophoresis, *Journal of Chromatography A*, 985 (2003) 447

4. Weidong Qin, Sam Fong Yau Li, An ionic liquid coating for determination of sildenafil and UK-103, 320 in human serum by capillary zone electrophoresis-ion trap mass spectrometry, *Electrophoresis*, 23 (2002) 4110

5. Weidong Qin, Sam Fong Yau Li, Electrophoresis of DNA in ionic liquid coated capillary, *Analyst*, 128 (2003) 37

6. Weidong Qin, Sam Fong Yau Li, Determination of chlorophenoxy acid herbicides by capillary electrophoresis with integrated potential gradient detection, *Electrophoresis*, 24 (2003) 2174

7. Weidong Qin, Sam Fong Yau Li, Determination of ammonium and alkali, alkaline-earth metals ions by capillary electrophoresis-potential gradient detection using ionic liquid as background electrolyte and covalent coating reagent, submitted to *Journal of Chromatography A*, revising according to the referee's comments

8. Weidong Qin, Sam Fong Yau Li, Free solution electrophoresis of DNA in ionic liquid coated capillary, submitted to *Electrophoresis*

9. Weidong Qin, Sam Fong Yau Li, Ionic liquids as additives for separation of benzoic acid and chlorophenoxy acid herbicides by capillary electrophoresis, submitted to *Electrophoresis*

Conference paper

10. Weidong Qin, Hongping Wei, Sam Fong Yau Li, Study of the 1-ethyl-3-methylimidazolium based ionic liquids as background electrolyte in capillary electrophoresis, *The 25th International Symposium on Capillary Chromatography*, Riva del Garda, Italy, 13-17 May, 2002